

Technical Report Series
Number 77-6

HYDROGRAPHIC OBSERVATIONS
IN ONSLOW BAY, NORTH CAROLINA
(JULY - AUGUST 1976/OBIS V):
DATA GRAPHICS

CIRCULATING COPY
Sea Grant Library

by
J. J. Singer
L. P. Atkinson
W. S. Chandler
and
P. G. O'Malley

Georgia Marine Science Center
University System of Georgia
Skidaway Island, Georgia

HYDROGRAPHIC OBSERVATIONS
IN
ONslow BAY, NORTH CAROLINA
(JULY - AUGUST 1976/OBIS V): DATA GRAPHICS

J. J. Singer
L. P. Atkinson
W. S. Chandler
P. G. O'Malley

Skidaway Institute of Oceanography
P. O. Box 13687
Savannah, Georgia 31406

The Technical Report Series of the Georgia Marine Science Center is issued by the Georgia Sea Grant Program and the Marine Extension Service of the University of Georgia on Skidaway Island (P. O. Box 13687, Savannah, Georgia 31406). It was established to provide dissemination of technical information and progress reports resulting from marine studies and investigations mainly by staff and faculty of the University System of Georgia. In addition, it is intended for the presentation of techniques and methods, reduced data and general information of interest to industry, local, regional, and state governments and the public. Information contained in these reports is in the public domain. If this prepublication copy is cited, it should be cited as an unpublished manuscript.

ACKNOWLEDGEMENTS

The authors would like to thank all those who participated in this study, both at sea and ashore. These include the following scientists, technicians and students.

Larry Atkinson	Mark Kelly
Carroll Baker	Greg McIntyre
Bill Chandler	Patrick O'Malley (at Skidaway)
Don Deibel	Gus Paffenhofer
Bill Dunstan	Carol Porter
Fran Gonsoulin	Joe Sands
Eileen Hofmann	Jim Singer
Jean Hosford	Kathie White

Of these, special thanks go to Carroll Baker for his invaluable assistance in keeping the CTD-Rosette system operational, to Eileen Hofmann for directing nutrient analysis and to Jean Hosford for temporarily taking over shipboard cooking responsibilities in addition to carrying out her other duties as a technician. Additional thanks go to Amy Edwards and Lynn Rubicam for their contributions in computer generated data graphics and data work up. Captain James Rouse, Lee Knight and mates Paul Glenn and Jim Walker and Gene Brogdon are sincerely thanked for their dedication and perserverance in completing this project. Mary Lou Neuhauser is thanked for filling in as ship's cook during the second half of this project.

Laboratory and dock space at Beaufort, North Carolina was generously provided by Duke University Marine Laboratory. Dick Barber and Eric Nelson are gratefully acknowledged for their assistance during our stay at DURL. Dan Perlmutter and Dan McIntosh provided drafting assistance and Paula Vopelak typed the text.

Funding for this research was provided by the U. S. Energy Research and Development Administration under Contract E(38-1)-889.

This report is published as a part of the Georgia Marine Science Center's Technical Report series issued by the Georgia Sea Grant Program under NOAA Office of Sea Grant #04-7-158-44126.

TABLE OF CONTENTS

	<u>Page</u>
Acknowledgements.	i
List of Tables.	iii
List of Figures	iv
Introduction.	1
Methods	4
Biogrids.	4
Hydrogrids.	6
Chemical and Physical Procedures.	7
CTD Data Acquisition.	8
CTD Data Processing	9
CTD Calibration	11
CTD Error Analysis.	16
Meteorological Conditions	19
Results	22
Horizontal Distribution of Temperature.	22
Horizontal Distribution of Salinity	23
Horizontal Distribution of Nutrients.	24
Vertical Distribution of Physical and Chemical Properties (Hydro Grids)	38
Hydro Grid I.	38
Hydro Grid II	39
Hydro Grid III(A-2)	39
XBT Grid III	40
Hydro Grid IV	40
Vertical Distribution of Physical and Chemical Properties (Bio Grids)	62
Bio Grid I.	62
Bio Grid II	63
Bio Grid III.	63
Bio Grid IV	64
T-S Plot.	85
Nitrate Vs. Phosphate	85
Salinity Vs. Silicate	85
Summary and Conclusions	89
List of References.	90
Appendix. Summary of Events: (OBIS V).	92

LIST OF TABLES

	<u>Page</u>
Table 1. OBIS V (Summer 1976).	1
Table 2. CTD/Data Flow: Shipboard acquisition to NODC submission.	10
Table 3. Salinity offset for OBIS V.	11
Table 4. Specifications for Plessey Model 9400 CTD system.	16
Table 5. Effects of depth on salinity for OBIS V data.	17
Table 6. Sources of salinity error due to the reported accuracy of the sensors and the salinity equation.	17

LIST OF FIGURES

	<u>Page</u>
Figure 1. Location of the study area.	2
Figure 2. Approximate current meter mooring locations during OBIS V.	3
Figure 3. Standard base grid for Onslow Bay, North Carolina . . .	5
Figure 4. Salinity offsets for Hydro I and Bio I.	12
Figure 5. Salinity offsets for Hydro/Bio II and aborted Hydro III's	13
Figure 6. Salinity offsets for Bio III and Hydro/Bio IV	14
Figure 7. Salinity offset for aborted Hydro V	15
Figure 8. Wind data (Cape Hatteras - July 1976)	20
Figure 9. Wind data (Cape Hatteras - August 1976)	21
Figure 10. Cruise tracks for Hydro Grids I, II and IV and XBT Grid III.	26
Figure 11. Cruise tracks for aborted grids	27
Figure 12. Surface temperature (Hydro Grids I, II and IV and XBT Grid III)	28
Figure 13. Bottom temperature (Hydro Grids I, II and IV and XBT Grid III)	29
Figure 14. Surface salinity (Hydro Grids I, II and IV)	30
Figure 15. Bottom salinity (Hydro Grids I, II and IV).	31
Figure 16. Surface nitrate (Hydro Grids I, II and IV).	32
Figure 17. Surface phosphate (Hydro Grids I, II and IV).	33
Figure 18. Surface silicate (Hydro Grid IV).	34
Figure 19. Bottom nitrate (Hydro Grids I, II and IV)	35
Figure 20. Bottom phosphate (Hydro Grids I, II and IV)	36
Figure 21. Bottom silicate (Hydro Grid IV)	37
Figure 22. Vertical distribution of temperature (Hydro Grid I) . .	42
Figure 23. Vertical distribution of salinity (Hydro Grid I). . .	43
Figure 24. Vertical distribution of sigma-t (Hydro Grid I) . . .	44

LIST OF FIGURES (continued)

	<u>Page</u>
Figure 25. Vertical distribution of nitrate (Hydro Grid I). . .	.45
Figure 26. Vertical distribution of phosphate (Hydro Grid I). . .	.46
Figure 27. Vertical distribution of temperature (Hydro Grid II) .	.47
Figure 28. Vertical distribution of salinity (Hydro Grid II). . .	.48
Figure 29. Vertical distribution of sigma-t (Hydro Grid II)49
Figure 30. Vertical distribution of nitrate (Hydro Grid II)50
Figure 31. Vertical distribution of phosphate (Hydro Grid II) . .	.51
Figure 32. Vertical distribution of temperature (Hydro Grid III(A-2)).52
Figure 33. Vertical distribution of salinity and sigma-t (Hydro Grid III(A-2)).53
Figure 34. Vertical distribution of phosphate and silicate (Hydro Grid III(A-2)).54
Figure 35. Vertical distribution of temperature (XBT Grid III). .	.55
Figure 36. Vertical distribution of temperature (Hydro Grid IV) .	.56
Figure 37. Vertical distribution of salinity (Hydro Grid IV). . .	.57
Figure 38. Vertical distribution of sigma-t (Hydro Grid IV)58
Figure 39. Vertical distribution of nitrate (Hydro Grid IV)59
Figure 40. Vertical distribution of phosphate (Hydro Grid IV) . .	.60
Figure 41. Vertical distribution of silicate (Hydro Grid IV). . .	.61
Figure 42. Cruise tracks for Bio Grids I, II, III and IV.65
Figure 43. Vertical distribution of temperature (Bio Grid I). . .	.66
Figure 44. Vertical distribution of salinity (Bio Grid I)67
Figure 45. Vertical distribution of sigma-t (Bio Grid I).68
Figure 46. Vertical distribution of nitrate (Bio Grid I).69
Figure 47. Vertical distribution of phosphate (Bio Grid I).70
Figure 48. Vertical distribution of temperature, sigma-t and salinity (Bio Grid II)71

LIST OF FIGURES (continued)

	<u>Page</u>
Figure 49. Vertical distribution of nitrate and phosphate (Bio Grid II).72
Figure 50. Vertical distribution of temperature (Bio Grid III) .	.73
Figure 51. Vertical distribution of salinity (Bio Grid III). .	.74
Figure 52. Vertical distribution of sigma-t (Bio Grid III) . .	.75
Figure 53. Vertical distribution of nitrate (Bio Grid III) . .	.76
Figure 54. Vertical distribution of phosphate (Bio Grid III) .	.77
Figure 55. Vertical distribution of silicate (Bio Grid III). .	.78
Figure 56. Vertical distribution of temperature (Bio Grid IV). .	.79
Figure 57. Vertical distribution of salinity (Bio Grid IV) . .	.80
Figure 58. Vertical distribution of sigma-t (Bio Grid IV). . .	.81
Figure 59. Vertical distribution of nitrate (Bio Grid IV). . .	.82
Figure 60. Vertical distribution of phosphate (Bio Grid IV). .	.83
Figure 61. Vertical distribution of silicate (Bio Grid IV) . .	.84
Figure 62. T-S plot (OBIS V)86
Figure 63. Plot of nitrate Vs. phosphate87
Figure 64. Plot of salinity Vs. silicate88

INTRODUCTION

This data report is the third in a series on work in Onslow Bay, North Carolina (Atkinson et al., 1976a, b) (Figure 1). It, like the earlier reports, is intended to document the chemical and physical data obtained. The report covers cruises OB5-OB9 of the Onslow Bay project. These cruises comprise Onslow Bay Intrusion Study No. 5 (OBIS V) and were made aboard the R/V BLUE FIN during the summer of 1976 (Table 1). The hydrographic data sets are available from the National Oceanographic Data Center (NODC).

Table 1. OBIS V (Summer 1976)

Project Leg	Date	Cruise Number
HYDRO/BIO I	14-18 July	OB5
HYDRO/BIO II	21-23 July	OB6
HYDRO III (aborted three times)	28 July-2 August	OB7
XBT/BIO III	4-6 August	OB7
HYDRO/BIO IV	14-16 August	OB8
HYDRO V (aborted)	18 August	OB9

OBIS V

The objective of OBIS V like that of OBIS II was to collect temperature, chemical and biological data which could later be correlated with data recorded by twelve current meters and two thermographs (deployed by North Carolina State University) which were concurrently operative at seven locations in the study area (Fig. 2). No attempt will be made at this time, however, to correlate our data to these related records nor will any of the

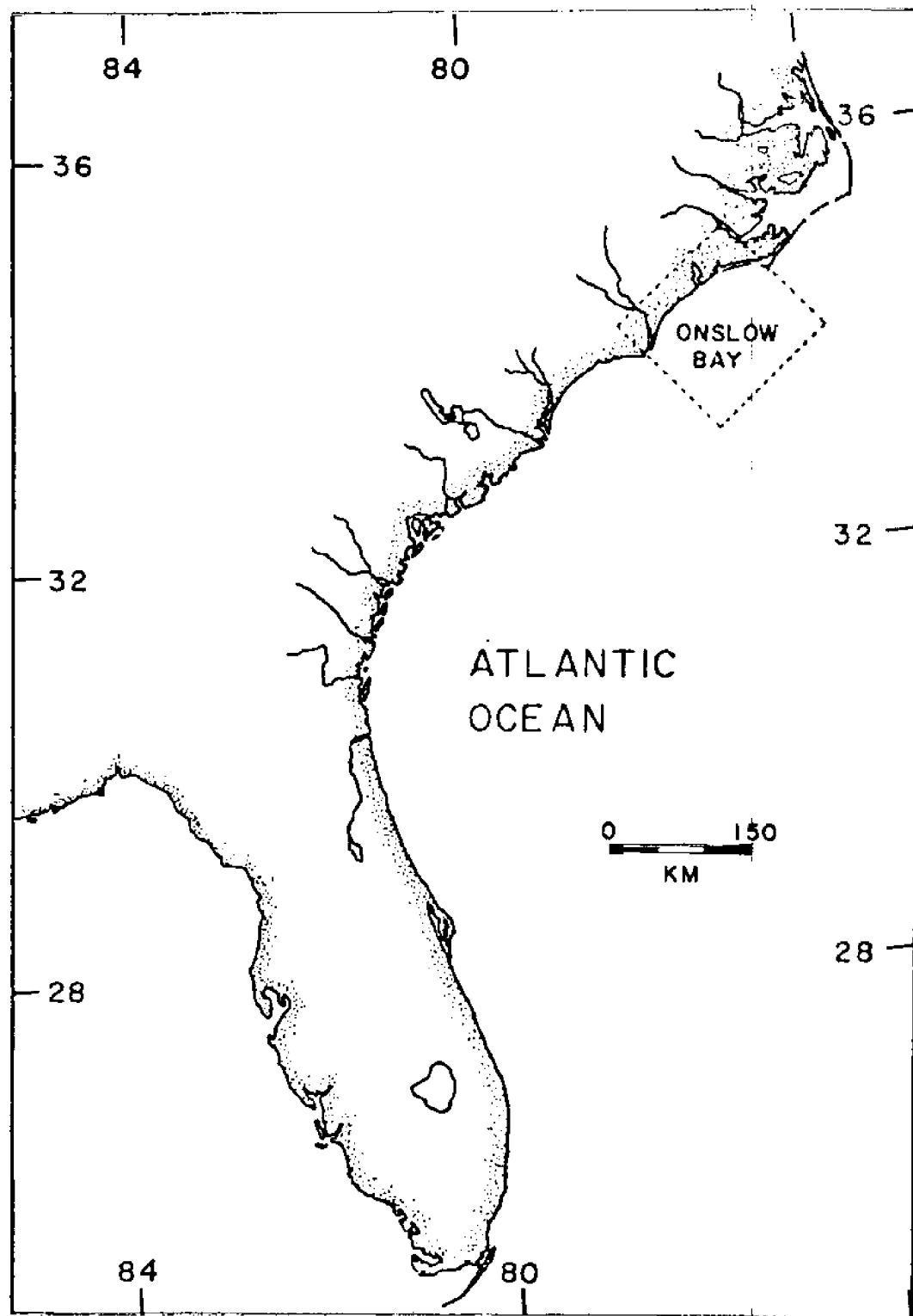


Figure 1. Location of the study area

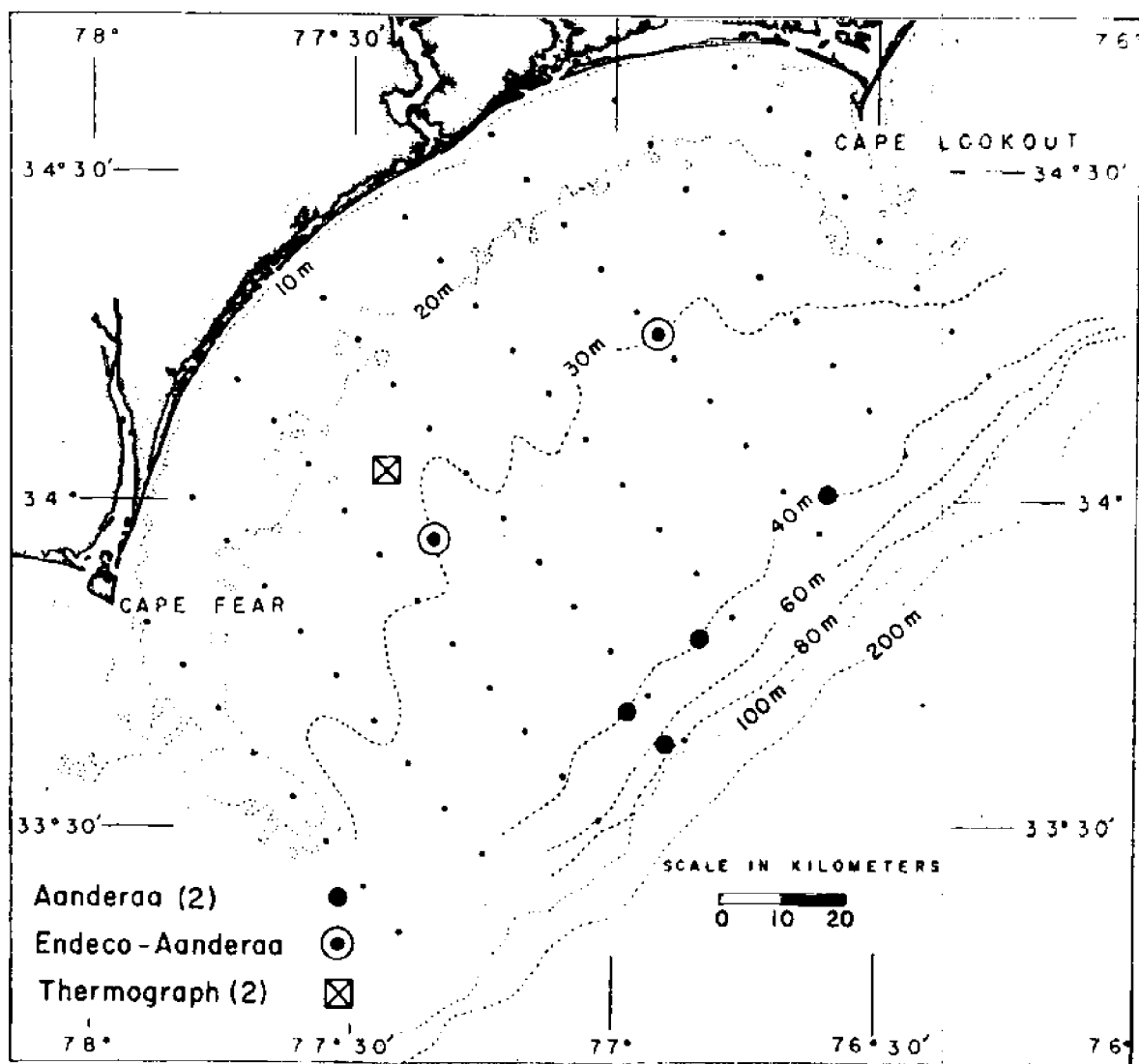


Figure 2. Approximate current meter mooring locations during OBIS V.

biological data be presented in this text. The current meter and biological data will appear in separate reports edited by Dr. L. Pietrafesa (N. C. State University) and Drs. W. Dunstan and G.-A. Paffenhofer (Skidaway Institute of Oceanography) respectively.

METHODS

The study area was assigned a standard base grid made up of eight onshore-offshore transects (Fig. 3). This was identical to the grid reported in earlier Onslow Bay work (Atkinson *et al.*, 1976a, b) except that one additional offshore station was on occasion added to the transects. The same permanent station numbers are used. Each alternating sampling grid (hydro or bio) was made up of some combination of the base grid's onshore/offshore transects, depending on the previously observed temperature structure, and/or the time lapse between cruises through the grid area.

The selected hydrogrid always represents a trade-off between fineness of scale and the achievement of synopticity. With this in mind alternate onshore/offshore transects were omitted, thereby decreasing the along-shore scale from that of our earlier work. However, it was felt that this would not significantly alter our view of the larger scale intrusion phenomenon we were investigating and that the reduced sampling time for a circuit of the Bay would generate, in number, more surveys. This in turn would permit us to better track a single intrusion from beginning to end (this advantage, however, was lost by such unscheduled factors as bad weather, equipment malfunction, and ship breakdown).

Biogrids

As originally conceived, a biological grid would detect changes in various parameters induced by the movement of intruding fronts and the variance of light conditions with time. It was composed of five stations

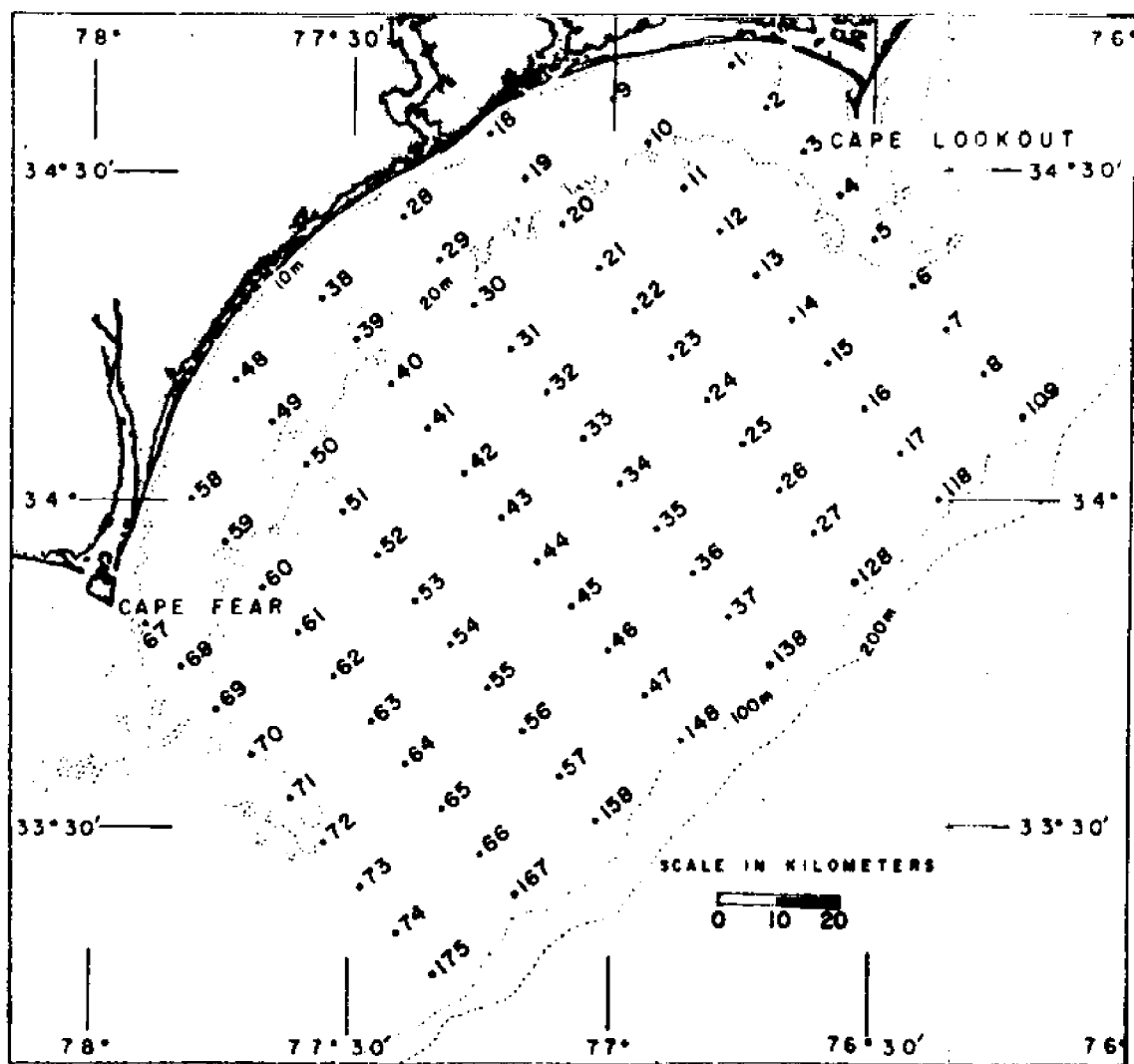


Figure 3. Standard base grid for Onslow Bay, North Carolina.

along one onshore/offshore transect which were selected for intensive sampling because of their proximity to an apparent intrusion core. Samples would be taken offshore and inshore of the intrusion core and in the core itself. The cruise track would go back and forth from end station, to center station, to opposite end station, generally sampling at three hour intervals over a 24 hour span. This would result in four complete transects of the grid with the center station being sampled four times. The two immediately adjacent stations would be less intensively sampled without regard to a specific time interval as the ship cruised to a center or end station. However, for the present work, though we started with the above format in mind, the biogrids ultimately varied from one another in the time between stations, the total time allotted, the number of stations sampled, and the number of repetitions of the selected cruise tracks. The variations were influenced by such factors as weather conditions and ship performance, etc.

Typically, at a bio station a CTD-Rosette cast and a zooplankton net tow were made. The sampling depths were determined by analysis of the temperature profile. If a thermocline was present, samples were taken at the surface, just above or below the thermocline, at the bottom and occasionally at other random depths. If no thermocline was present just surface and bottom samples were taken. Water samples were taken for the analysis of salinity, nitrate, phosphate, silicate, oxygen, in vivo chlorophyll, particle size, phytoplankton cells, zooplankton, and particulate carbon.

Hydrogrids

A hydrographic grid was designed to sample the entire Bay to obtain an updated look at the distribution of properties both preceding and following the biological sampling period. Such grids were generally on

the order of 24 to 42 hours in duration. Along a hydrographic grid track, either CTD-Rosette casts or XBT firings and Niskin bottle casts were made at all stations. Niskin sampling depths were determined after the temperature structure was obtained either from the CTD or XBT, and samples were taken near the surface, just above or below the thermocline, at the bottom and occasionally at other random depths. Samples were taken for analysis of salinity, nitrate, phosphate, silicate, oxygen and in vivo chlorophyll and occasionally for extracted chlorophyll, particle size and phytoplankton cell analysis.

Chemical and Physical Procedures

Salinity samples were analyzed conductometrically using a Plessey portable laboratory salinometer. The values so obtained were used to calibrate the Plessey model 9400 CTD system. Because of laboratory space problems aboard the research vessel, oxygen analysis was delayed until we returned to port after each cruise. The Winkler method was used. However, post project experiments have indicated that the samples were highly susceptible to thermal effects. Consequently, no oxygen values are presented. Temperature was determined by deep sea reversing thermometers, XBT's and the CTD system.

After collection, the nutrient samples were immediately frozen in polyethylene bottles and stored in the dark until thawed and analyzed ashore. Colorimetric determinations of nutrient concentrations were made with a Bausch and Lomb Spectronic 88 Spectrophotometer with a sample sipper. Silicate concentration was determined by the method of Mullin and Riley (1955) as modified by Strickland and Parsons (1965), and phosphate concentrations were determined by the method of Murphy and Riley (1962). Nitrate was determined by the cadmium column reduction technique as modified by Gardner et al. (1976).

CTD (Conductivity/Temperature/Depth) Data Acquisition

The CTD unit consisted of a Plessey model 9400 CTD sensor system with a model 8400 Digital Data Logger and Kennedy model 1600 incremental magnetic tape recorder for data acquisition and storage. A redundant 'XYZ' plot was made of all casts using a Hewlett-Packard model 7046A X-Y Recorder which was calibrated with a precision 10VDC source. The CTD sensor-unit was mated to a General Oceanics model 1015 Mark 5 Rosette multi-bottle array for water sampling. The Rosette was equipped with 1.7 and 5.0 liter Niskin bottles.

Digitized data was collected only during descent through the water column (generally less than 50 m deep) as the CTD was lowered at 15 m/min on single conductor cable. All three parameters (C, T and D) were sampled once each 229 milliseconds: every 6 cm at the 15 m/min lowering rate. For primary calibration of temperature and salinity a Niskin bottle equipped with a protected deep sea reversing thermometer was tripped after a three minute equilibration period at the maximum sample depth. Other water samples were collected during ascent following examination of the downcast temperature profile. Typical station time was less than 15 minutes.

The acquisition of CTD data during the downcast and water samples during the upcast creates some problems that are difficult to solve. The factors that come into play are:

- 1) The sensors are located at the bottom of the sub-surface unit to maximize response during the downward motion. During upward motion the CTD sensors lie in the wake of the Rosette. Thus CTD data is of higher quality during the downcast.
- 2) It is generally felt that water samples must be taken during the upcast. If they are taken during the downcast the surface samples may be subjected to dilution by deeper waters.

- 3) Differential horizontal advection may alter the coherence of downcast CTD data vs. upcast water sample data. However, since gradients in nutrients are typically quite low the minor advective motions during the time of a station cause negligible mismatch of nutrient data.

CTD Data Processing

The CTD plots were logged and stored with their respective station sheets. Data had to be manually digitized from some of these (HYDRO/BIO I and II) because of magnetic tape recording problems. The remainder of the data were recorded on tape and extracted and processed according to the flow scheme shown in Table 2. The flow scheme is essentially that described by Scarlet (1975). Computations and data manipulations were performed on a CDC CYBER 70.

MAGREAD converts binary coded data to decimal and CTDUNIT converts decimal units to engineering units. LAGFILT treats the data for the temperature lag of the temperature sensor and coarse filters the data for noise. Then, SIGSALP calculates uncorrected sigma-t and salinity values. At this stage, salinity and temperature offset corrections are made from the primary calibration data. Then flow is resumed by repeating SIGSALP with the added correction factors. DLATCH deletes lines with decreasing or repeated depths due to ship roll and CTDAVE presents the data in average one meter increments. NODCFO converts the data to NODC format and NODMER merges additional data (i.e., nutrients, weather, latitude, longitude, etc.) for submission to NODC. CEMLIST calculates specific volume anomaly, oxygen saturation and apparent oxygen utilization (from the International Oceanographic Tables, 1973), the distance between successive stations, and reads all other data and formats all data for presentation in a technical report. This final product

Table 2. CTD/Data flow: Shipboard Acquisition to NODC submission.

Data Source/Disposition	Program	Data File
Tape from Data Logger	MAGREAD (Converts binary coded data to decimal)	
		BIRANG
	CTDUNIT (Converts decimal units to engineering units)	
		LAG
	LAGFILT (Course filter and temperature lag)	
Primary calibration from bottle casts		CAL
	SIGSALP (Calculates sigma-t and salinity)	
		LATCH
	DLATCH (Removes decreasing and repeated depths)	
		CTDATA
	CTDAVE (One meter averaged data)	
		AVE
	NODCF0 (Converts to NODC format)	
		NODC + HEAD
	NODMER (Merges NODC data with Headers and chemical data)	
Submission to NODC		NODCFNL
	CEMLIST (Calculates specific volume anomaly, oxygen utilization, etc.)	
		TECHNICAL REPORT

is stored on magnetic tape in our computer system and all data (i.e., CTD, XBT, chemical etc.) are available through NODC.

CTD Calibration

The data derived from the CTD sensor system is critical to the correct interpretation of the oceanographic processes. To insure the highest quality data an extensive calibration scheme was performed.

The CTD system was calibrated against deep bottle casts in mixed layers: this was the only way to be sure the sensors and the bottles were both sampling the same water. However, since a mixed layer was not always observed, a comparison could not be made at every station. Consequently, the resulting mean offset for the mixed layer salinity data of each leg of the project was used for each entire data set. This offset decreased through the five week study period and is tabularized below (Table 3) and presented graphically in Figures 4 through 7. No temperature offset was made since the CTD temperature sensor agreed with the protected reversing thermometers within the range of accuracy of the two ($\pm .02^{\circ}\text{C}$). Likewise, no depth offset was necessary. The XBT system was found to agree with reversing thermometers to within $\pm .05^{\circ}\text{C}$ when compared during Hydro I.

Table 3. Salinity offset for OBIS V.

Project Leg	‰ Offset	Stand. Dev.	Data Source
HYDRO I (c.s. 1-26)	+ .138	+ .030	XYY' Plotter
(c.s. 32-36)	+ .333*	+ .023	"
BIO I	+ .099	+ .008	"
HYDRO/BIO II	+ .090	+ .017	"
ABORTED HYDRO III	+ .101	+ .022	Magnetic Tape
BIO III	+ .073	+ .026	"
HYDRO/BIO IV			
(c.s. 1-31)	+ .064	+ .021	"
(c.s. 32-42)	+ .019	+ .008	"
ABORTED HYDRO V	+ .068	+ .009	"

*The sharp increase in offset during HYDRO I came after field repairs of the CTD system.

c.s. = consecutive station.

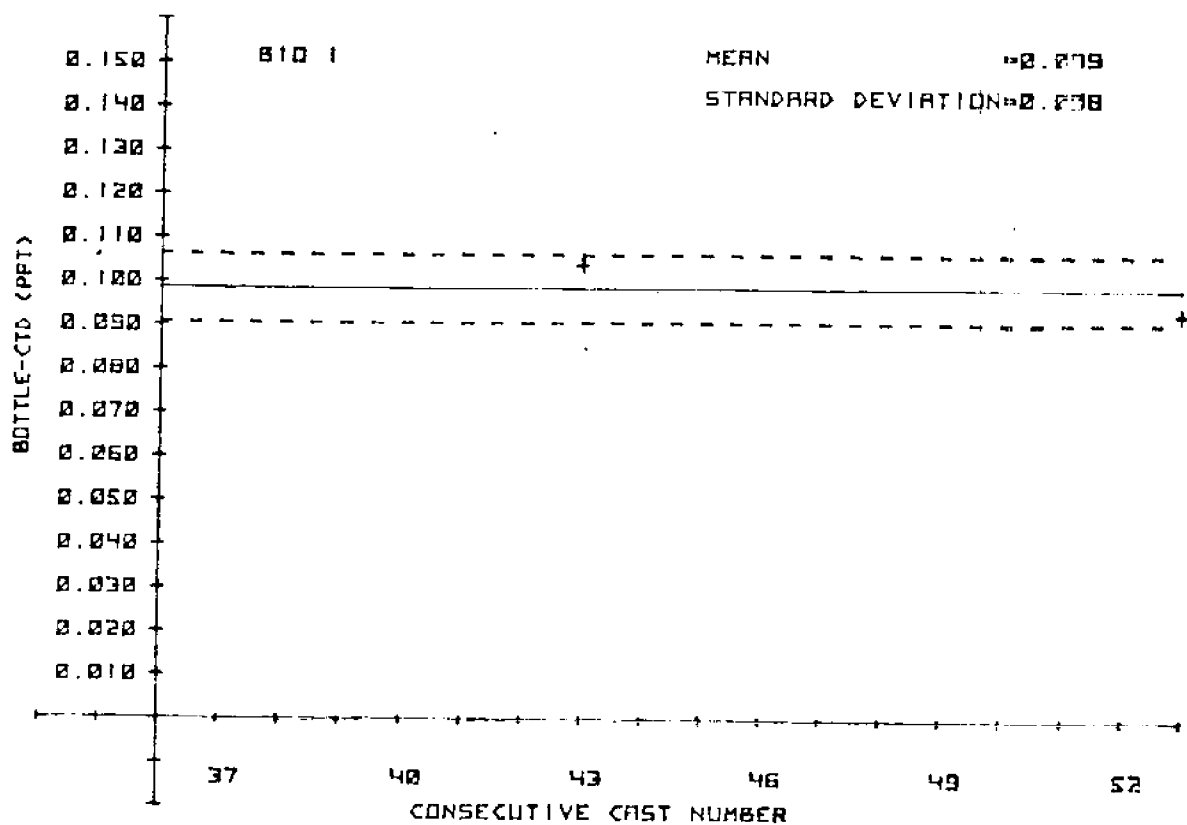
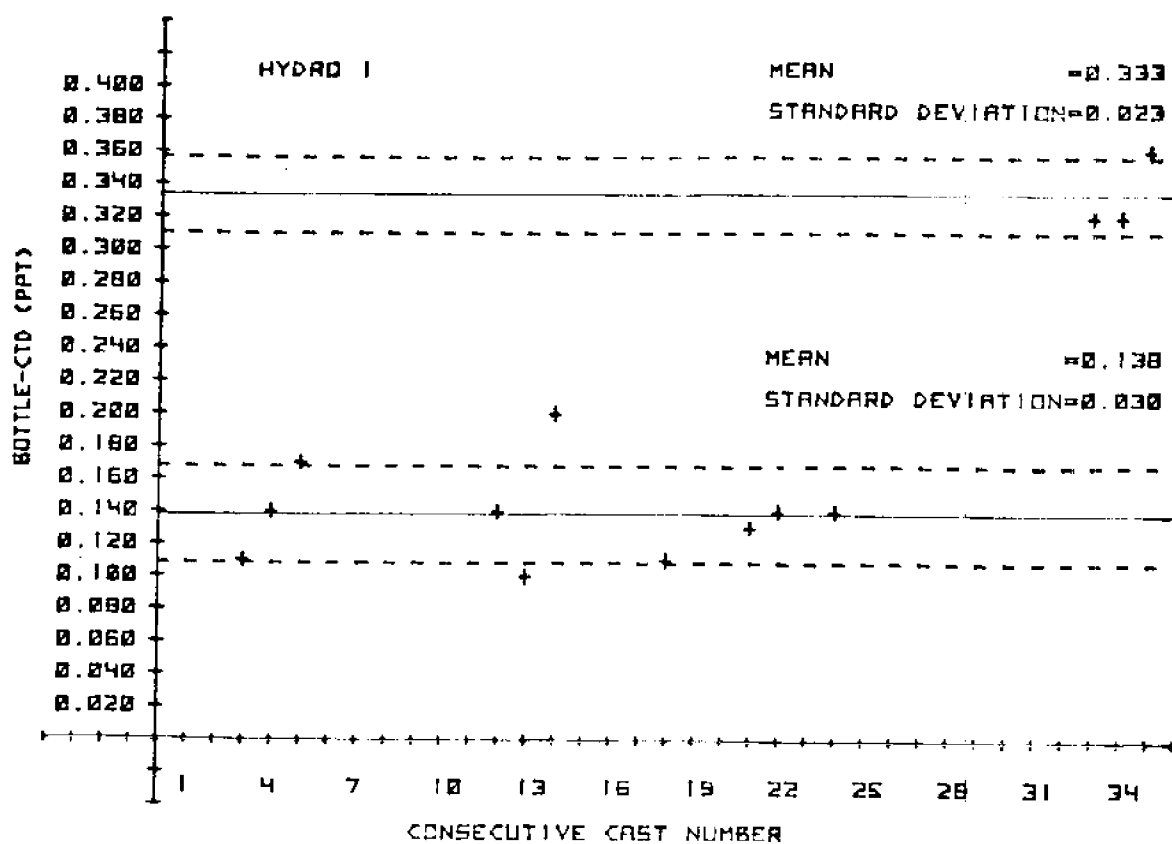


Figure 4. Salinity offsets for Hydro I and Bio I (— mean offset; -- standard deviation).

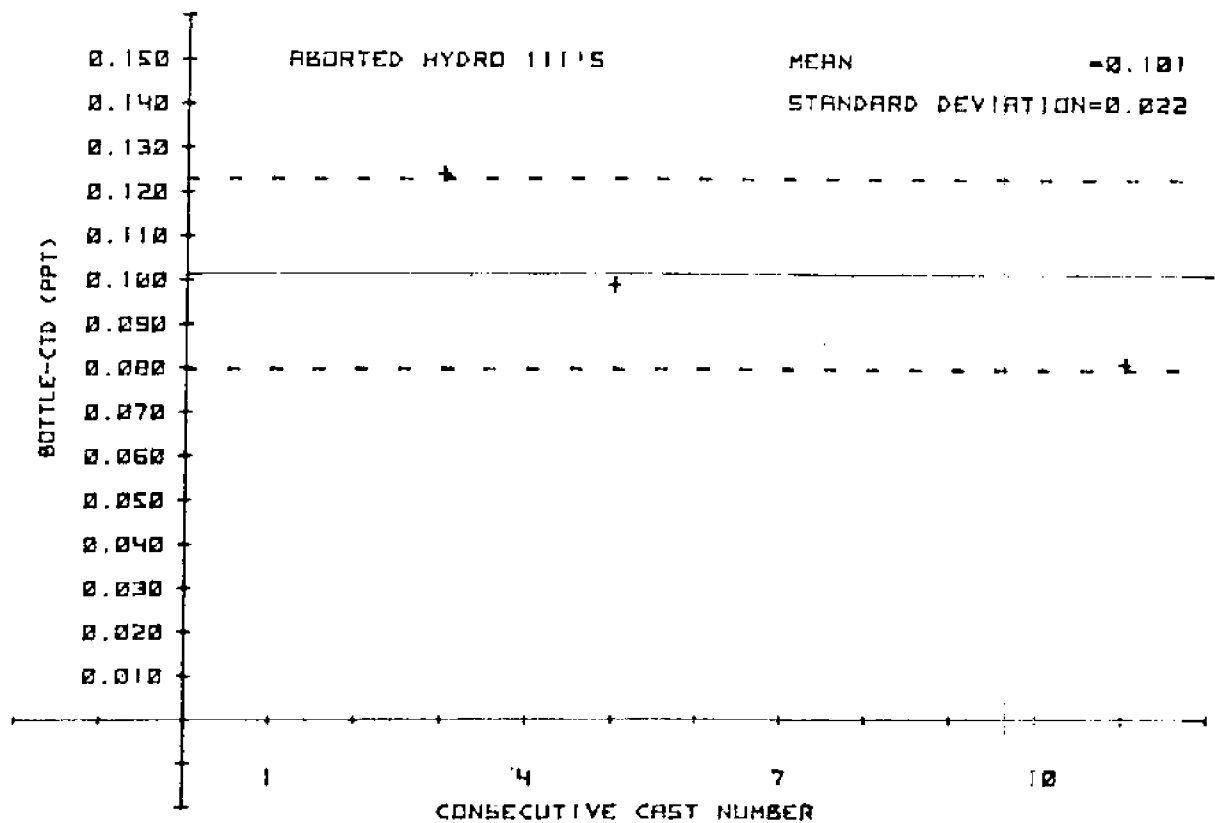
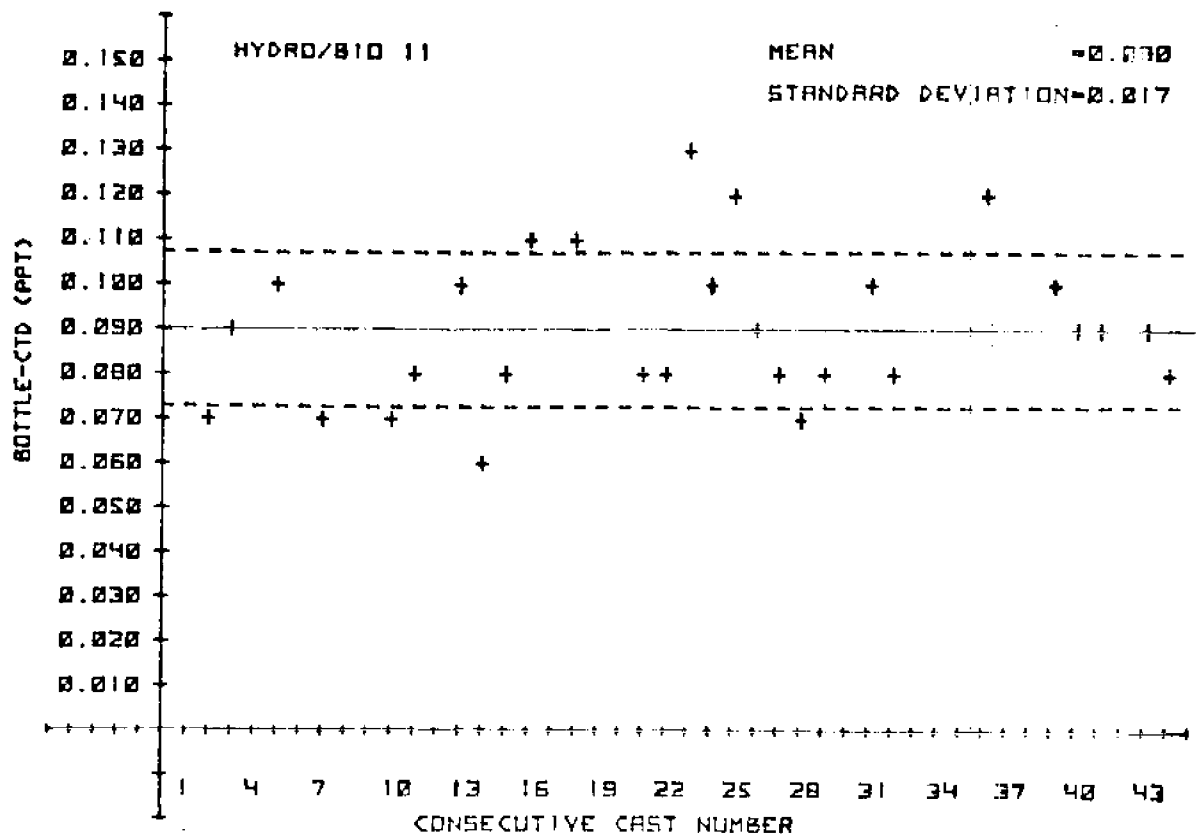


Figure 5. Salinity offsets for Hydro/Bio II and aborted Hydro III's
(— mean offset; -- standard deviation).

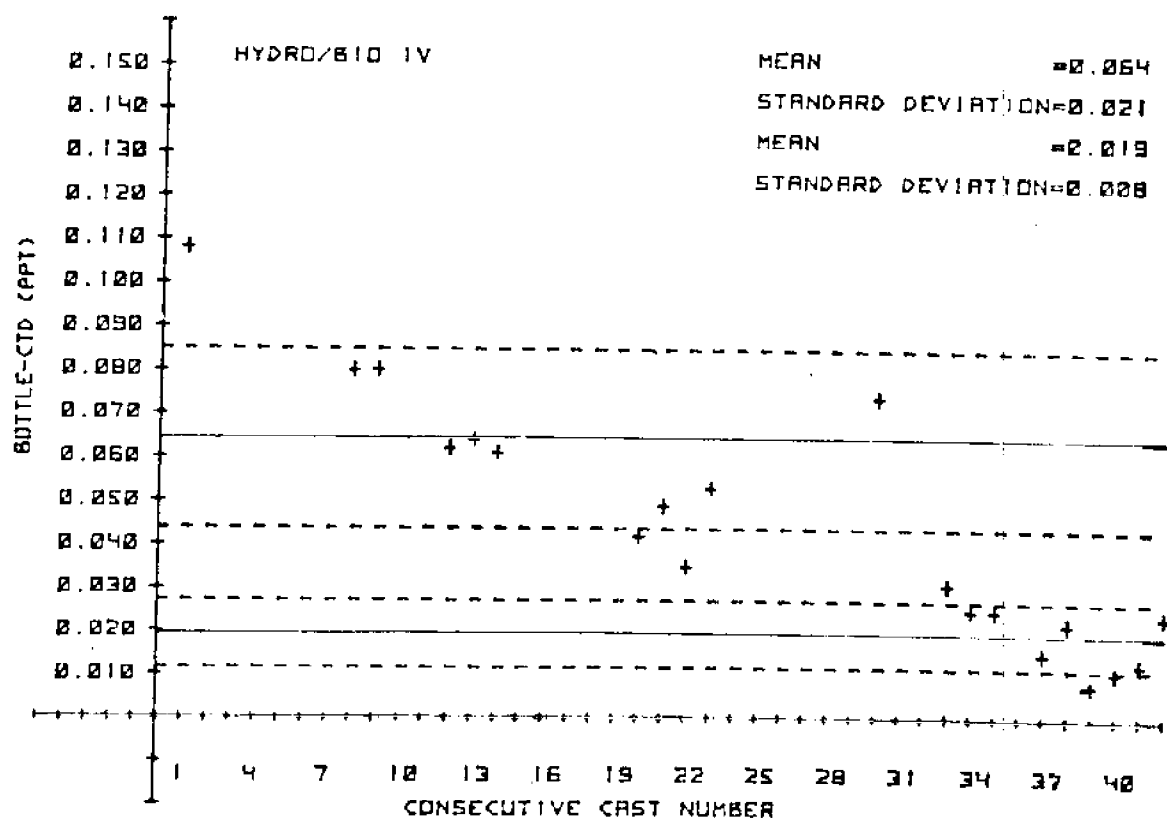
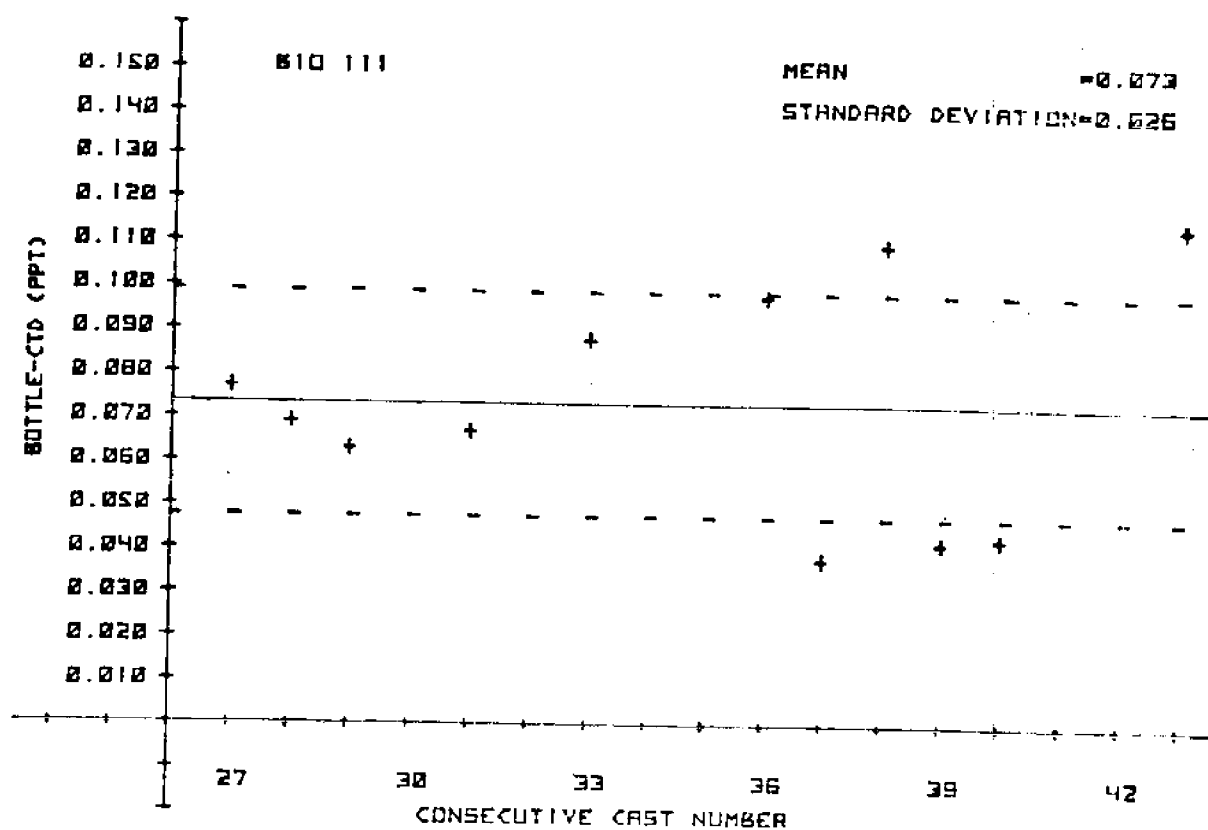


Figure 6. Salinity offsets for Bio III and Hydro/Bio IV (+ mean offset; -- standard deviation).

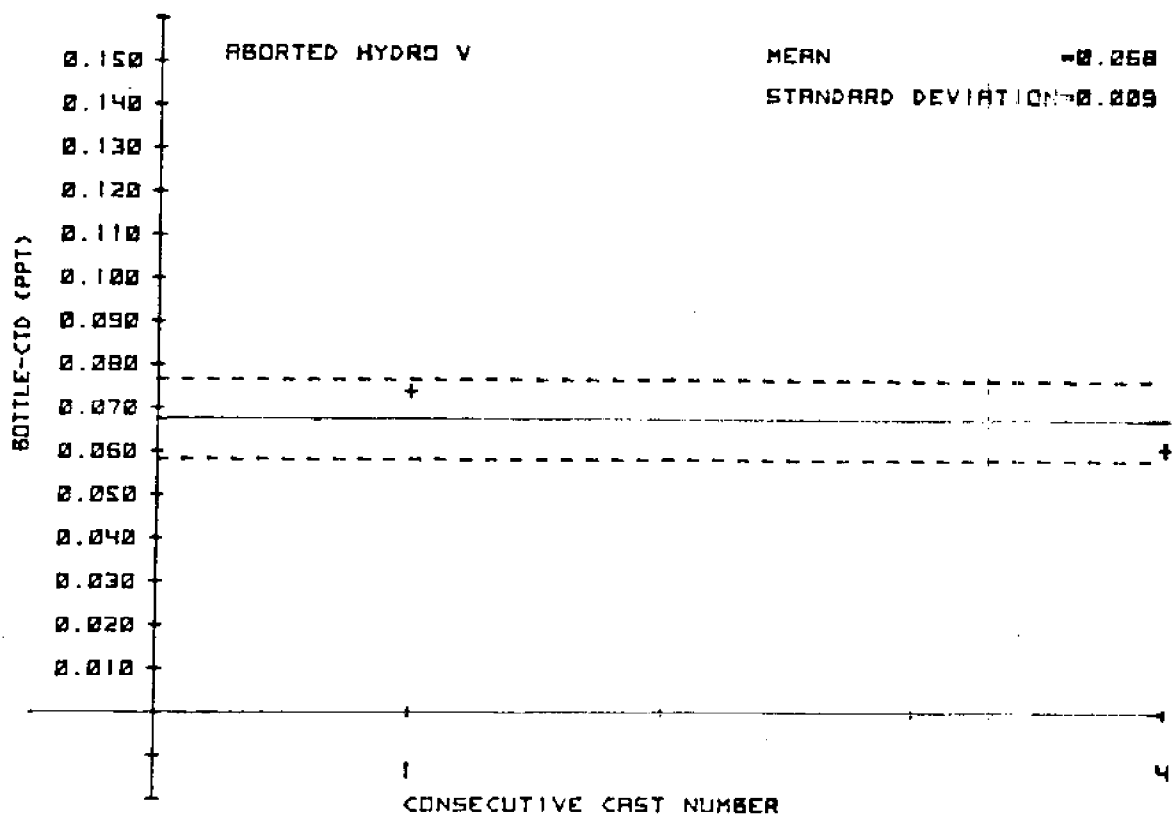


Figure 7. Salinity offset for aborted Hydro V (— mean offset; -- standard deviation).

CTD Error Analysis

The Plessey model 9400 CTD system has the following rated accuracy, resolution and time constants (Table 4).

Table 4. Specifications for Plessey model 9400 CTD system.

	Conductivity	Temperature	Depth
Accuracy	± 0.03 mmho/cm	$\pm 0.02^{\circ}\text{C}$	± 1.5 m
Resolution	0.0001 mmho/cm	0.0001 $^{\circ}\text{C}$	0.0012 m
Time Constant	0.1 sec	0.35 sec	0.1 sec

Since salinity was not measured directly it had to be calculated from the above parameters. For this work, salinity was determined by the equation of Knowles (1973) for shallow water ($p \approx 0$) using the coefficients of a third order polynomial he determined for Reeburgh Normal water ($C1 = 19.369^{\circ}/\text{oo}$) as a means of estimating $C(35, t, o)$:

$$C(35, t, o) = 29.03862 + 0.86024t + 0.46931 \times 10^{-2}t^2 - 0.27022 \times 10^{-4}t^3 \text{ and } C(s, t, p) \approx C(s, t, o) \\ \text{and } R_t = C(s, t, o)/C(35, t, o).$$

Then, from the International Oceanographic Tables (1966):

$$\Delta_{15} = R_{15} - R_t \text{ or } R_{15} = \Delta_{15} + R_t \\ \text{where } \Delta_{15} = 10^{-5} R_t (R_t - 1) (t - 15) \{ 96.7 - 72.0 R_t + 37.3 R_t^2 - (0.63 + 0.21 R_t^2) (t - 15) \} \text{ and } S^{\circ}/\text{oo} = -0.08996 + 28.29720 R_{15} + 12.80832 R_{15}^2 - 10.67869 R_{15}^3 + 5.98624 R_{15}^4 - 1.32311 R_{15}^5.$$

The absolute accuracy of this method is not known. However, for the temperature and salinity range observed during this study (16 - 29°C , 34.5 - $36.5^{\circ}/\text{oo}$) this expression was found to result in calculated salinities deviating $-0.010 \pm .002^{\circ}/\text{oo}$ from a table of measured experimental values reported by Jaeger (1973).

Since this equation ignores the influence of pressure on the conductivity sensor, a table of pressure effects on salinity has been compiled (Table 5). One hundred fifty-six of the 164 casts were made to depths less than or equal to 40 meters for which it has been estimated that the pressure effect could increase the calculated salinity by only $+0.014^{\circ}/\text{oo}$ (Bradshaw and Schleicher, 1965). The effect on the deepest cast (55 meters) has been calculated to be $+0.020^{\circ}/\text{oo}$.

Table 5. Effects of depth on salinity for OBIS V data.

Temp. ($^{\circ}\text{C}$)*	$^{\circ}/\text{oo}$	Depth (m)	$^{\circ}/\text{oo}$ Effect
25.00	35.50	10	$+0.003$
25.00	36.00	20	$+0.006$
23.50	36.00	30	$+0.010$
22.00	36.00	40	$+0.014$
19.50	36.00	50	$+0.018$
19.00	36.00	55	$+0.020$

*Averaged over data set or maximum temperature listed by Bradshaw and Schleicher, 1965.

Other sources of error are attributable to the reported accuracy of the conductivity and temperature sensors and are summarized below (Table 6).

Table 6. Sources of salinity error due to the reported accuracy of the sensors and the salinity equation.

Parameter	Maximum Error
Conductivity	$\pm .023^{\circ}/\text{oo}$
Temperature	$\pm .016^{\circ}/\text{oo}$
Depth	$\pm .014^{\circ}/\text{oo}$ (95% of casts)
Equation*	$\pm .002^{\circ}/\text{oo}$
Total	$+ .055$ to $-.041^{\circ}/\text{oo}$

*The negative component of the equation error is not included because it is compensated for by an offset factor added to the data set.

The total error reported above is applicable to all data recorded on magnetic tape and does not consider the digitizing errors which may have occurred for HYDRO/BIO's I and II. We estimate that temperature was digitized to an accuracy of $\pm .005^{\circ}\text{C}$ and conductivity to $\pm .01 \text{ mho/cm}$. Such accuracy could result in additional salinity errors of $\pm .005^{\circ}/\text{oo}$ and $\pm .009^{\circ}/\text{oo}$, respectively.

Actually, the largest standard deviation of all the mixed layer samples taken for salinity calibration purposes implies an accuracy, after offset, of $\pm .030^{\circ}/\text{oo}$. This value is probably a more realistic measure of the quality of the data set except in strong thermoclines ($>1^{\circ}\text{C}$ change/m) than the composite maximum error reported above for the sensor package.

METEOROLOGICAL CONDITIONS

Wind data from Cape Hatteras, North Carolina¹ are presented in Figures 8 and 9. These data are derived from the monthly summaries for July and August 1976 (U. S. Department of Commerce, July and August 1976) and are plotted in GMT at six hour intervals.

The data show that the winds were generally southwesterly during July 1976 with three brief (2-3 days or less) periods of northeasterly winds. The average wind velocity for July was 4.4 meters/second. In August, periods of both northeasterly and southwesterly winds were observed. These were separated by a period of variable winds which included the highest observed velocities (10.7 meters/second). This variable direction and highest velocity period coincided with the passage of Hurricane Belle 87 kilometers southeast of Cape Hatteras (141 kilometers east of Cape Lookout) at 1300 GMT on 9 August. The closest approach of the eye of the hurricane to the study area came at 1000 GMT on 9 August when it was 91 km east of the shelf break (200 m isobath) in the northeastern sector of the Bay along the 34°00.0" north latitude line. The average wind velocity for August was 3.9 meters/second.

The average high and low air temperatures for the entire study period were 28.9°C and 21.7°C respectively. Meteorological data were also collected by the ship's crew at each station. These additional data are available through NODC.

¹Cape Hatteras lies 116 kilometers northeast of Cape Lookout.

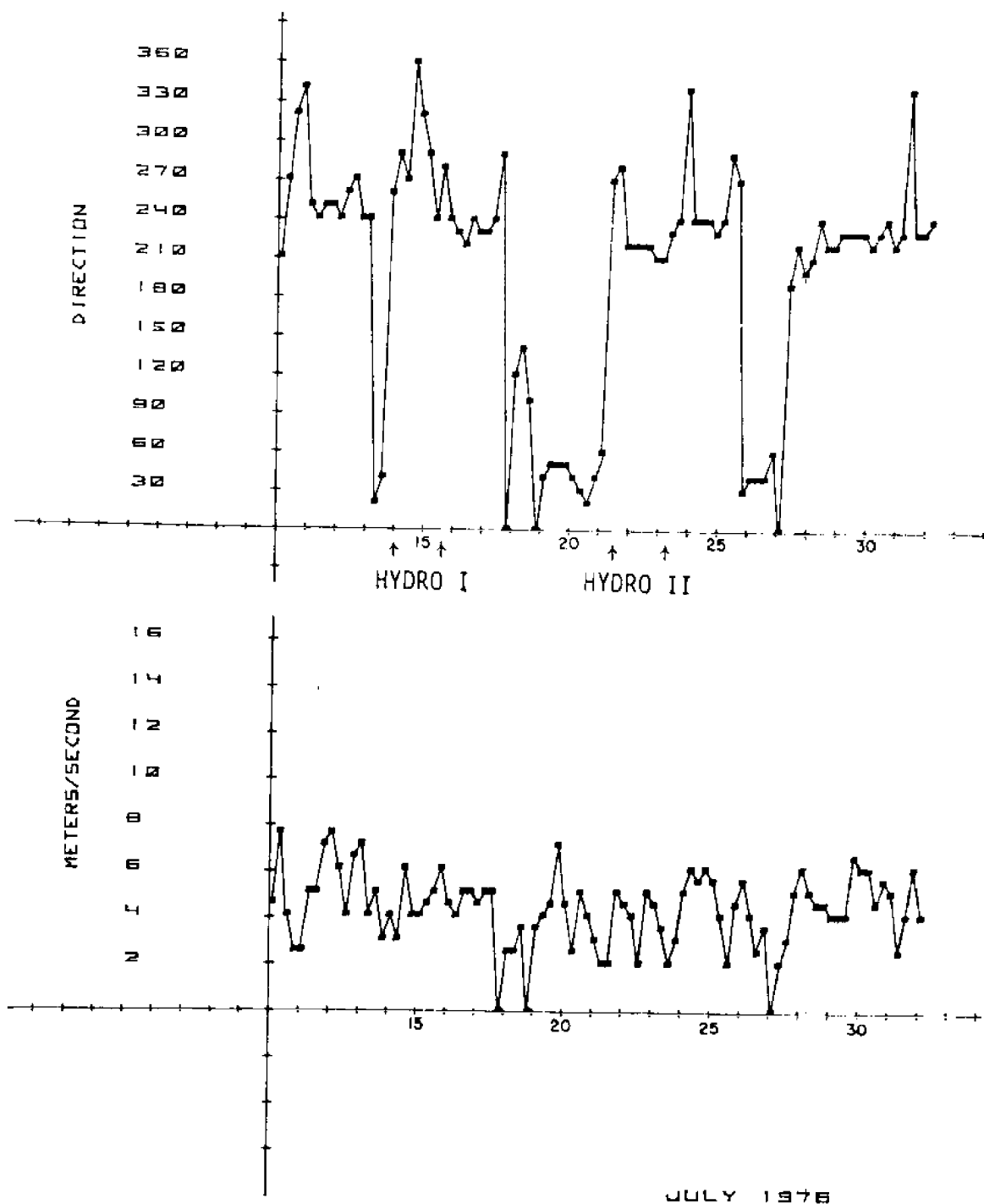


Figure 8. Wind data (Cape Hatteras - July 1976).

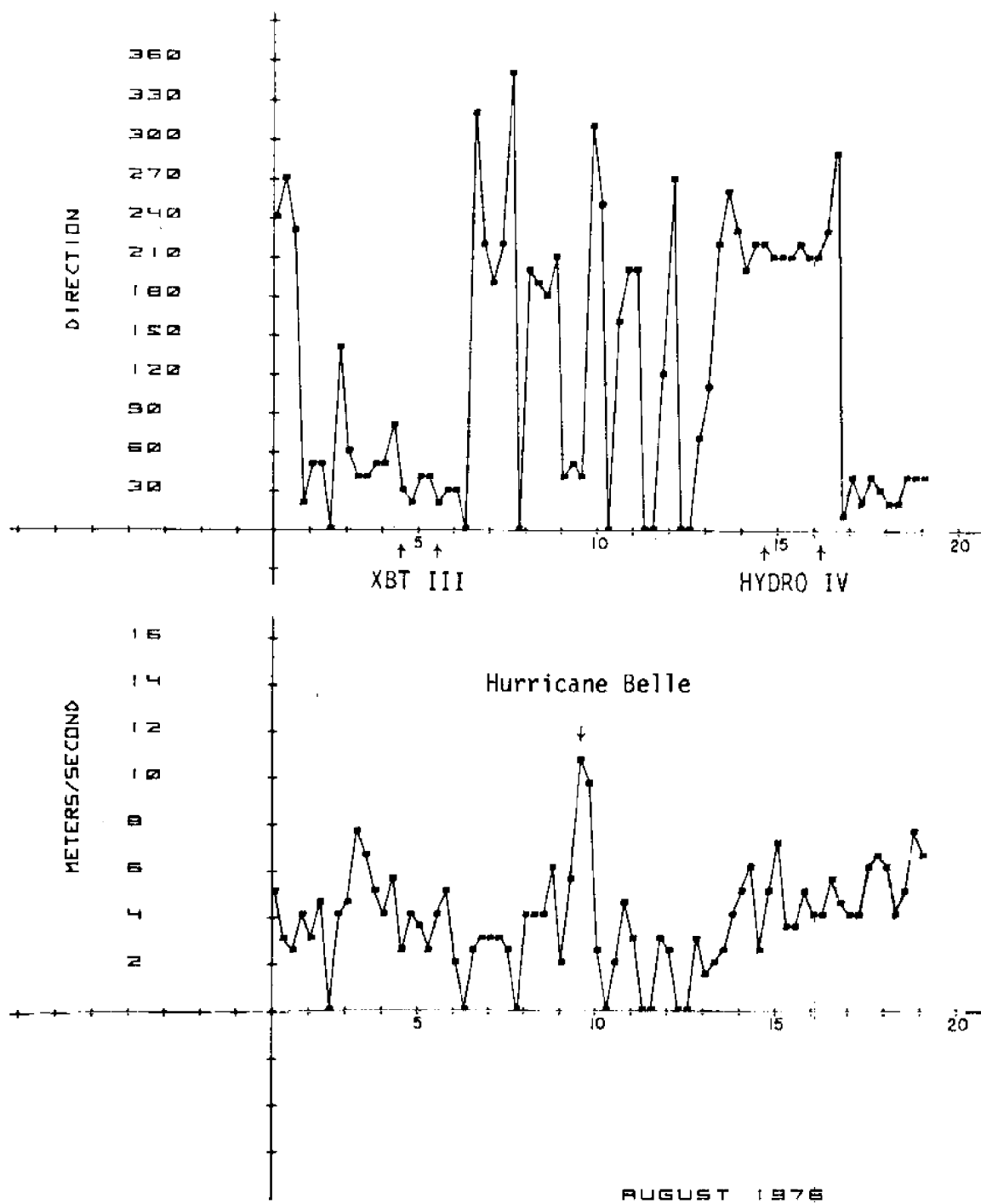


Figure 9. Wind data (Cape Hatteras - August 1976).

RESULTS

Horizontal Distribution of Temperature

The cruise tracks for Hydro Grids I, II and IV and XBT Grid III are shown in Figure 10. All subsequent surface and bottom horizontal plots are derived from data collected along these cruise tracks. Several cruises were aborted (Figure 11) and no horizontal plots are presented.

Figures 12 and 13 show the surface and bottom temperature distribution throughout the Bay during each grid. These plots are derived from both CTD and XBT data sets. Surface temperatures are generally taken from depths of 1 to 2 meters below the surface and bottom temperature either from depths 2 to 3 meters above the bottom as indicated by the shipboard fathometer system for CTD data or at the bottom for XBT data.

Surface temperatures ranged from a low of 25.5°C to a high of 29.0°C over the course of the study period. The lowest temperatures were observed off Cape Fear and the highest temperatures were found offshore and parallel to the shelf break. Some surface structure is apparent in the temperature plots for regions off Cape Fear and in Figure 12(d) one can see the thermal wall of the Gulf Stream.

Figure 13 shows the bottom temperature structure observed during the study period. The movement of colder water onto the shelf and/or the appearance of cold cores is evident in all plots. The early stage of an intrusion event is shown in Figure 13(a) with waters as low as 21.5°C having moved onto the shelf in the southernmost offshore corner. This is the same region in which intrusions were observed to move onto the shelf in our earlier work (Atkinson et al., 1976). In Figure 13(b) there is evidence of an intrusion moving onto the shelf in this same region. There is also evidence of another intrusion which has moved shoreward and

has been isolated. It is defined by the 23.0°C isotherm. Conceivably, this older and warmer core could be a stranded portion of the intrusion first observed in Figure 13(a) (the time lapse between the two plots is roughly seven days). Current meter data collected by Dr. L. Pietrafesa will help in ascertaining whether or not this is in fact the case.

In Figure 13(c) another intrusion is stranded on the shelf. It is a different intrusion than that shown stranded in Figure 13(b). This conclusion is based on the lower temperatures exhibited (21.5 vs. 23.0°C). Also, it is unlikely that this core is related to the one shown just moving onto the shelf in Figure 13(b) since still another intrusion was observed moving onto the shelf during an aborted hydro grid made between these two (Figure 32, page 52).

In Figure 13(d) there is an old intrusion isolated on the shelf as indicated by the 23.0°C core. This could be the same core as depicted in Figure 13(c) although it is unlikely. Actual confirmation should come from the current meter data. Also in this figure, there is clear evidence of the movement of deeper Gulf Stream waters onto the shelf,

Horizontal Distribution of Salinity

Horizontal salinity plots are given for Hydro Grids I, II and IV. Since no hydrography was done during XBT Grid III no salinities are available for that grid. Surface samples were taken within 1 to 2 meters of the surface and bottom samples were taken generally within 2 to 3 meters of the bottom as indicated by the fathometer. The data presented are a composite of that which was collected with the CTD system as calibrated against bottom mixed layer water samples, and near surface and bottom bottle samples taken when the CTD system was inoperable.

The surface salinity in Onslow Bay ranged from a low of $34.40^{\circ}/\text{oo}$ to a high of $36.10^{\circ}/\text{oo}$. In Figure 14(a) and 14(b) low salinity waters

appear to be moving into the Bay from the southwest (possibly emanating from the vicinity of Cape Fear and the mouth of the Cape Fear River). Both observations were in part during or following periods of southwesterly winds (Figure 8). Also, in Figure 14(a) other low salinity waters appear to be advecting from the northeast (Cape Lookout). These combined observations suggest a complex surface circulation in the Bay. In addition, there are various mixing processes apparent along the outer third of the shelf. Figure 14(d) clearly depicts the edge of the Gulf Stream with its associated high salinities.

The bottom horizontal salinity structure is by comparison much simpler. Salinities here generally range from a low of $35.80^{\circ}/\text{oo}$ near-shore to a high of $36.40^{\circ}/\text{oo}$ offshore. The higher salinities (36.30 to $36.40^{\circ}/\text{oo}$) are coincident with intruded Gulf Stream waters. In Figures 15(b) and 15(d) mid-bay salinity cores of $>36.30^{\circ}/\text{oo}$ and $>36.20^{\circ}/\text{oo}$ respectively are representative of the two cores depicted in the temperature structure of Figures 13(b) and 13(d). In addition, the Cape Lookout area appears to be a source of low salinity waters (Figure 15[a]). This same trend was seen in surface waters for this region.

Horizontal Distribution of Nutrients

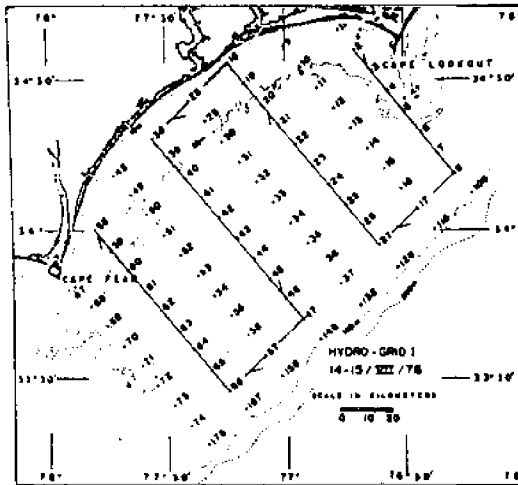
Data sets for nutrients are available only for Hydro Grids I, II and IV. In addition, silicate data is available only for Hydro Grid IV. Surface samples were taken within 1 to 2 meters of the surface and bottom samples were taken generally within 2 to 3 meters of the bottom.

Surface nitrate concentrations were generally less than $0.5 \mu\text{mole/liter}$ for the three hydro grids (Figure 16). The only exception occurred in Hydro Grid I (Figure 16[a]) where highs of 2.7 and $0.8 \mu\text{mole/liter}$ were observed in the northern nearshore region of the Bay. An explanation is not obvious and no corresponding highs in phosphate concentrations were observed (Figure 17[a]). Offshore of this same region there is an area

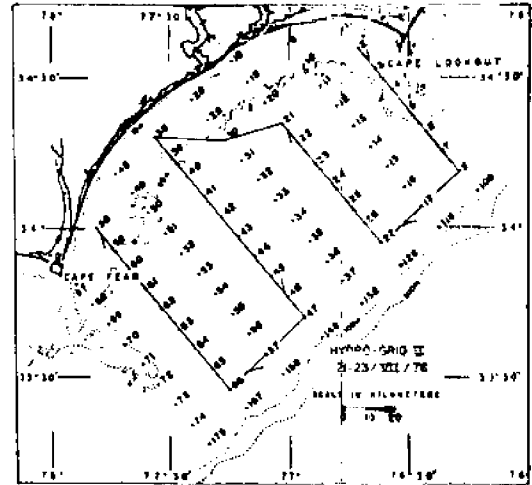
of higher nitrate ($>0.5 \mu\text{mole/liter}$) which corresponds to a region of higher phosphate ($>0.05 \mu\text{mole/liter}$) (Figure 17[a]). Figures 12(a) and 14(a) also reveal this to be an isolated region of lower temperature ($<26.0^{\circ}\text{C}$) and higher salinity ($>35.50^{\circ}/\text{oo}$) than the surrounding waters.

Surface phosphate concentrations were low (generally $<0.05 \mu\text{mole/liter}$) for Hydro Grid II (Figure 17[b]), but during Hydro Grid IV (Figure 17[d]), possible upwelling effects were exhibited near the shelf break where deeper Gulf Stream waters had moved onto the shelf. Phosphate concentrations as high as $0.10 \mu\text{mole/liter}$ are noted. Likewise, the movement of Gulf Stream waters onto the shelf can be seen in the surface silicate plot of Figure 18(d) where silicate concentrations range from 1.0 to $2.0 \mu\text{mole/liter}$ along the outer third of the shelf.

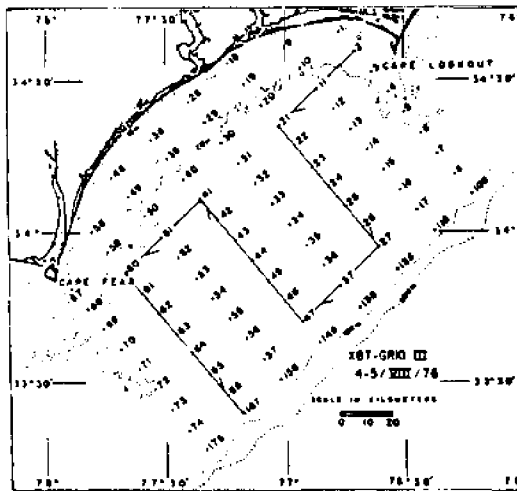
Elevated bottom nutrient concentrations (Figures 19, 20 and 21) appear to be associated with newly intruding waters. This, in fact, is essentially the sole source of detected nitrate (Figure 19). The phosphate plots, however, suggest nearshore influences which are probably associated with runoff (Figure 20[a] and [b]). In addition, plots 20(b) and (d) show traces of older intrusion cores stranded on the shelf. This latter observation suggests that nitrate is depleted more rapidly than phosphate, that phosphate is in excess, or that phosphate is regenerated. Finally, the silicate plot (Figure 21[d]) along with depicting newly intruded waters on the shelf, also suggests a source of high silicate waters in the vicinity of Cape Lookout. From this observation it is apparent that silicate is a good indicator of both intruding Gulf Stream waters and some specific low salinity nearshore waters.



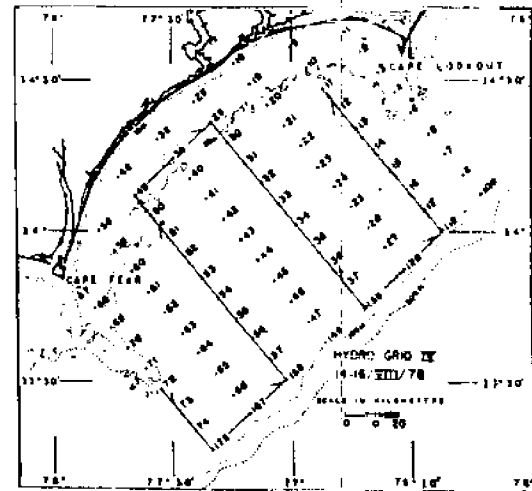
(a)



(b)

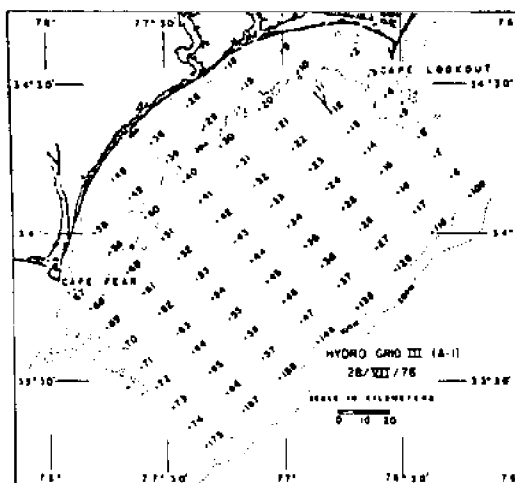


(c)

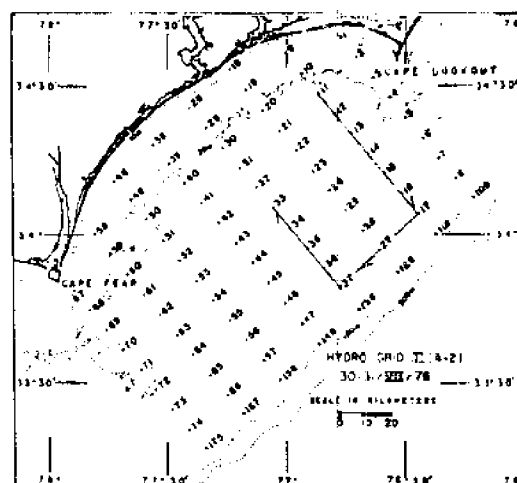


(d)

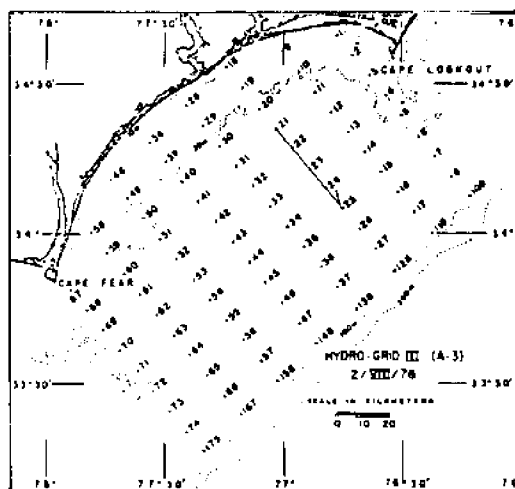
Figure 10. Cruise tracks for Hydro Grids I, II and IV and XBT Grid III.



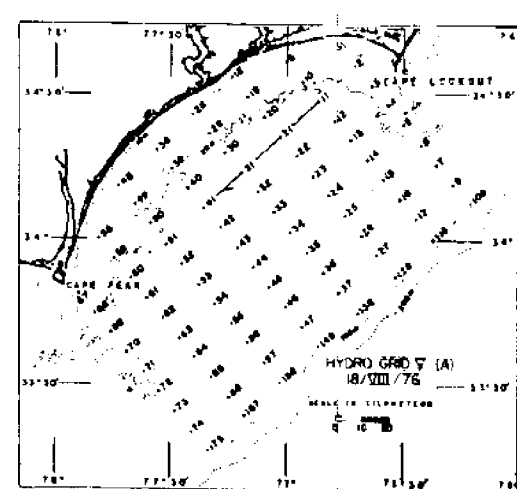
(a)



(b)

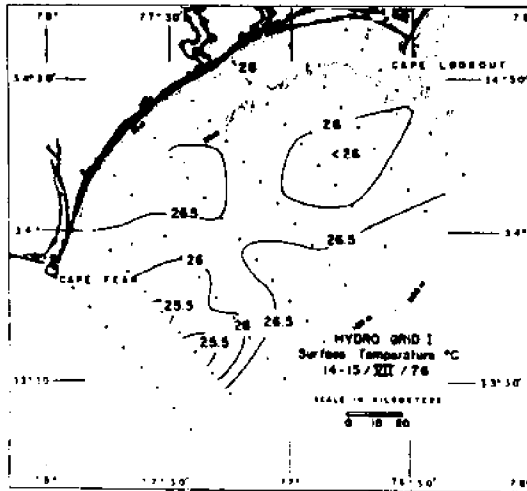


(c)

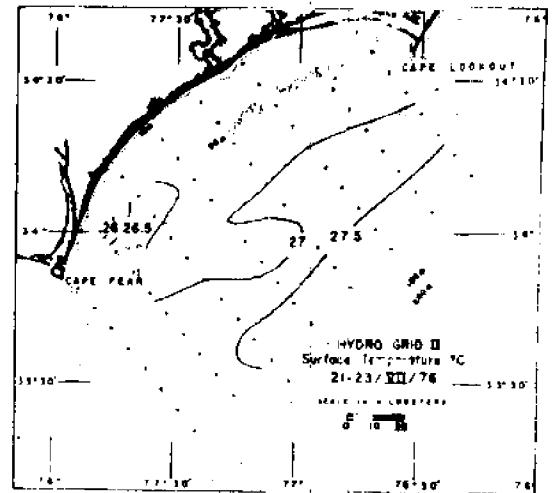


(d)

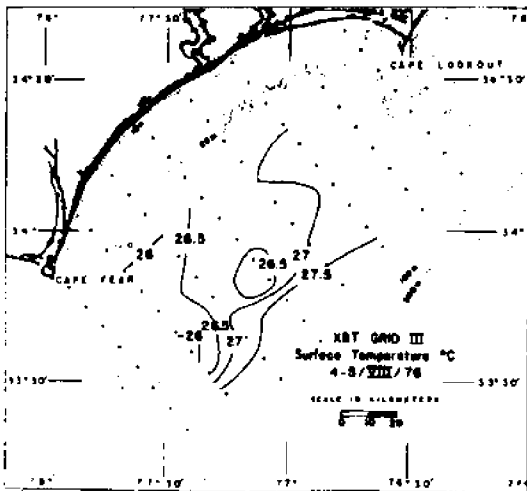
Figure 11. Cruise tracks for aborted grids.



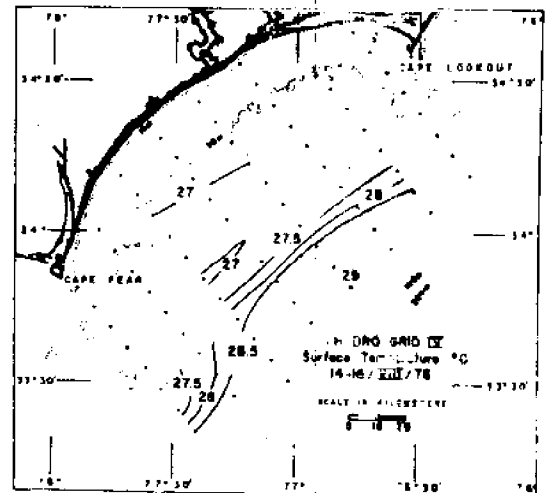
(a)



(b)

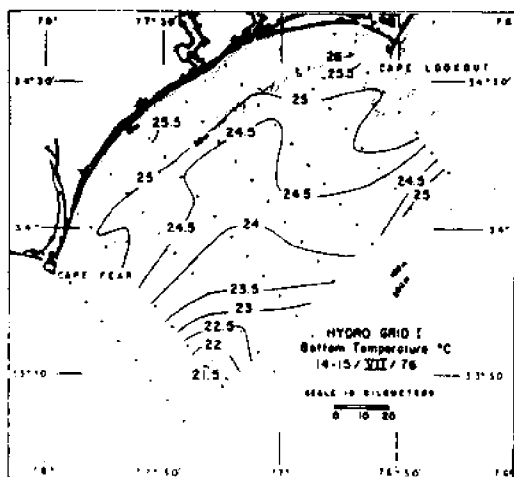


(c)

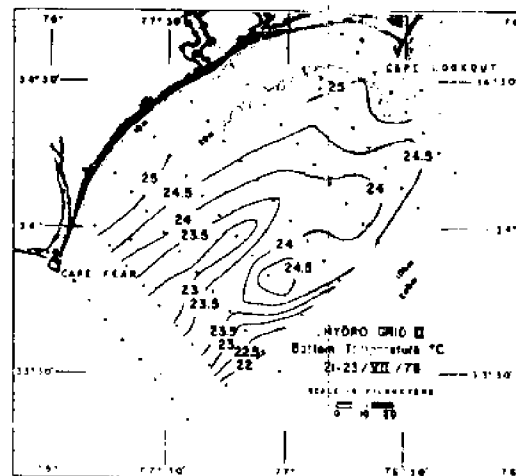


(d)

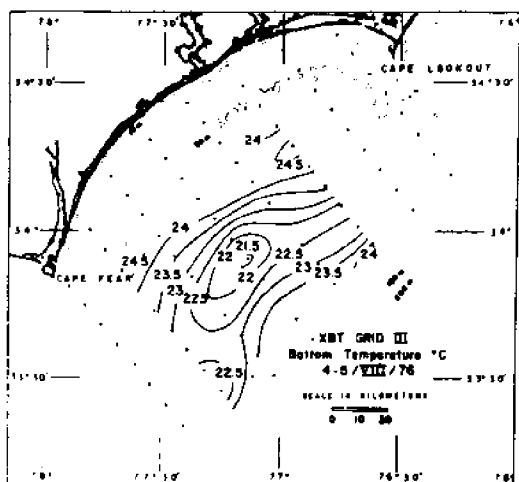
Figure 12. Surface temperature (Hydro Grids I, II and IV and XBT Grid III).



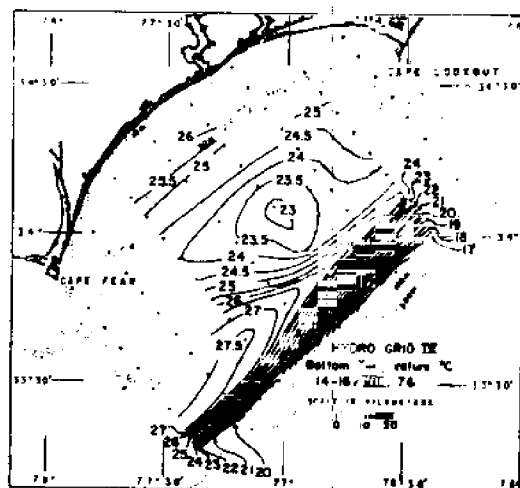
(a)



(b)

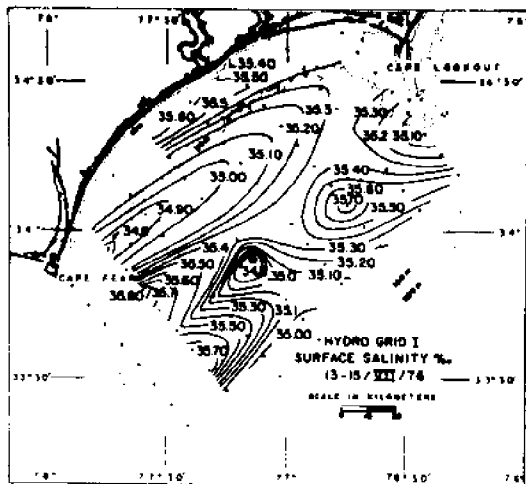


(c)

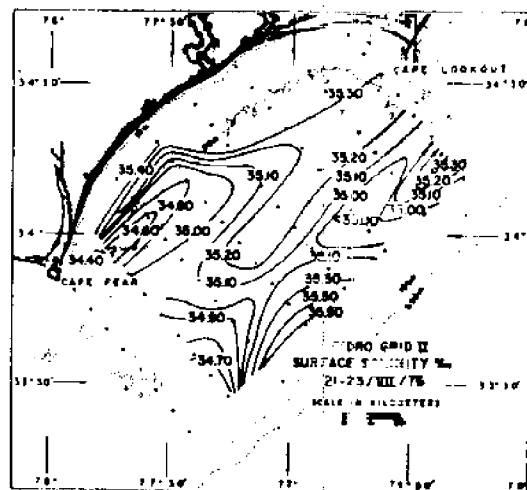


(d)

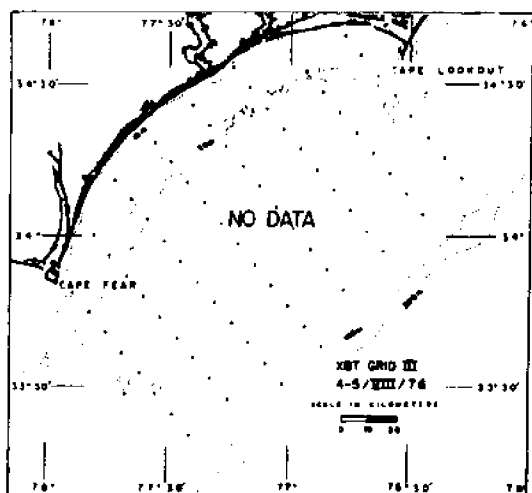
Figure 13. Bottom temperature (Hydro Grids I, II and IV and XBT Grid III).



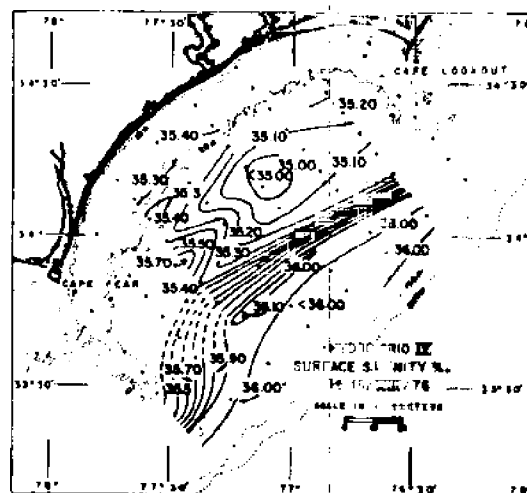
(a)



(b)

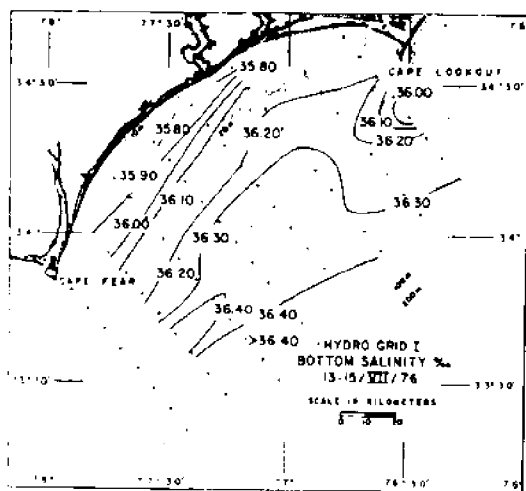


(c)

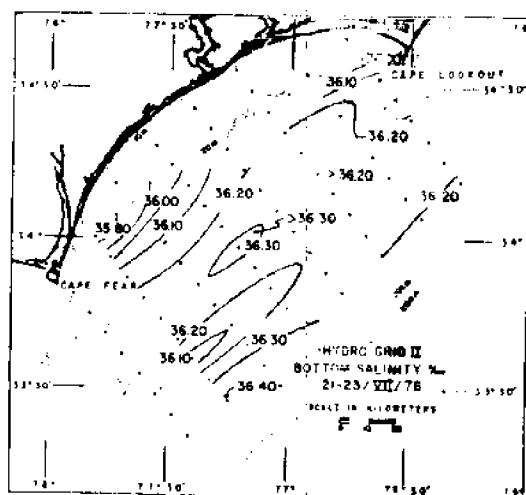


(d)

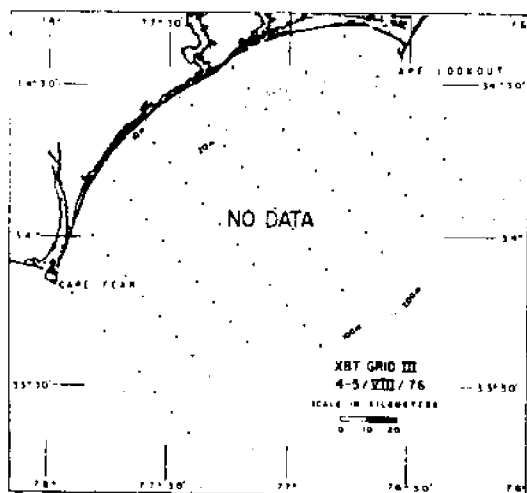
Figure 14. Surface salinity (Hydro Grids I, II and IV).



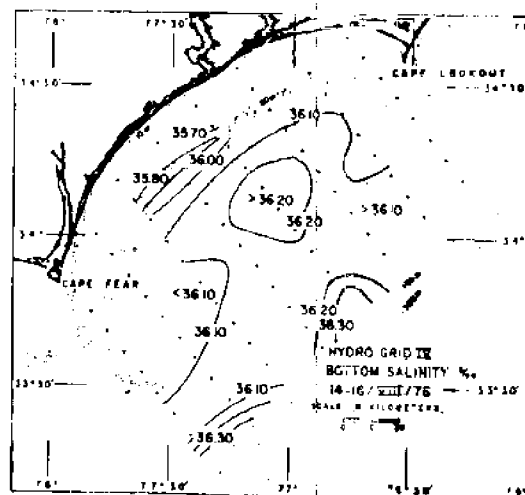
(a)



(b)

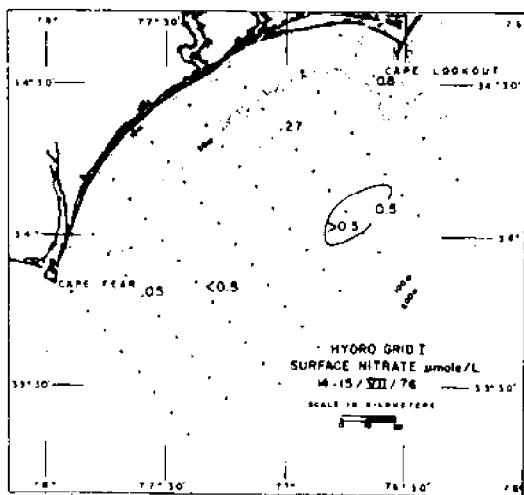


(c)

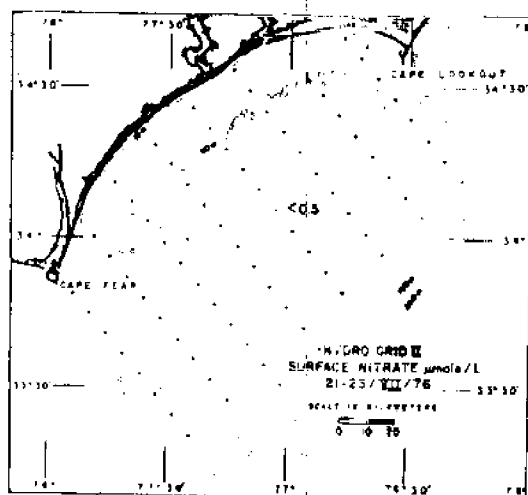


(d)

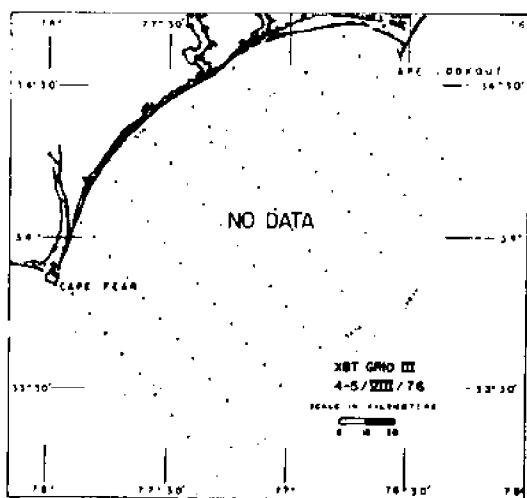
Figure 15. Bottom salinity (Hydro Grids I, II and IV).



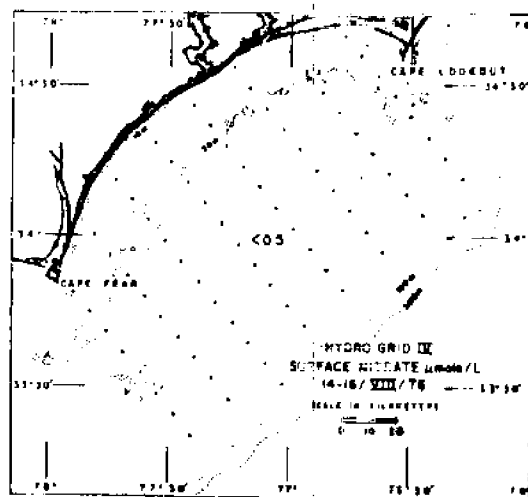
(a)



(b)

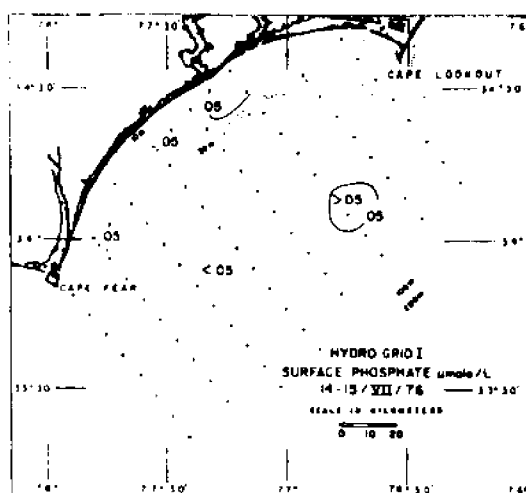


(c)

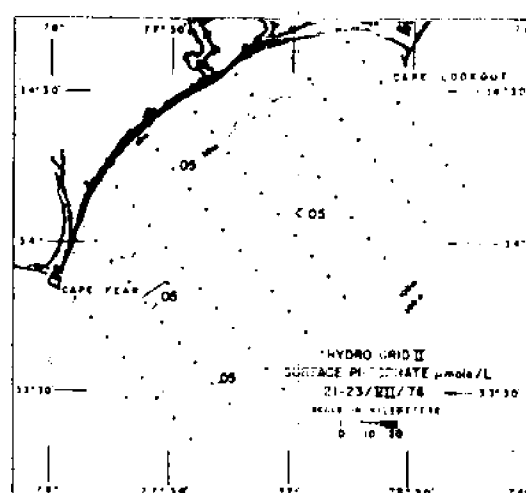


(d)

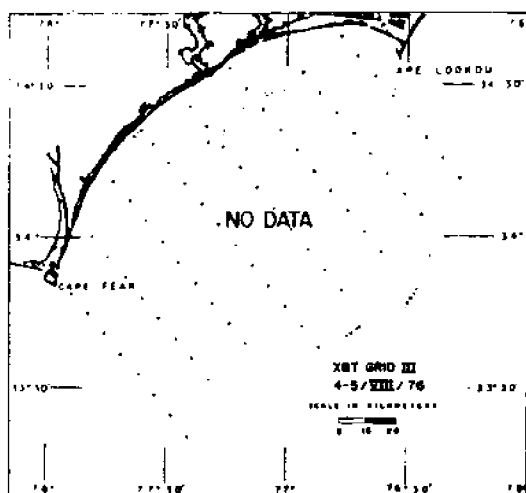
Figure 16. Surface nitrate (Hydro Grids I, II and IV).



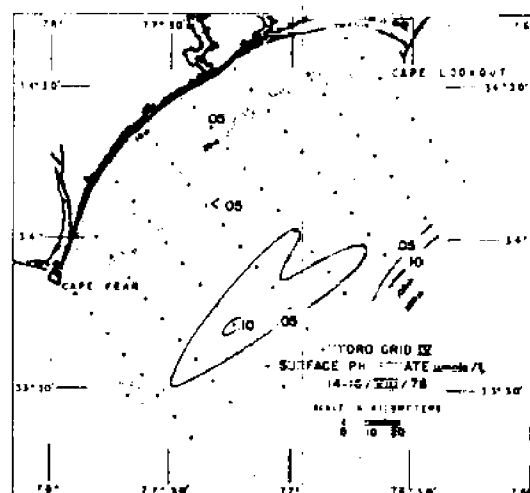
(a)



(b)

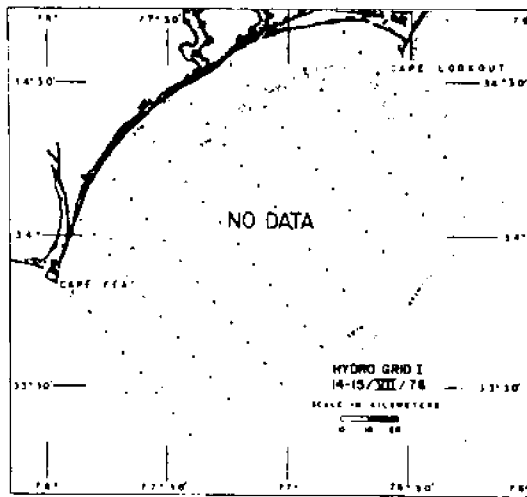


(c)

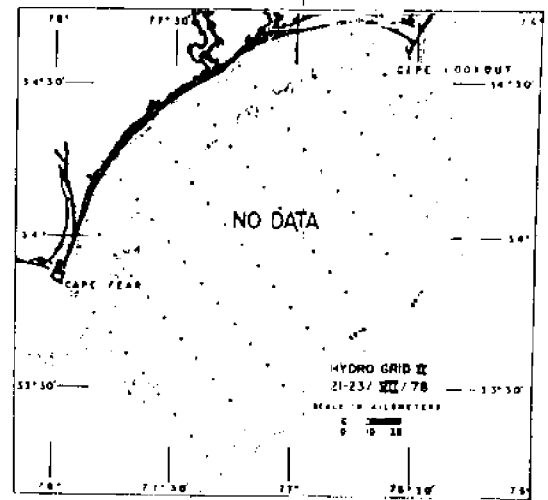


(d)

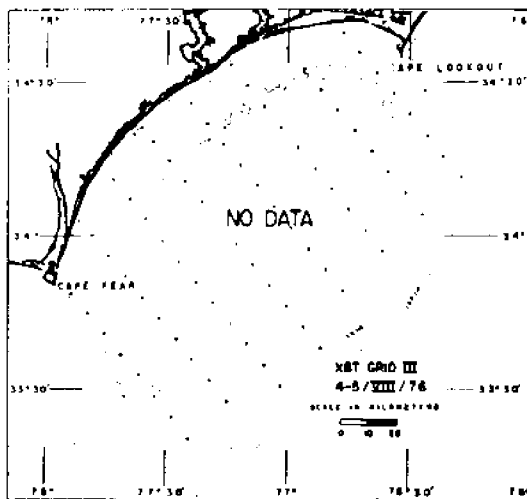
Figure 17. Surface phosphate (Hydro Grids I, II and IV).



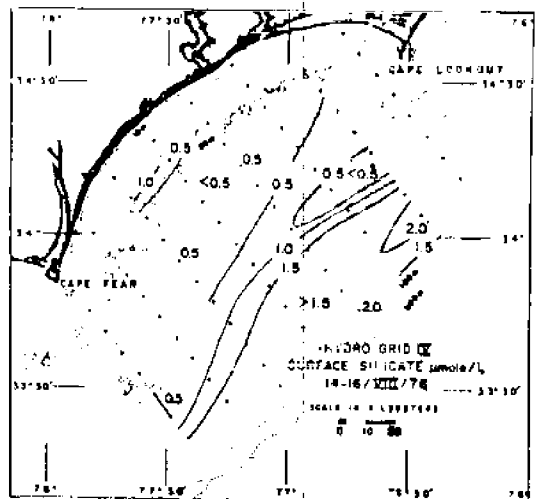
(a)



(b)

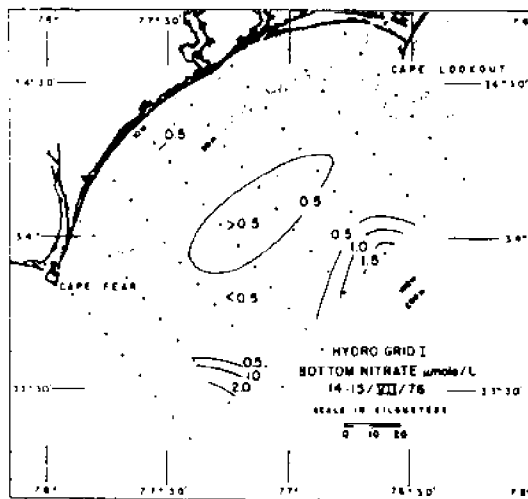


(c)

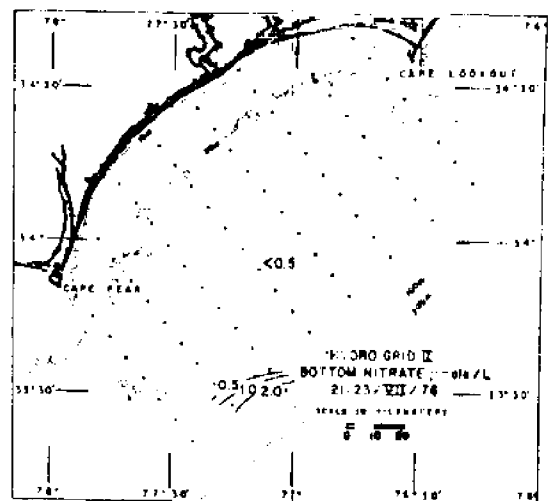


(d)

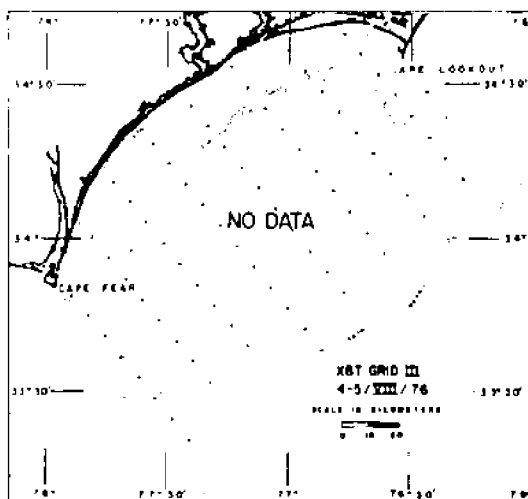
Figure 18. Surface silicate (Hydro Grid IV).



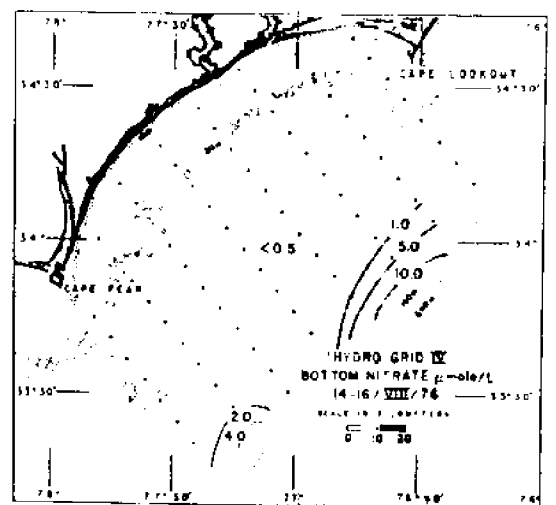
(a)



(b)

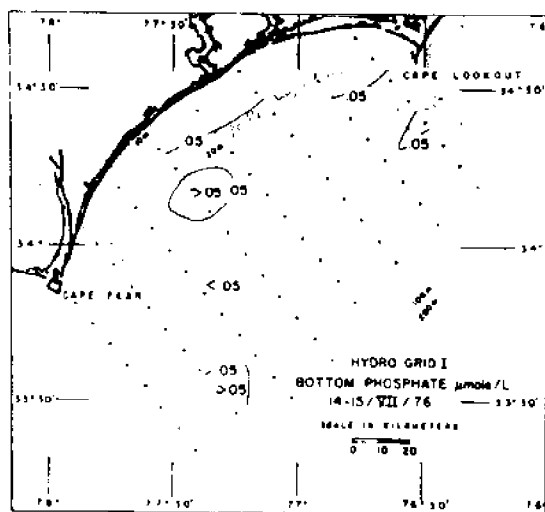


(c)

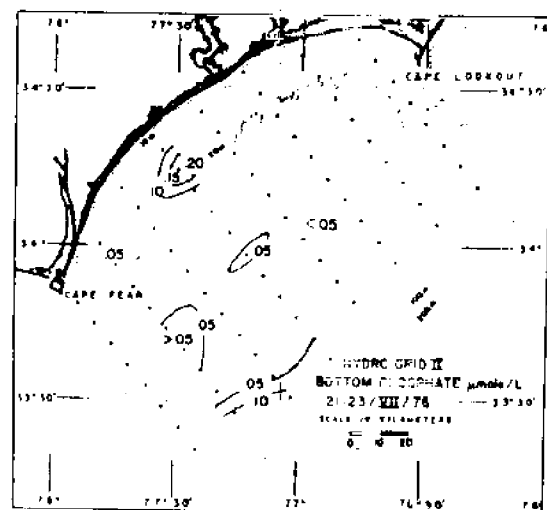


(d)

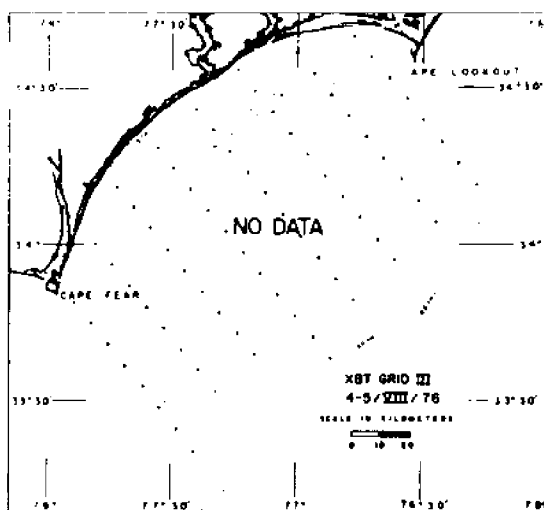
Figure 19. Bottom nitrate (Hydro Grids I, II and IV).



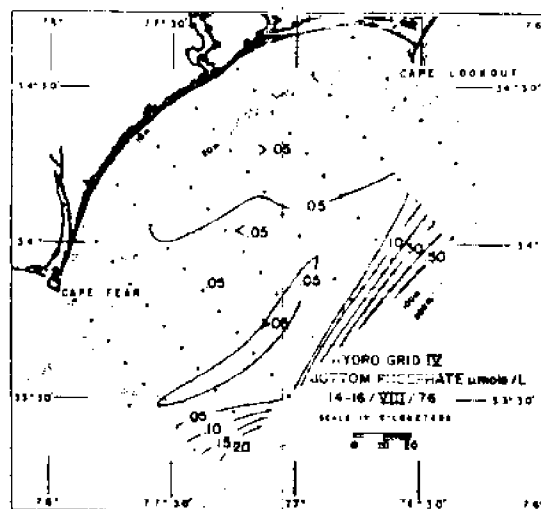
(a)



(b)

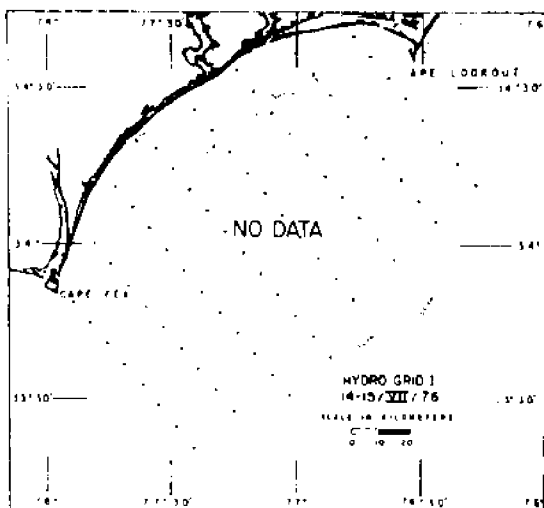


(c)

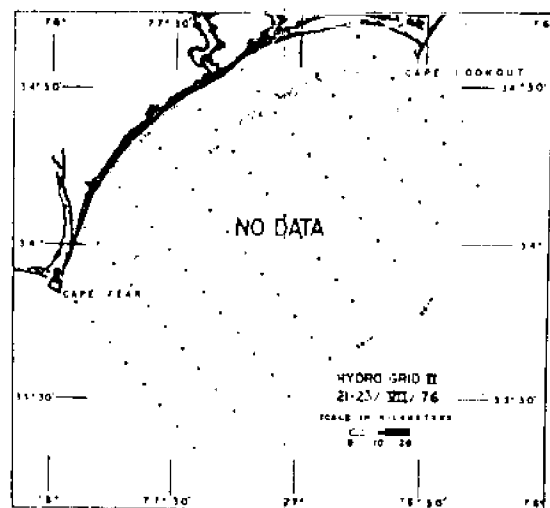


(d)

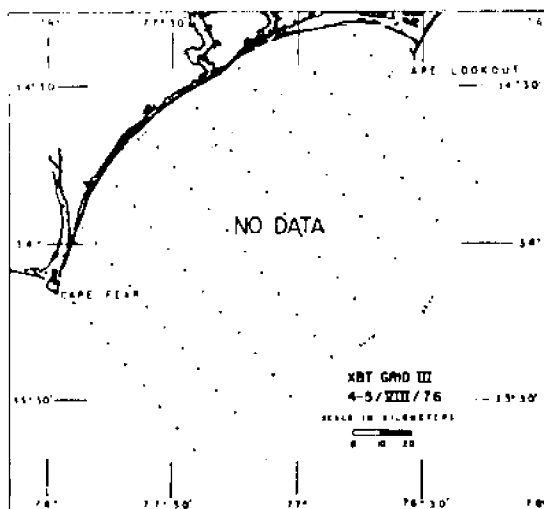
Figure 20. Bottom phosphate (Hydro Grids I, II and IV).



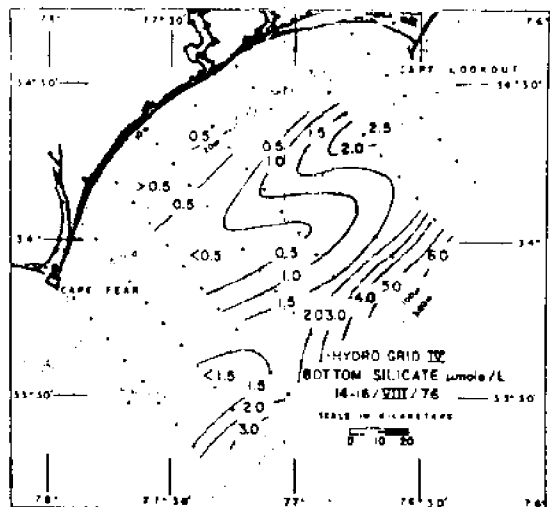
(a)



(b)



(c)



(d)

Figure 21. Bottom silicate (Hydro Grid IV).

Vertical Distribution of Physical and Chemical Properties (Hydro Grids)

In the following figures the arrows indicate the cruise direction. The transects have been arranged to give the cusp shape nature of the Bay and the proper relationship of stations along one onshore/offshore transect to those of the next. In this way a three dimension view of the Bay is obtained. The bottom bathymetry is an averaged value from the various cruises along the given transects. Temperature plots are derived from CTD and XBT data; salinity plots from CTD and/or bottle samples; sigma-t from available data as reported above; and nutrients (NO_3 , PO_4 and SiO_3) from water samples collected at selected depths as indicated on the respective plots.

Hydro Grid I. The vertical temperature structure during Hydro Grid I (Figure 22) demonstrates the temperature gradient which is characteristic of intrusions and shows that intrusions are not restricted to the shelf break. Note the apparent movement of colder waters far onto the shelf along the bottom in transect (d) and the presence of a warmer core (24.5°C) isolated along transect (a). The corresponding salinity and sigma-t plots (Figures 23 and 24) also show strong vertical gradients with increasing salinity and sigma-t values with depth. Such trends confirm the off shelf origin of these waters.

The movement of colder bottom waters onto the shelf serves as a mechanism for the transport of nutrients onto the shelf. Nitrate concentrations as high as $2.0 \mu\text{mole/liter}$ are observed along transect (d) (Figure 25) which had the coldest (21.5°C) penetration of off shelf waters (Figure 22[d]). Concentrations as high as $1.5 \mu\text{mole/liter}$ are noted for station 27 where the coldest waters were only 24.5°C . Furthermore, at station 47 where 23.0°C water were observed, no significant nitrate concentrations are detected. Further onshore along transect (c)

there is a core of high nitrate water with values as high as $2.8 \mu\text{mole/liter}$ in slightly warmer water than that found closer to the shelf break. A satisfactory explanation for this last observation is not provided beyond the possibility of a bad sample. Phosphate concentrations (Figure 26) directly attributable to an intrusion are shown only for transect (d). No silicate data are available.

Hydro Grid II. In Figure 27 the vertical temperature structure in the Bay during Hydro Grid II is presented. This figure is the vertical counterpart of Figure 13(b). Once again there is an intrusion apparently moving onto the shelf along the two southern transects. Also, there is evidence of another older intrusion core ($23.0 - 24.0^{\circ}\text{C}$) centered at stations 25, 43 and 62. Salinity of $36.25^{\circ}/\text{oo}$ and sigma-t's of 24.5 and 25.0 correspond to both the older and new intrusions (Figures 28 and 29). Both the nitrate and phosphate plots (Figure 30 and 31) show high concentrations at station 66 coincident with the new intrusion and its coldest tongue. However, only the phosphate plot shows any evidence of the older intrusion, but only along the transects which pass through the two coldest cores. High phosphates reported at station 39 are probably due to runoff. No silicate data are available.

Hydro Grid III(A-2). Figure 32 shows the vertical temperature structure along two northern transects made during the second aborted attempt at Hydro Grid III. There is no corresponding horizontal plot, and salinity, sigma-t, phosphate and silicate data are available only for transect (a). Figure 32 exhibits an isolated intrusion core and a newer intrusion apparently moving onto the shelf. Both of these features are outlined by the 24.0°C isotherms. In Figure 33, salinity and sigma-t values of $36.25^{\circ}/\text{oo}$ and 24.5 respectively represent these intrusion cores on the shelf and, in Figure 34, near bottom silicate values of $2.0 \mu\text{mole/liter}$ roughly approximate these cores as well. The phosphate plot in

this latter figure is less conclusive though it does exhibit two regions of higher concentrations. No nitrate data are available.

XBT Grid III. Figure 35 shows the vertical temperature structure during XBT Grid III. This figure corresponds to the horizontal plot of Figure 13(c). It clearly shows a cold core (21.5°C to 22.5°C) along the length of the Bay and suggests the possibility of another core having moved further nearshore in transect (a) (station 21). Such an observation is not inconsistent with our findings in September 1975 (Atkinson et al., 1976). No salinity, sigma-t or nutrient data are available in conjunction with this grid. However, a bio grid was run across stations 53-57 and will be presented later (page 63).

Hydro Grid IV. In Figure 36, the vertical temperature structure during Hydro Grid IV is shown. It reveals a stranded intrusion with a core of 23.0 to 24.0°C along much of the length of the Bay. It also shows evidence of other waters moving onto the shelf behind it. This is not surprising in view of the horizontal plot of Figure 13(d) which shows a rather massive movement of bottom waters onto the shelf along its entire length. In Figures 37 and 38 high salinity and sigma-t values ($36.25^{\circ}/\text{oo}$ and 24.5 respectively) correlate only to station 33, the coldest region on the mid-shelf. Similarly high, and higher values are noted for the outer edge of the shelf. It is also noted here that the coldest penetration of this particular intrusion occurs along the northern transects of the Bay. This is the first documentation we have of intruding waters moving into the northern offshore section of the Bay in advance of the southern sector. This observation and the overall movement of Gulf Stream waters onto the shelf at this time may have been influenced by the passage of Hurricane Belle on 9 August.

The nitrate, phosphate and silicate plots of Figures 39-41 support the obvious conclusion that the intrusion centered around station 33 is the older of the two. That is, all three nutrient species are found to be either negligible or very low, thereby suggesting that they have been used up. Of course, there is the possibility that there were no nutrients to begin with. In contrast, looking at the waters moving onto the shelf one can see considerable quantities of nutrients along three of the transects. Nitrate, phosphate and silicate concentrations as high as 8.4, 0.50 and 6.1 $\mu\text{mole/liter}$ respectively are observed. No sign of these high nutrient waters is seen along transect (c). This is due generally to a lack of onshore penetration of the colder waters exhibited along the other three transects. High silicate values (2.5 $\mu\text{mole/liter}$) at station 13 are unrelated to the intrusion phenomenon. They appear to be due to the movement of waters south from the Cape Lookout area (see Figure 21[d]).

TEMPERATURE °C
HYDRO GRID I
14-15/VIII/76

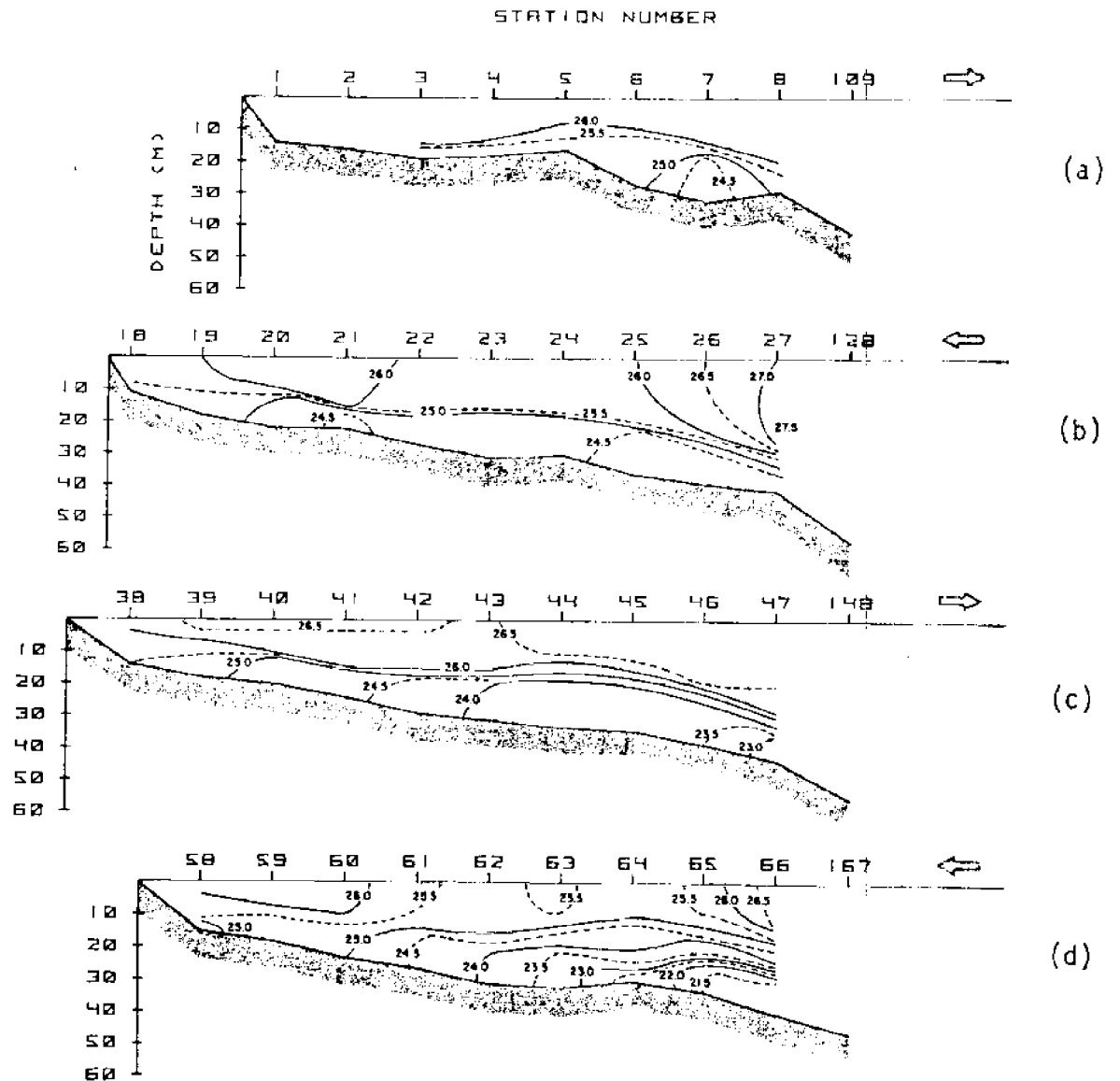


Figure 22. Vertical distribution of temperature (Hydro Grid I).

SALINITY ‰
HYDRO GRID I
14-15/VII/76

STATION NUMBER

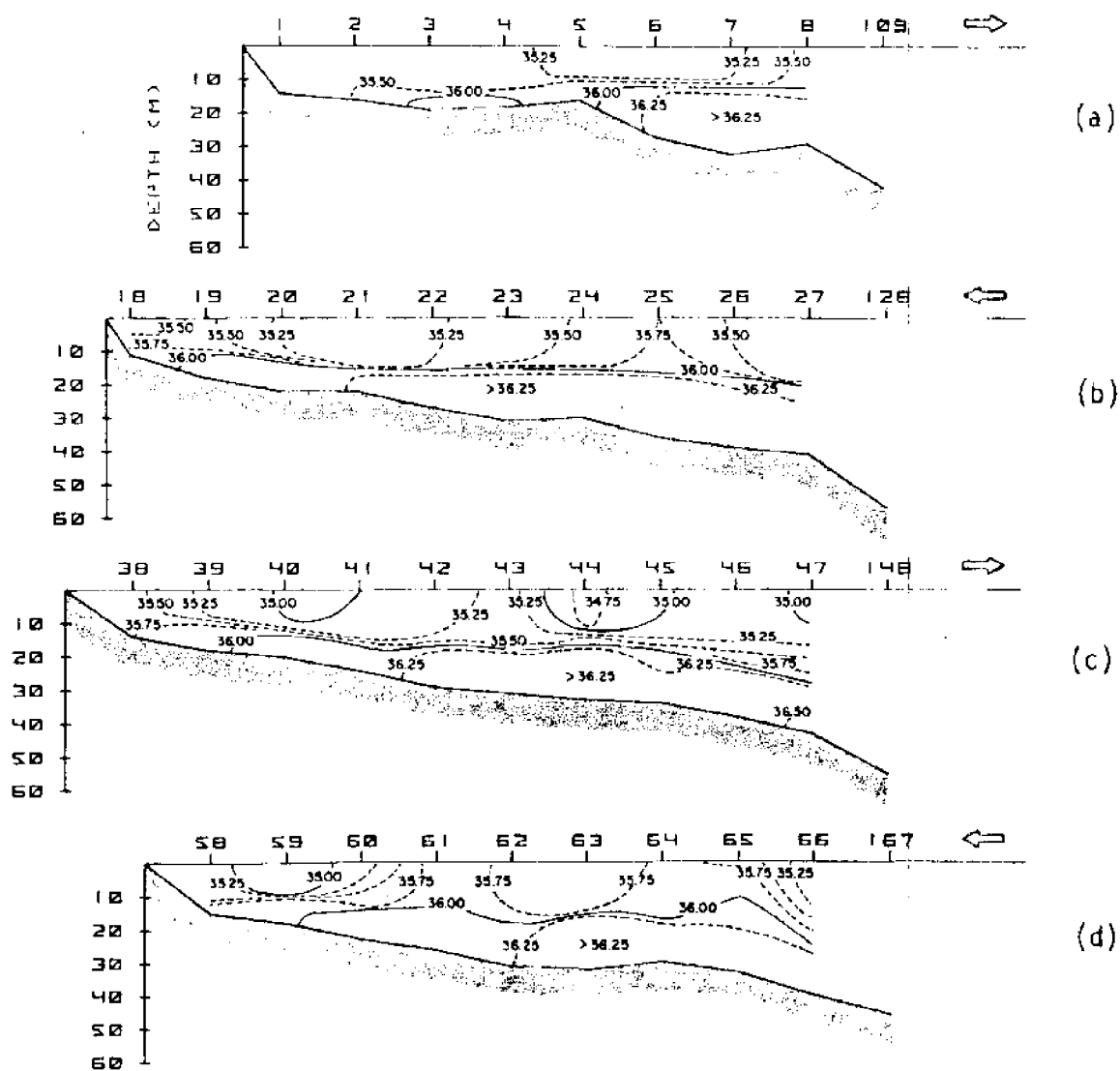


Figure 23. Vertical distribution of salinity (Hydro Grid I).

SIGMA-T
HYDRO GRID I
14-15/V.LI/76

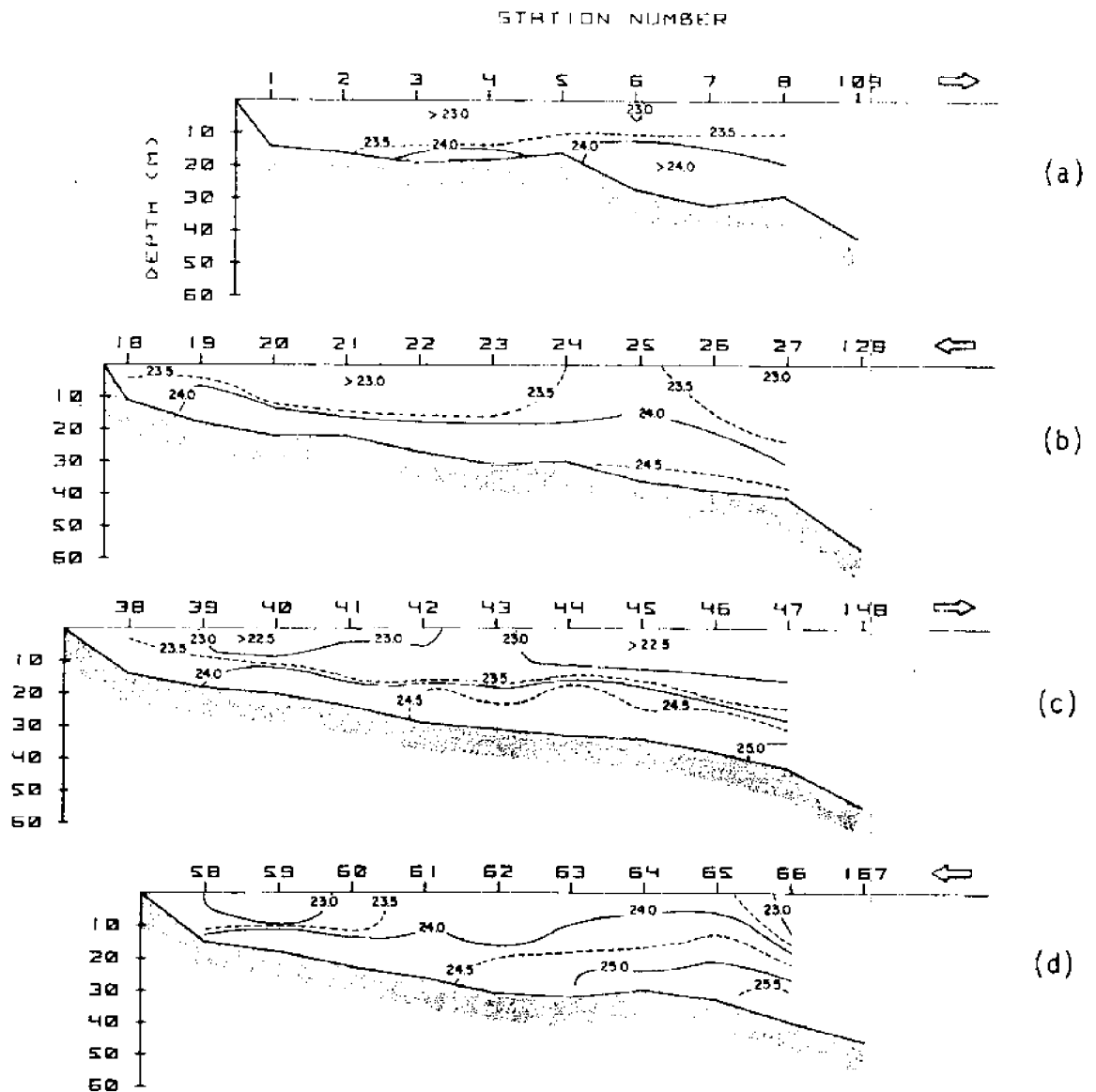


Figure 24. Vertical distribution of sigma-t (Hydro Grid I).

NITRATE ($\mu\text{MOLE/L}$)
 HYDRO GRID I
 14-15/VII/76

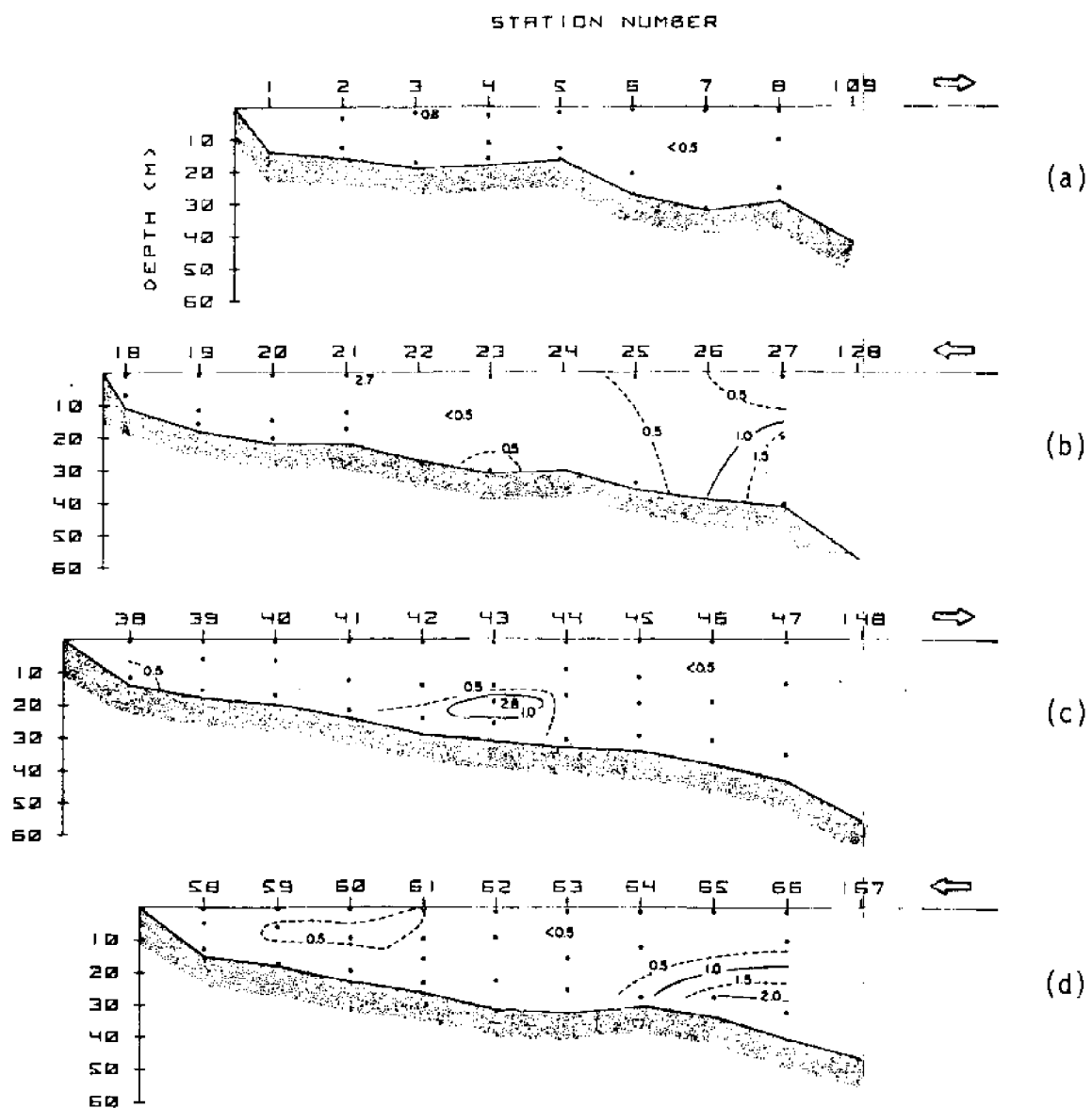


Figure 25. Vertical distribution of nitrate (Hydro Grid I).

PHOSPHATE ($\mu\text{MOLE/L}$)
 HYDRO GRID I
 14-15/VII/76

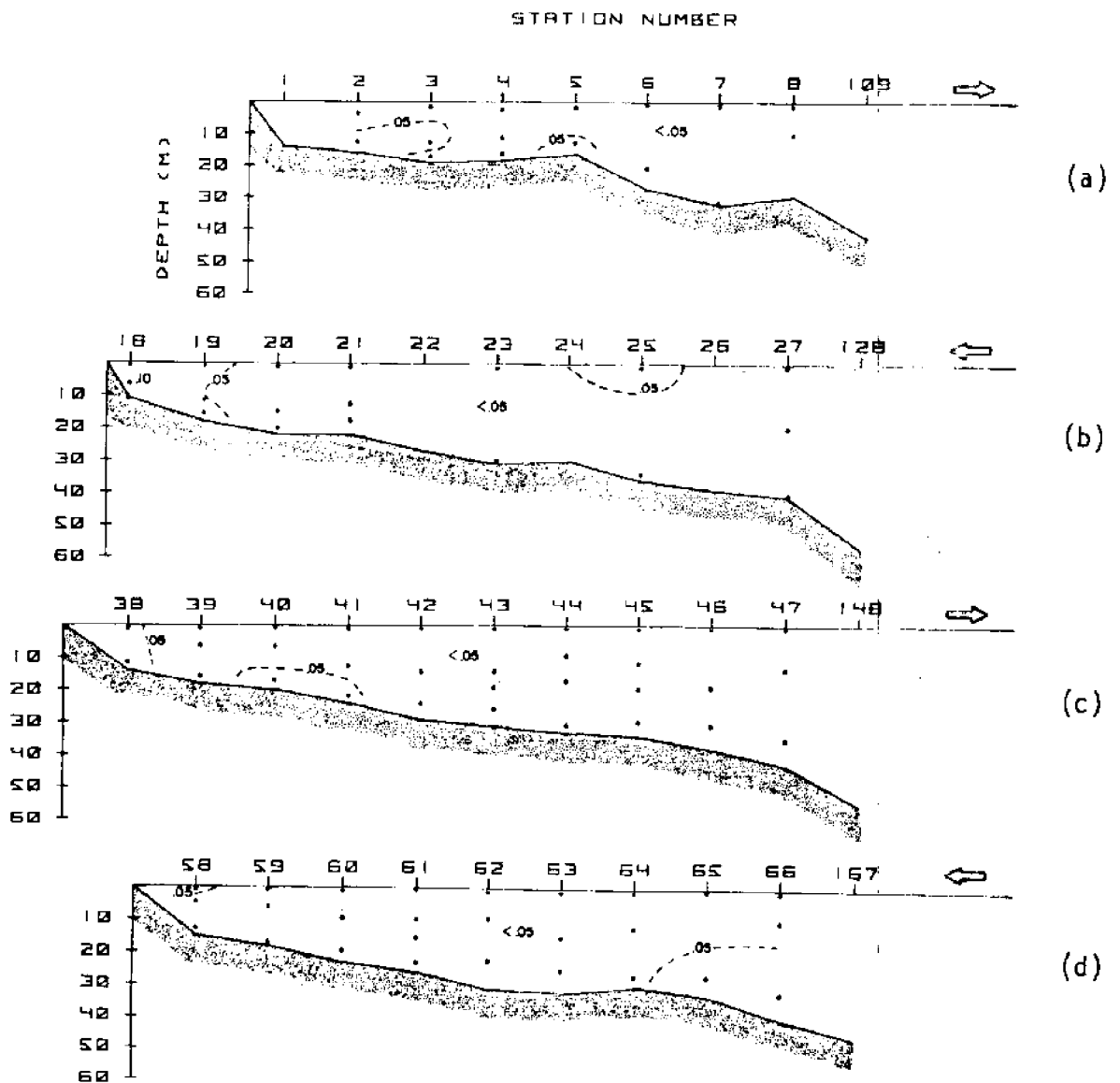


Figure 26. Vertical distribution of phosphate (Hydro Grid I).

TEMPERATURE °C
HYDRO GRID II
21-23/VII/76

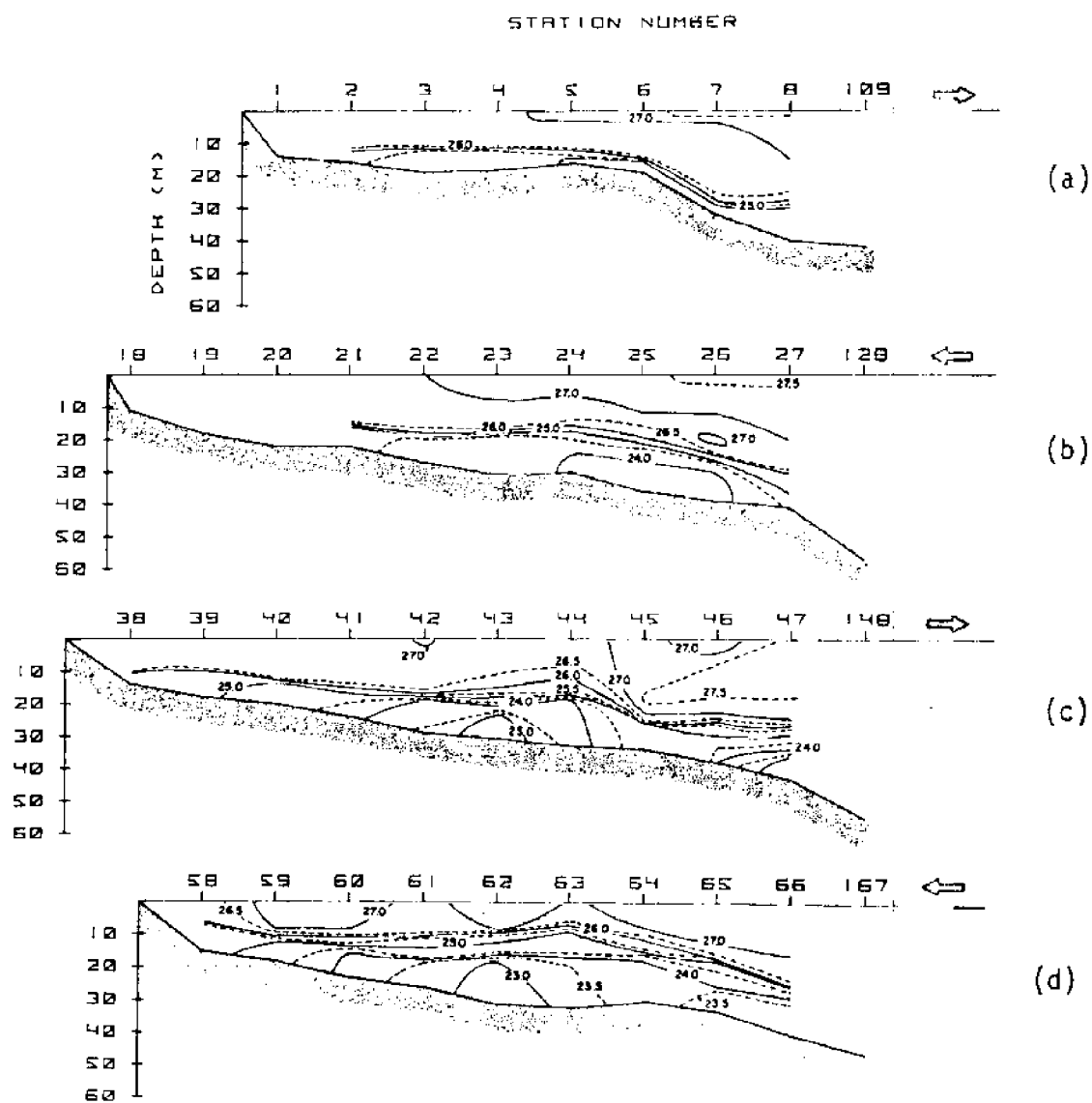


Figure 27. Vertical distribution of temperature (Hydro Grid II).

SALINITY ‰
HYDRO GRID II
21-23/VII/76

STATION NUMBER

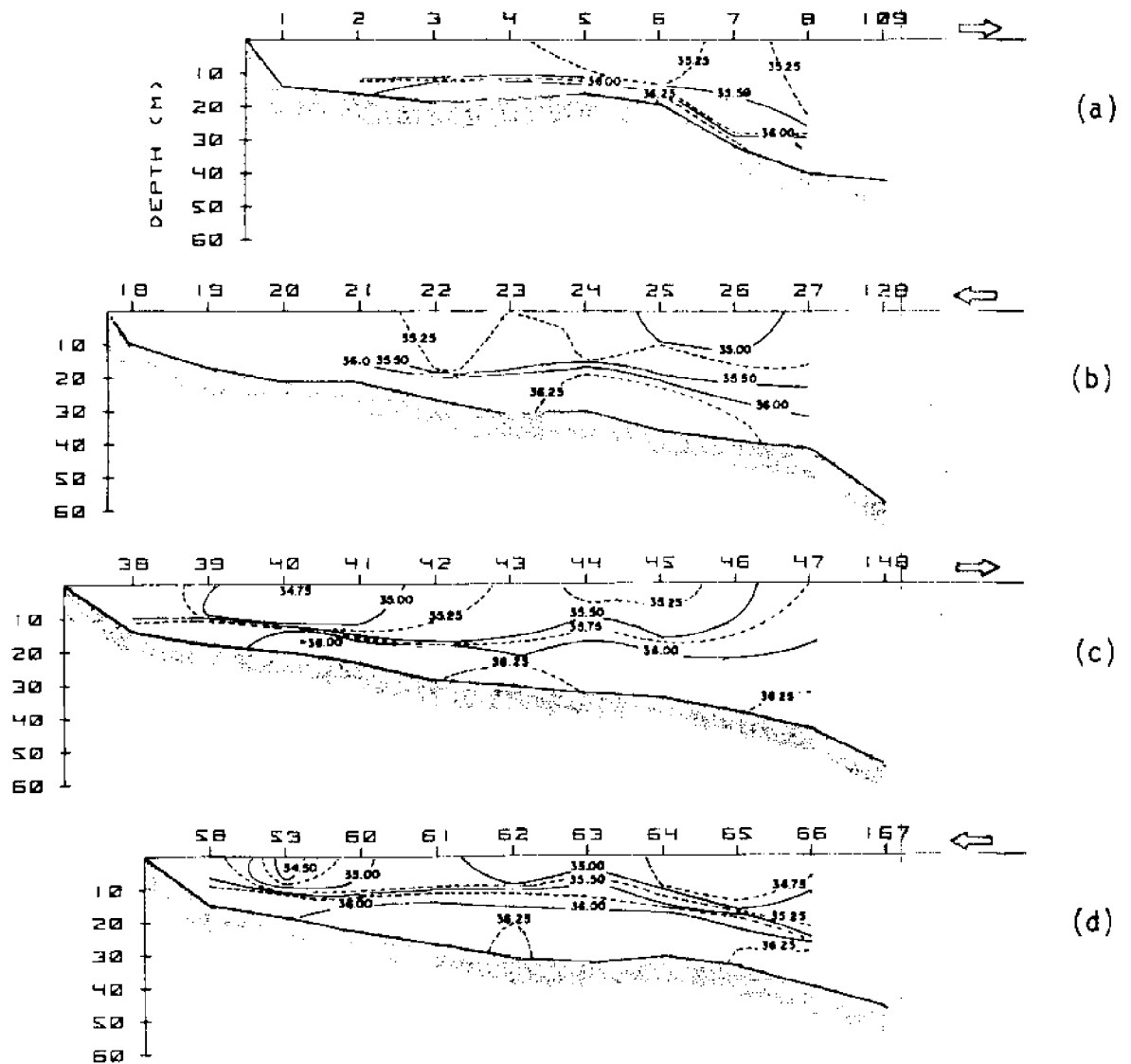


Figure 28. Vertical distribution of salinity (Hydro Grid II).

SIGMA-T
HYDRO GRID II
21-23/VII/76

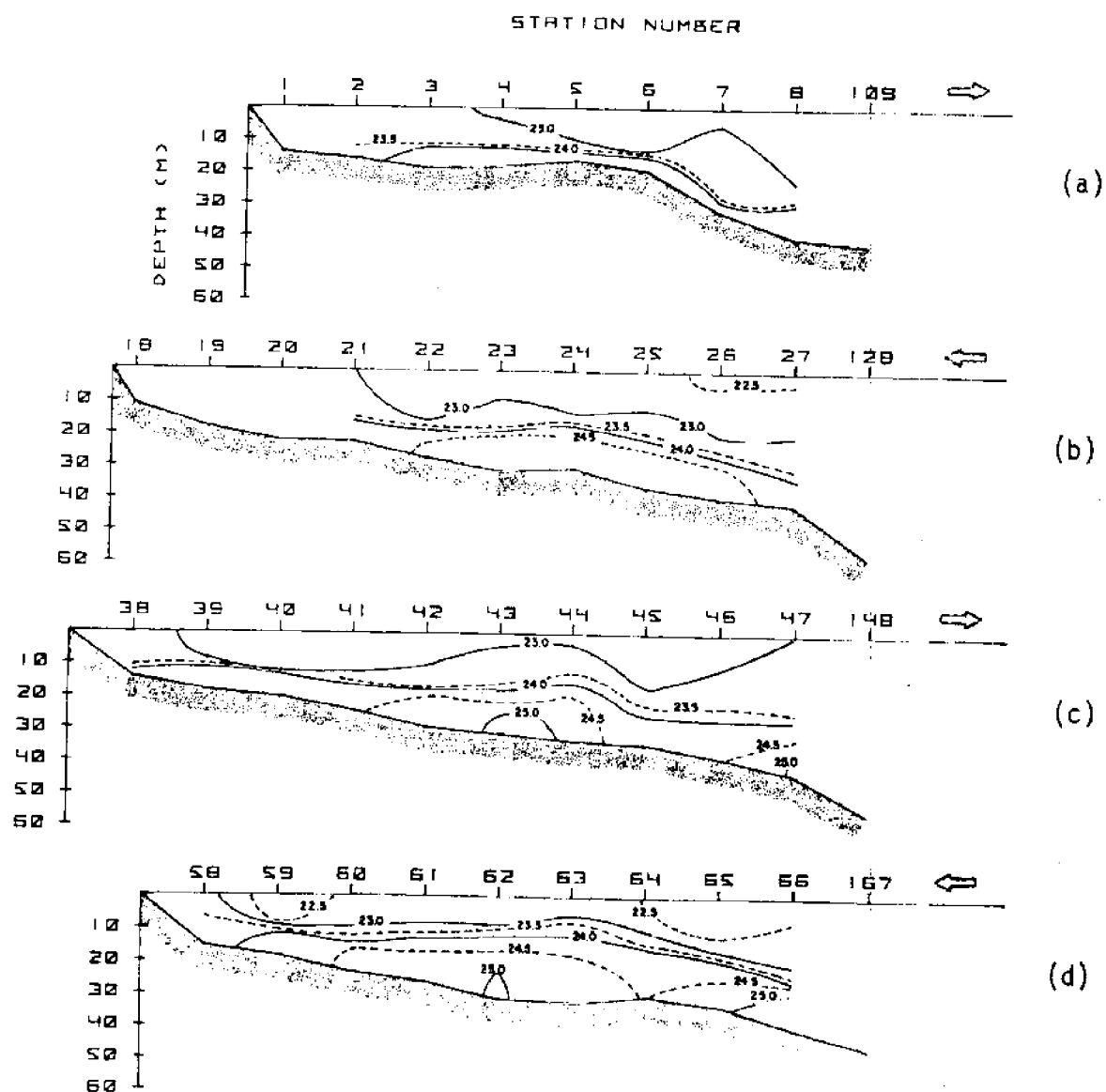


Figure 29. Vertical distribution of sigma-t (Hydro Grid II).

NITRATE ($\mu\text{MOLE/L}$)

HYDRO GRID II

21-23/VII/76

STATION NUMBER

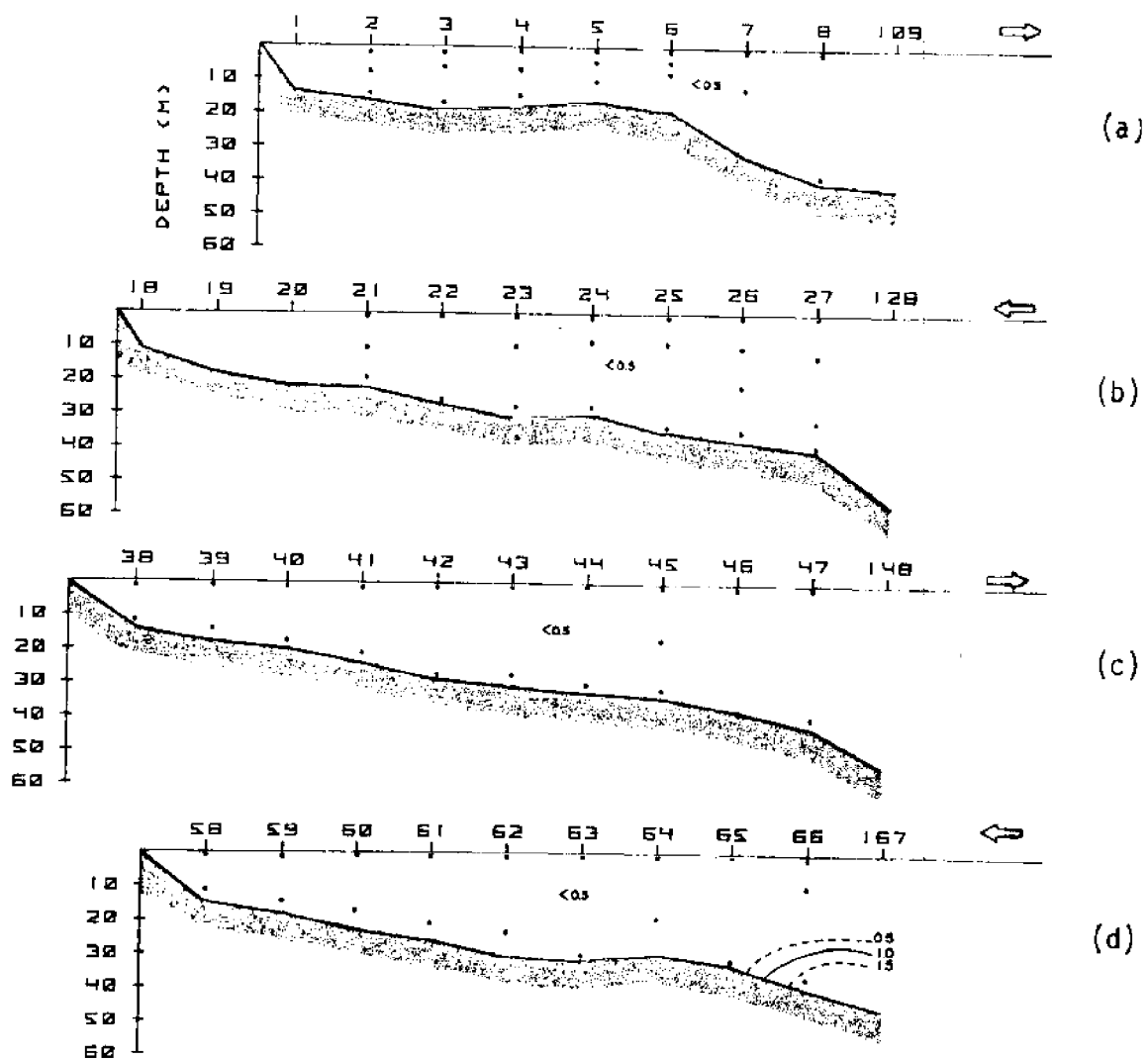


Figure 30. Vertical distribution of nitrate (Hydro Grid II).

PHOSPHATE ($\mu\text{MOLE/L}$)
 HYDRO GRID II
 21-23/VII/76

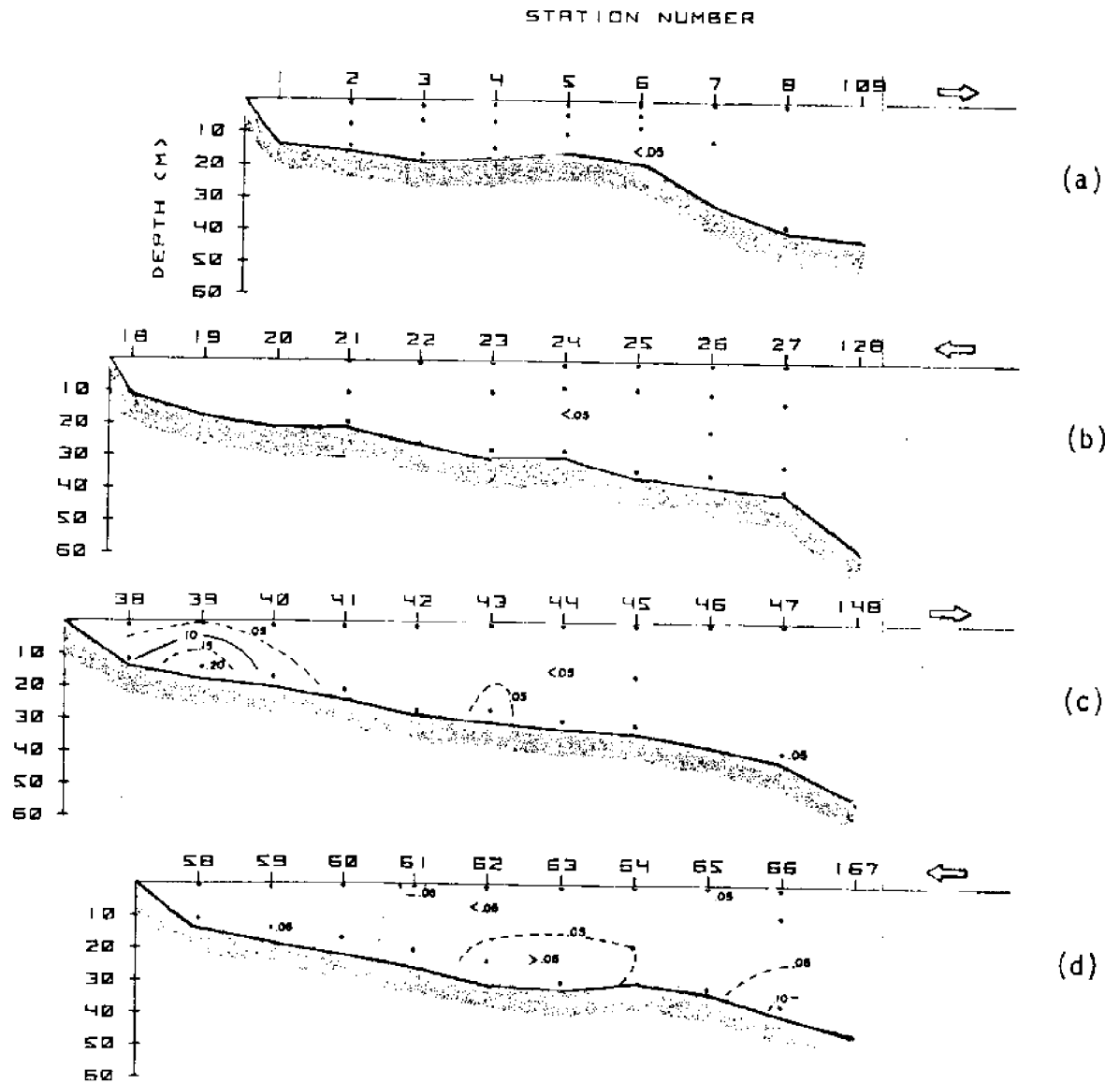
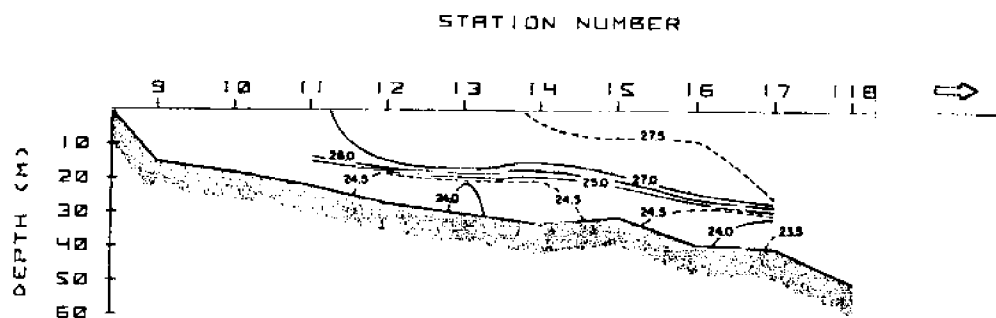
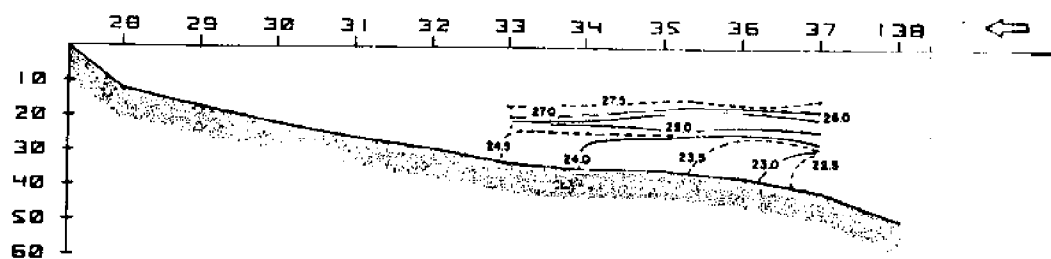


Figure 31. Vertical distribution of phosphate (Hydro Grid II).

TEMPERATURE °C
HYDRO GRID III (A-2)
30-31/VIII/76



(a)



(b)

Figure 32. Vertical distribution of temperature (Hydro Grid III (A-2)).

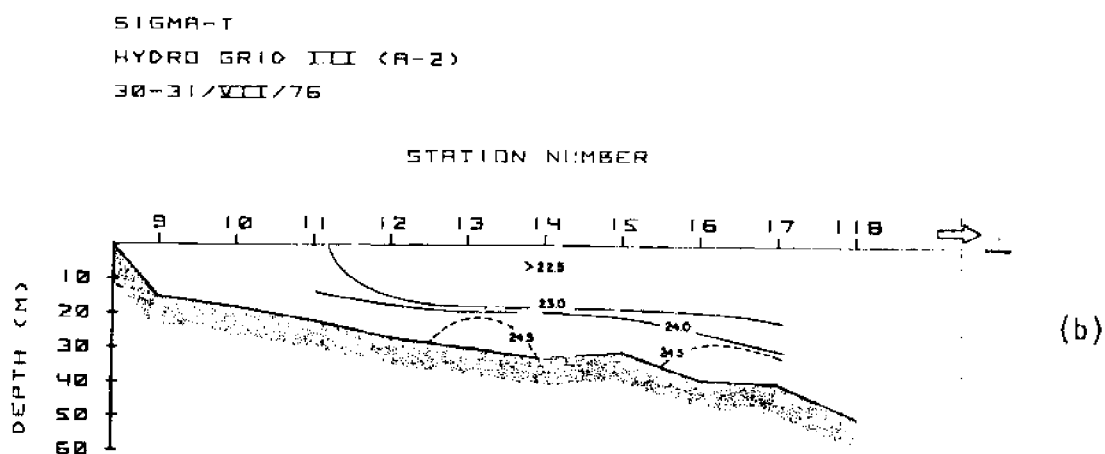
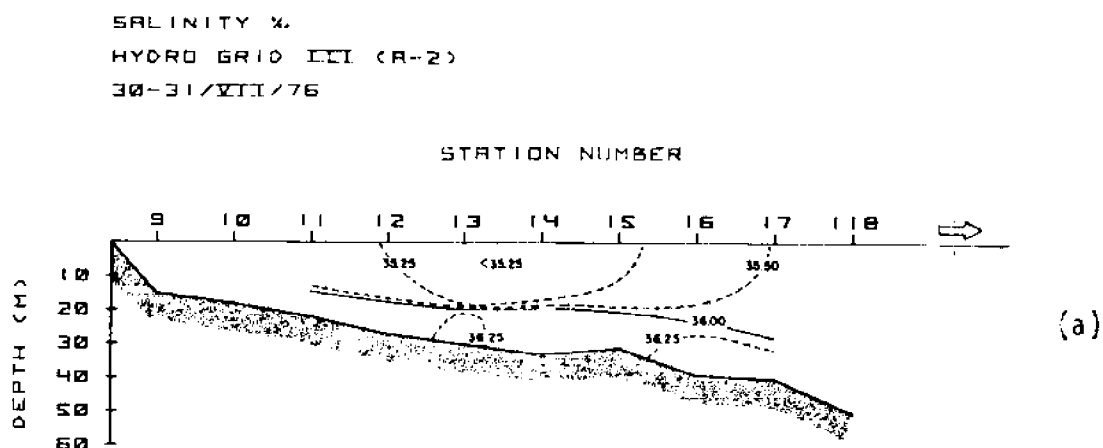
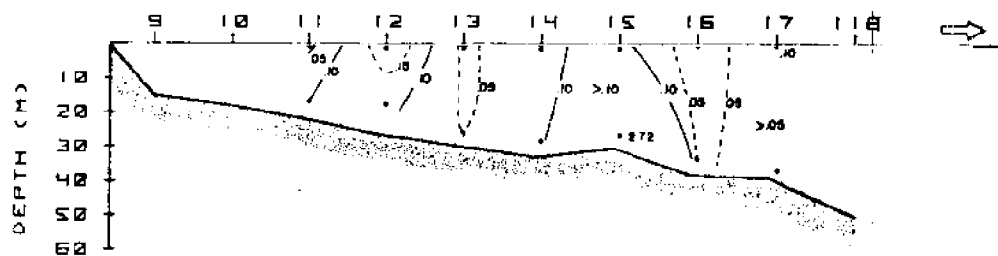


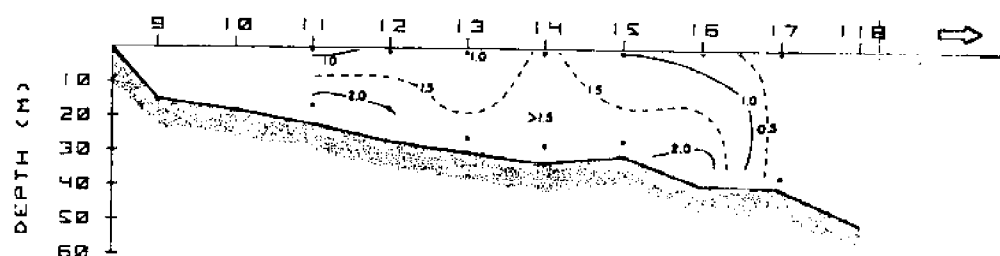
Figure 33. Vertical distribution of salinity and sigma-t (Hydro Grid III(A-2)).

STATION NUMBER



(a)

STATION NUMBER

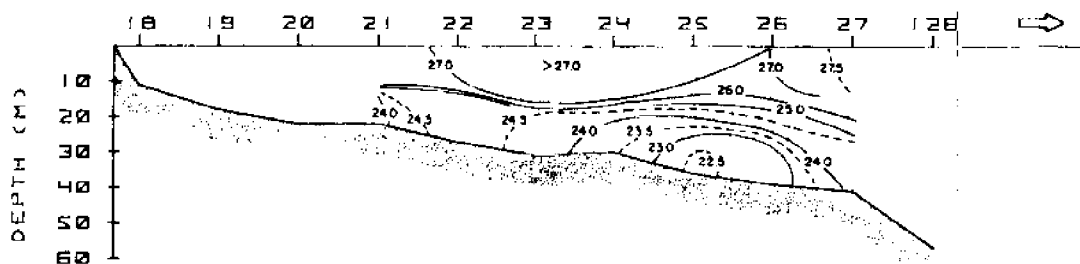


(b)

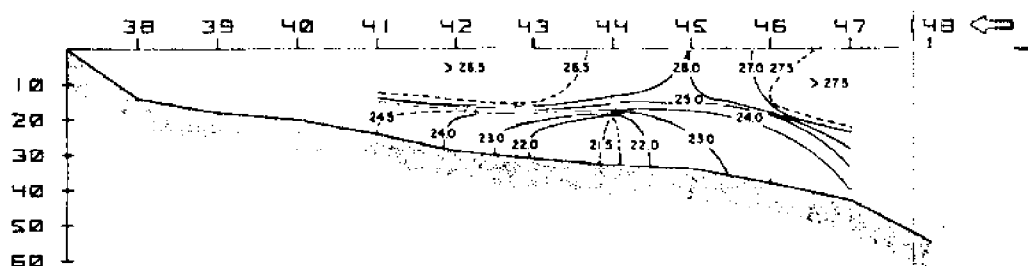
54.

TEMPERATURE °C
 XBT GRID III
 4-5/VIII/76

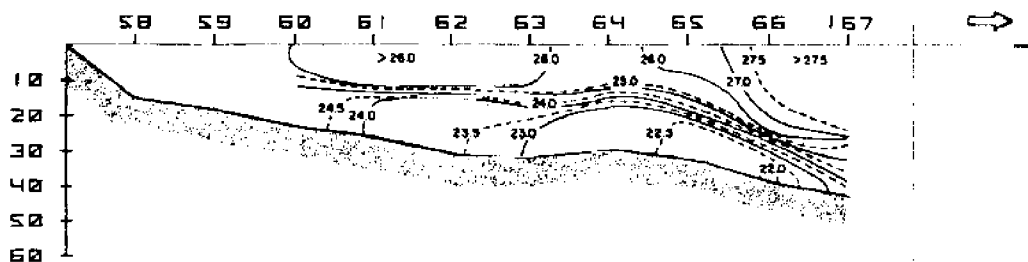
STATION NUMBER



(a)



(b)



(c)

Figure 35. Vertical distribution of temperature (XBT Grid III).

TEMPERATURE °C
HYDRO GRID IV
14-16/VIII/76

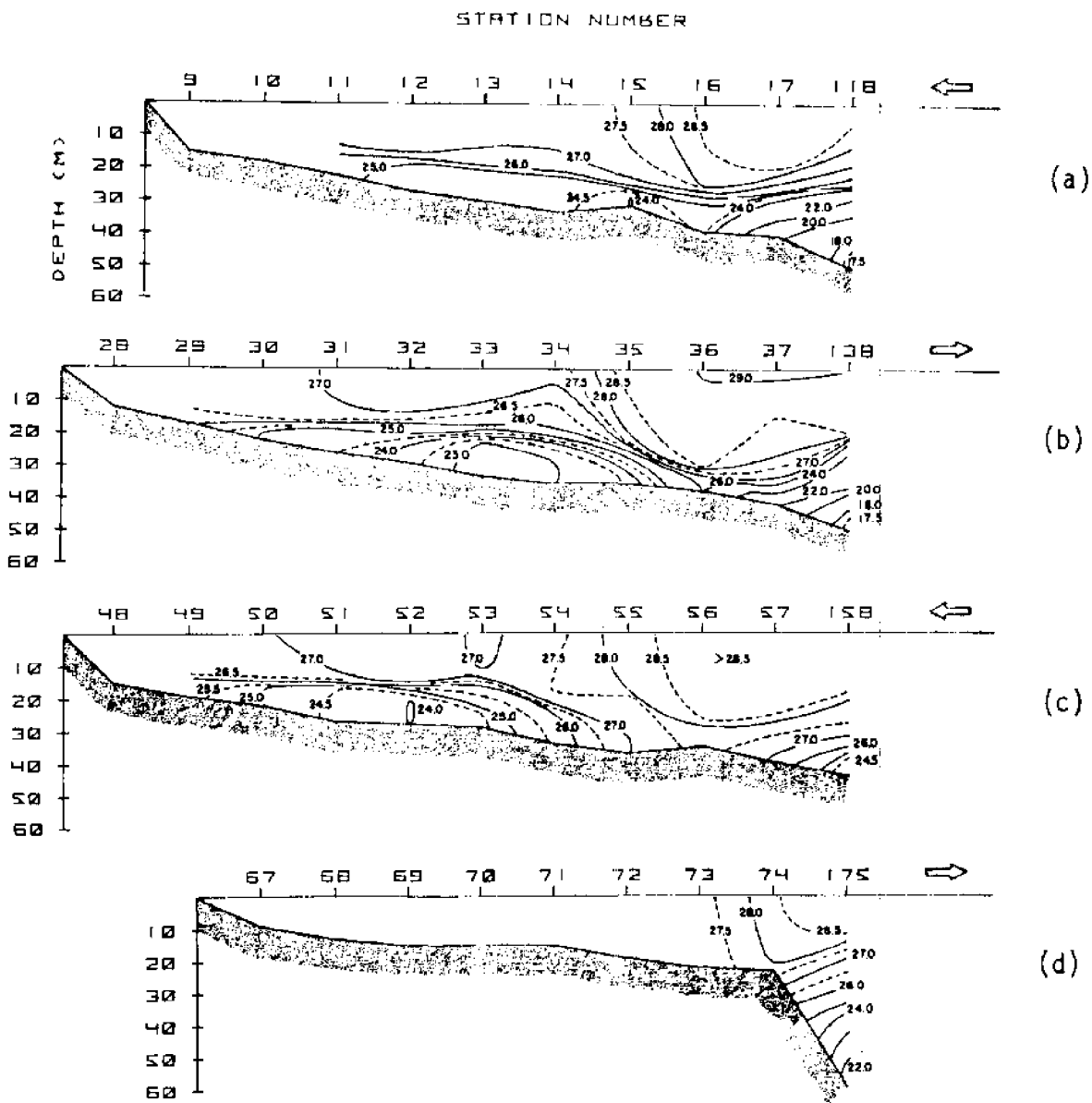
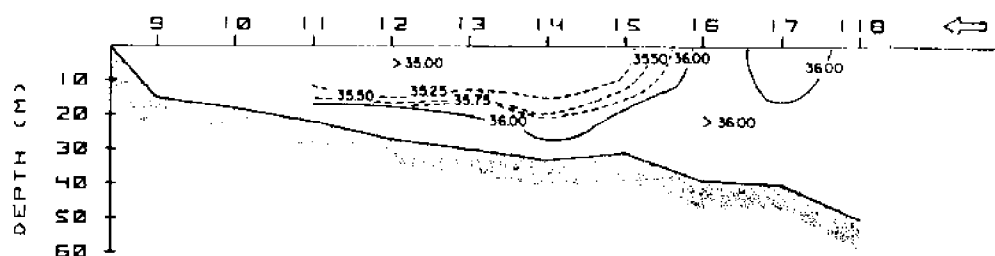


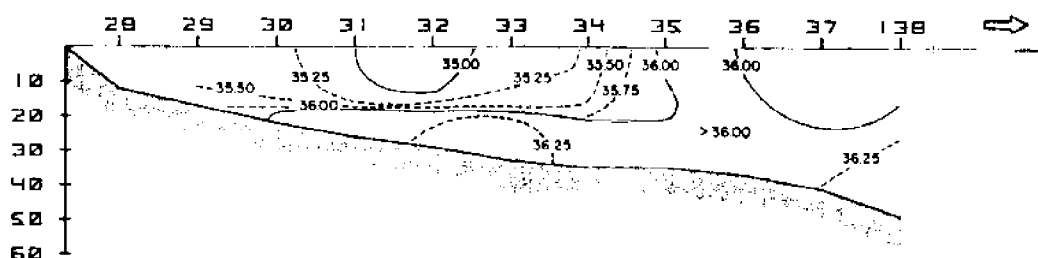
Figure 36. Vertical distribution of temperature (Hydro Grid IV).

SALINITY ‰
HYDRO GRID IV
14-16/VIII/76

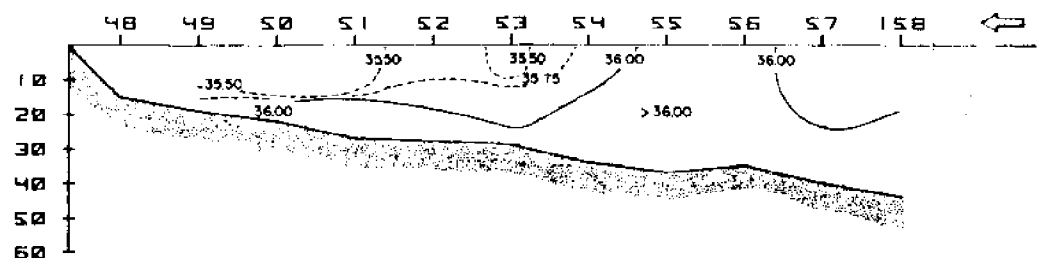
STATION NUMBER



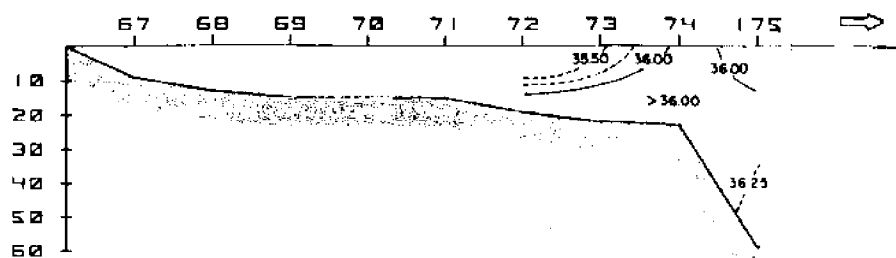
(a)



(b)



(c)



(d)

Figure 37. Vertical distribution of salinity (Hydro Grid IV).

SIGMA-T
HYDRO GRID IV
14-16/VIII/76

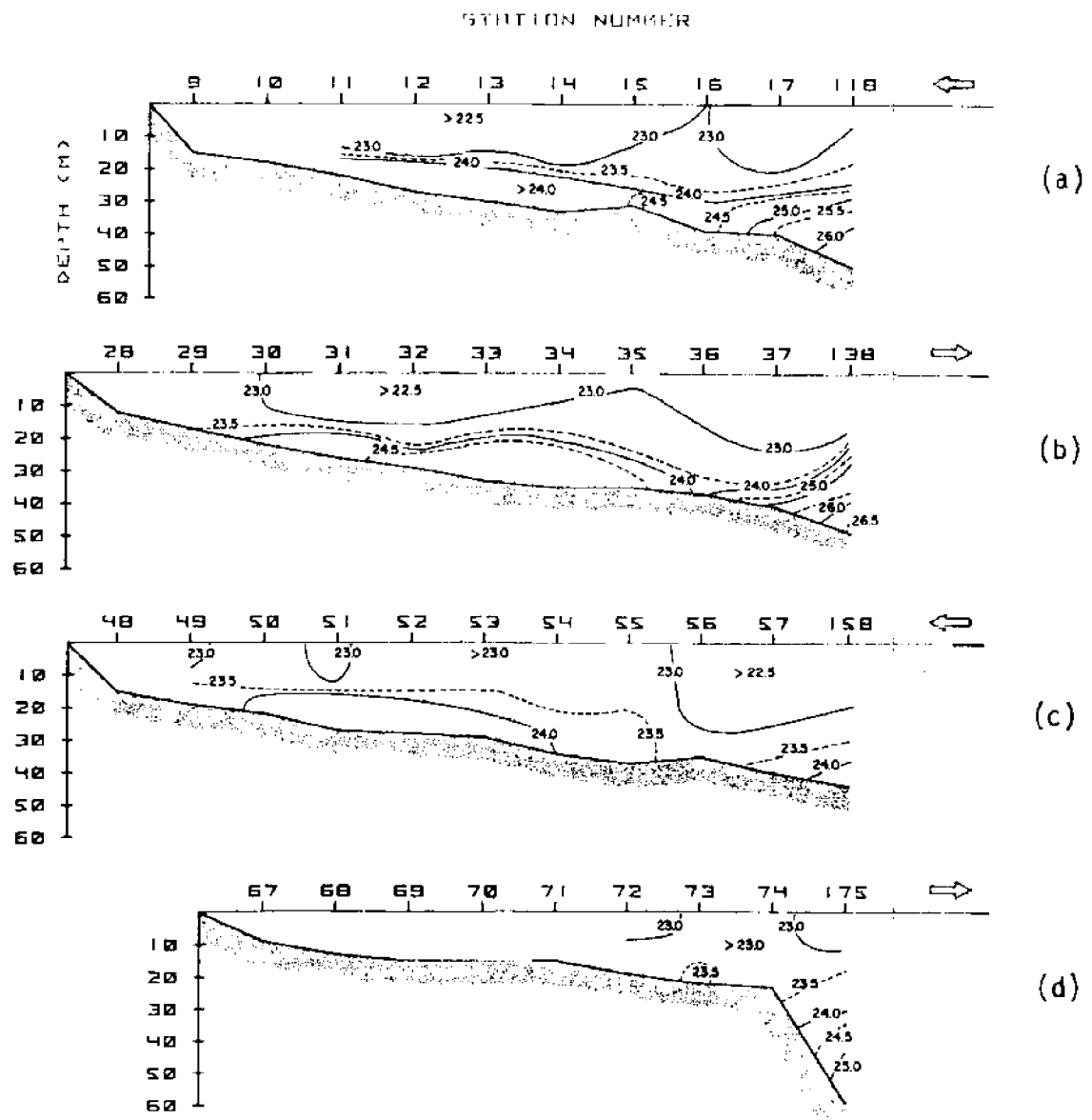


Figure 38. Vertical distribution of sigma-t (Hydro Grid IV).

NITRATE (MILLIMOL/L)
 HYDRO GRID IV
 14-16/VIII/78

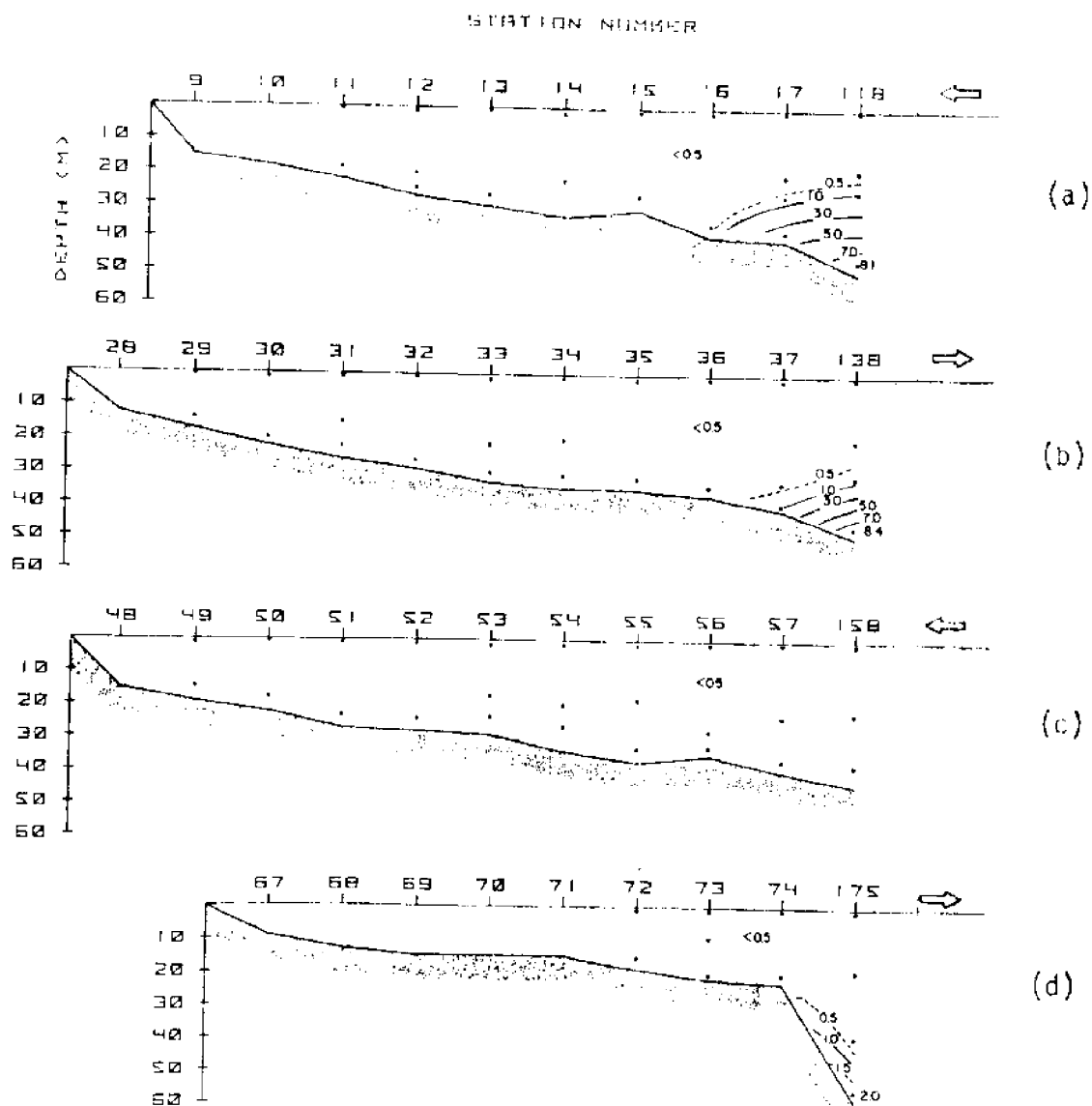


Figure 39. Vertical distribution of nitrate (Hydro Grid IV).

PHOSPHATE ($\mu\text{MOL/L}$)
 HYDRO GRID IV
 14-16/VIII/76

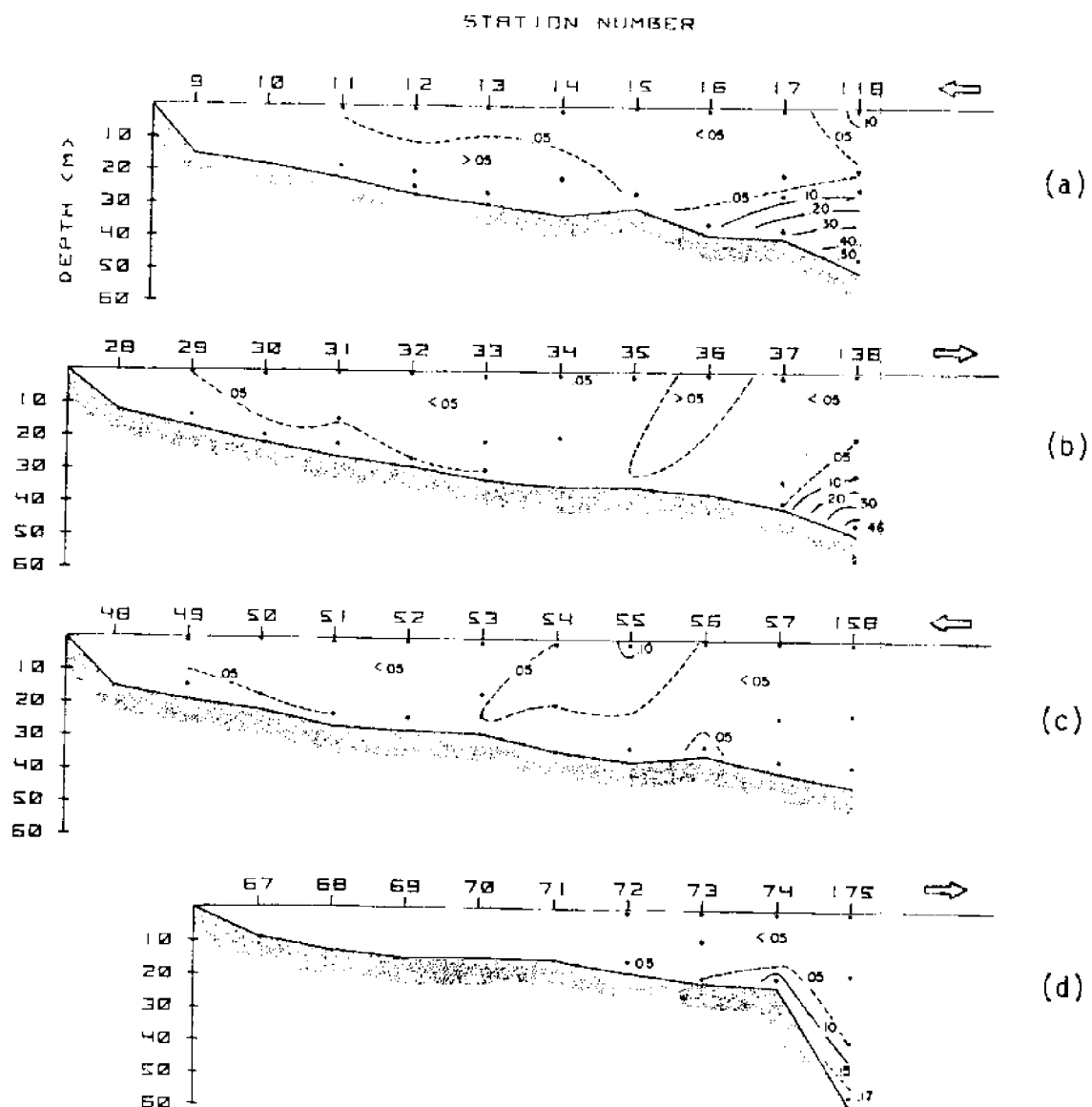


Figure 40. Vertical distribution of phosphate (Hydro Grid IV).

SILICATE ($\mu\text{MOLE/L}$)
 HYDRO GRID IV
 14-16/VIII/76

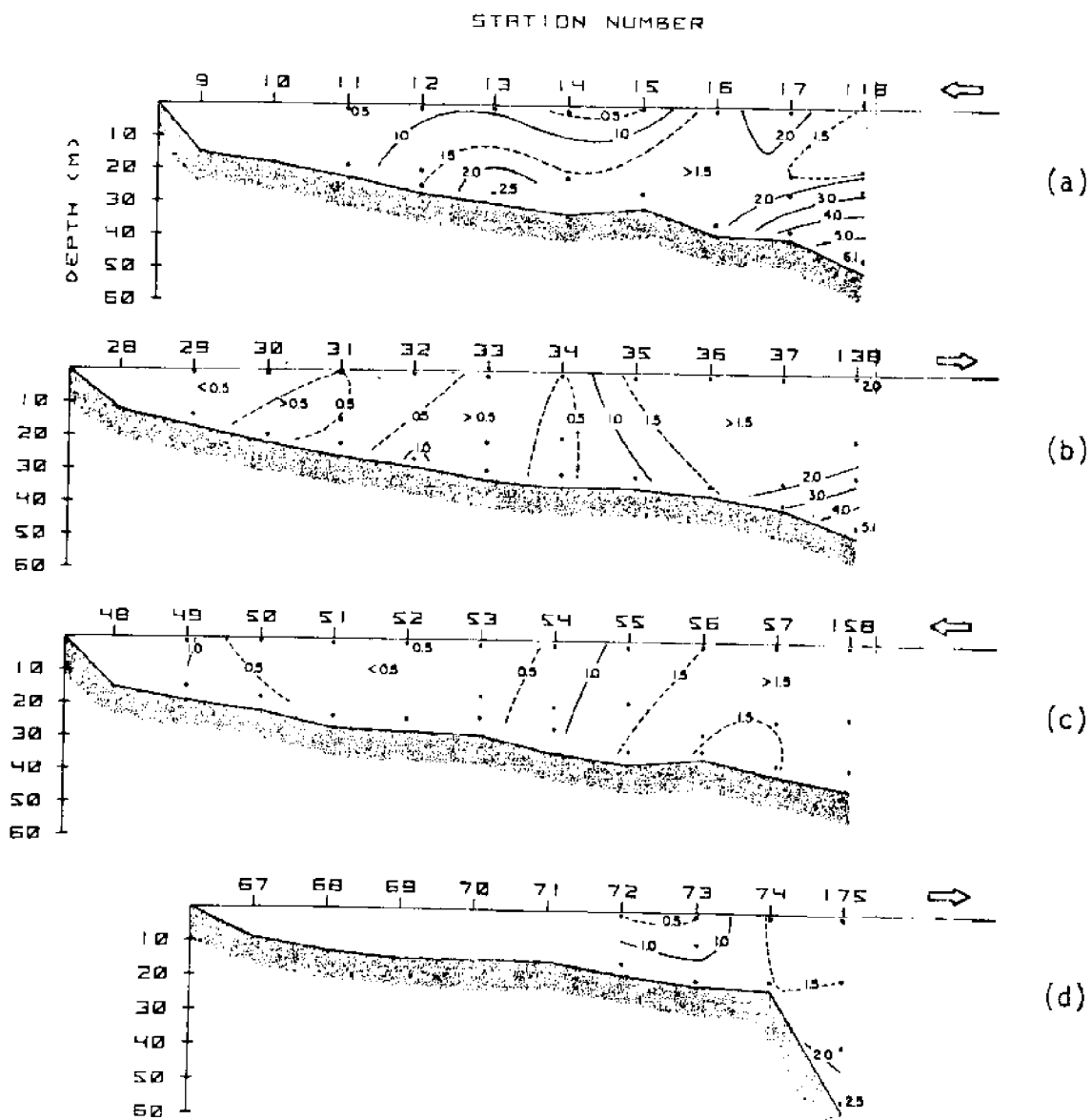


Figure 41. Vertical distribution of silicate (Hydro Grid IV).

Vertical Distribution of Physical and Chemical Properties (Bio Grids)

The tracks for the four bio grids made during this study period are shown in Figure 42. These correspond to regions of particular interest as ascertained from the hydro grids discussed in the preceding section. Only tracks (a) and (c) (Bio Grids I and III) were completed as originally conceived: four complete transects of the selected set of stations in a 24 hour period. Bio Grid II consisted of one passage along the indicated transect over a 12 hour span and Bio Grid IV consisted of two samplings of the indicated stations over a 9 hour span. For repeated transects, data collected at the end or turning station of one plot were used for the same station in the next plot. Sampling was identical to that reported earlier.

Bio Grid I. Bio Grid I suggests the recent separation of a cold core from an intruding tongue (Figure 43). This is probably related to the intrusion first observed moving onto the shelf 2 1/2 days earlier during Hydro Grid I (Figure 22). At that time a bottom temperature of 21.5°C was observed at station 65 and still colder waters appeared to be moving onto the shelf. During the Bio Grid, temperatures at this same station were observed to increase. In particular, note the change in the 22.0°C isotherm with time in Figure 43. It flattens and disappears. This change is possibly due to horizontal and vertical diffusion or to advection laterally along the shelf or to a combination of the two. Figures 44 and 45 characterize this region of intruded waters with typically high salinity and sigma-t values.

Figure 46 indicates that by the end of the second leg of the Bio Grid detectable nitrate concentrations at station 65 (the 22.0°C core) had fallen below $0.5\text{ }\mu\text{mole/liter}$. During the earlier Hydro Grid (Figure 25, page 45) concentrations as high as $2.0\text{ }\mu\text{mole/liter}$ had been observed. This suggests that even in a relatively young and cold intrusion core most of

the nitrate may be used up before the core has moved very far onto the shelf. In contrast, phosphate exhibited its greatest concentrations in the Bio Grid at station 65. This is shown in Figure 47(a) and (d). The lack of similar cores in plots (b) and (c) is thought to be due to the sampling method. The core of high phosphate water was apparently quite small vertically and was not sampled every time. No silicate data are available.

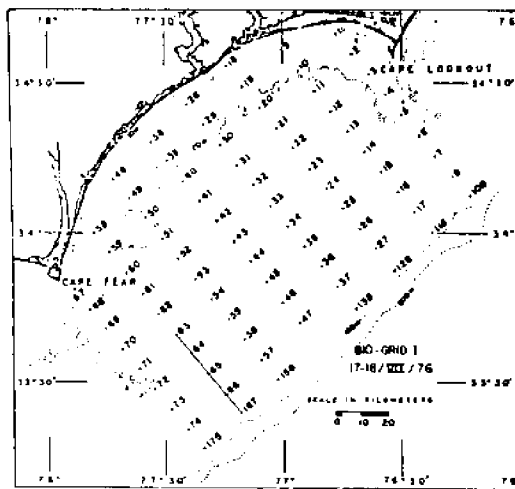
Bio Grid II. Bio Grid II consists of one transect the width of the shelf. The temperature, sigma-t and salinity plots (Figure 48) show an intrusion along the outer shelf with temperatures as low as 20.5°C at station 158. Also there is an older intrusion at mid-shelf with a core of 23.0°C. Both of these features were observed during Hydro Grid II along transects both north and south of this one, the most recent of which passed over the 23.0°C core 10 hours earlier (Figure 27, page 47). As was the case for the hydro grid, no trace of the older core is seen in the nitrate data. In addition, what trace there was of the older core in the phosphate record of Hydro Grid II is lost in Bio Grid II. The newer intrusion, however, is well defined by both nitrates and phosphates (Figure 49). No silicate data are available.

Bio Grid III. Bio Grid III is represented in the temperature, salinity and sigma-t plots of Figures 50-52. Note the well defined 22.0°C core on the shelf with its characteristic salinity and sigma-t profiles. The position of the 22.5°C isotherm suggests negligible onshore movement but perhaps some slight offshore movement over the 24 hour span of the bio grid. In addition, lateral movement along the shelf may have occurred. The apparent fluctuation in the size of the 22.0°C core is at least in part due to the scaling field for the parameter being contoured. Nitrate, phosphate and silicate concentrations as high as

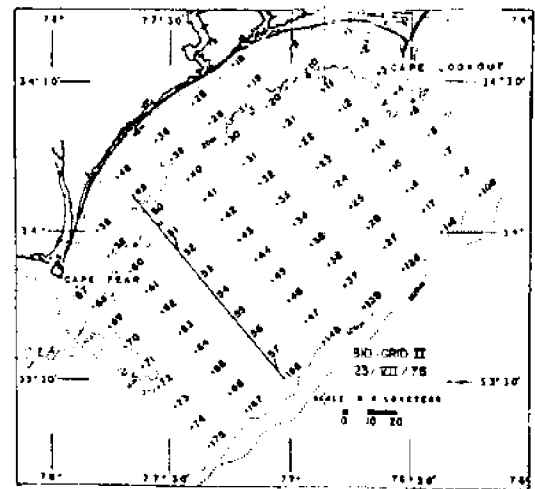
7.3, 0.18 and 3.5 $\mu\text{mole/liter}$ respectively were observed (Figures 53-55) They also suggest an offshore movement.

It is interesting to note that this intrusion core is isolated on the shelf with significant nitrate and phosphate concentrations whereas earlier in Bio Grid I an intrusion with a similar 22.0°C core exhibited negligible nitrate but similar phosphate concentrations. A possible explanation may lie in the relative age of the two.

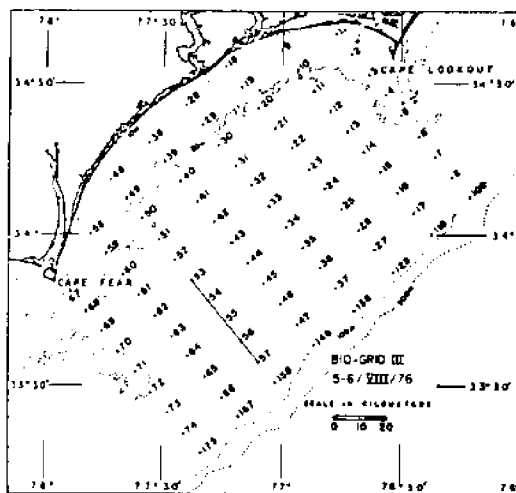
Bio Grid IV. Bio Grid IV consists of two passages along one transect. It was made nearly 24 hours later than the previous passage over this same transect during Hydro Grid IV (Figure 36). The 23.0°C core is still well defined as are the high salinity and sigma-t features (Figures 56-58). No significant onshore/offshore movement is apparent with respect to the earlier grid. Nitrate concentration is negligible but phosphate data still show some traces as defined by the $0.05 \mu\text{mole/liter}$ contours (Figures 59 and 60). The silicate data (Figure 61) are difficult to interpret.



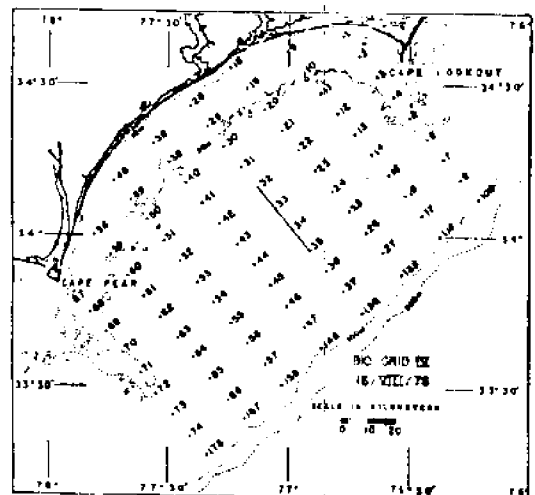
(a)



(b)



(c)



(d)

Figure 42. Cruise tracks for Bio Grids I, II, III and IV.

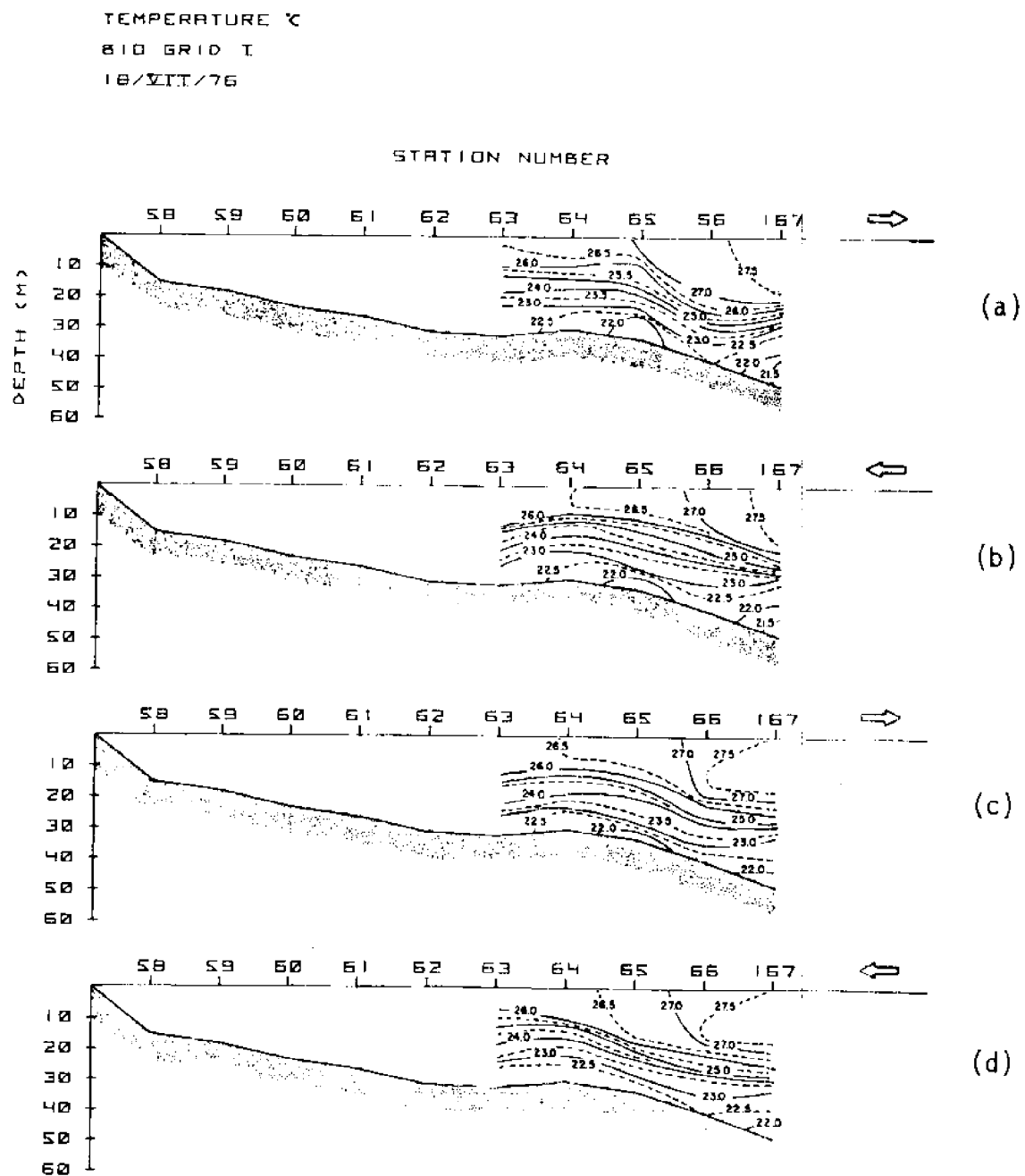


Figure 43. Vertical distribution of temperature (Bio Grid I).

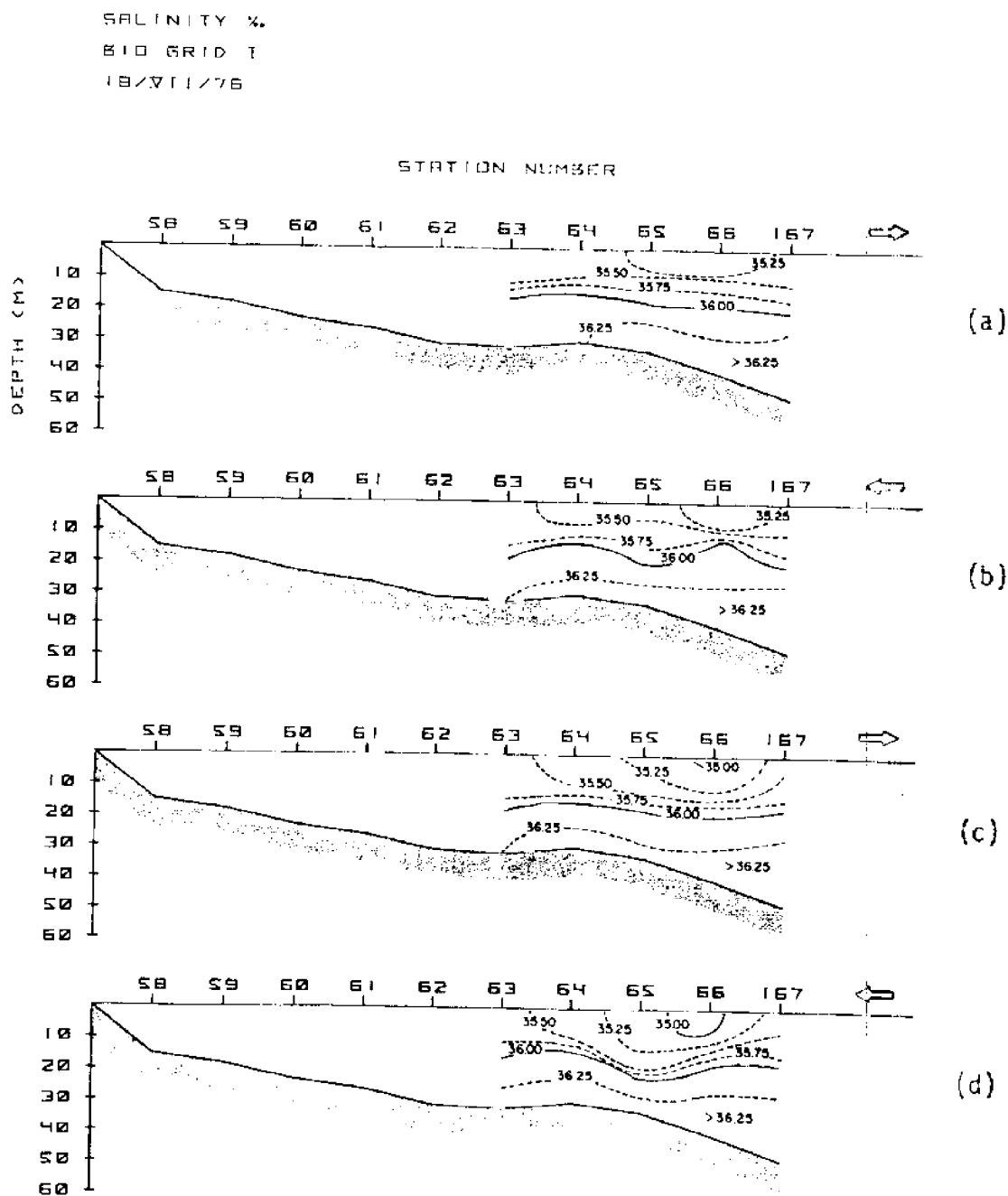


Figure 44. Vertical distribution of salinity (Bio Grid I).

SIGMA-T
BIO GRID 1
18/VII/76

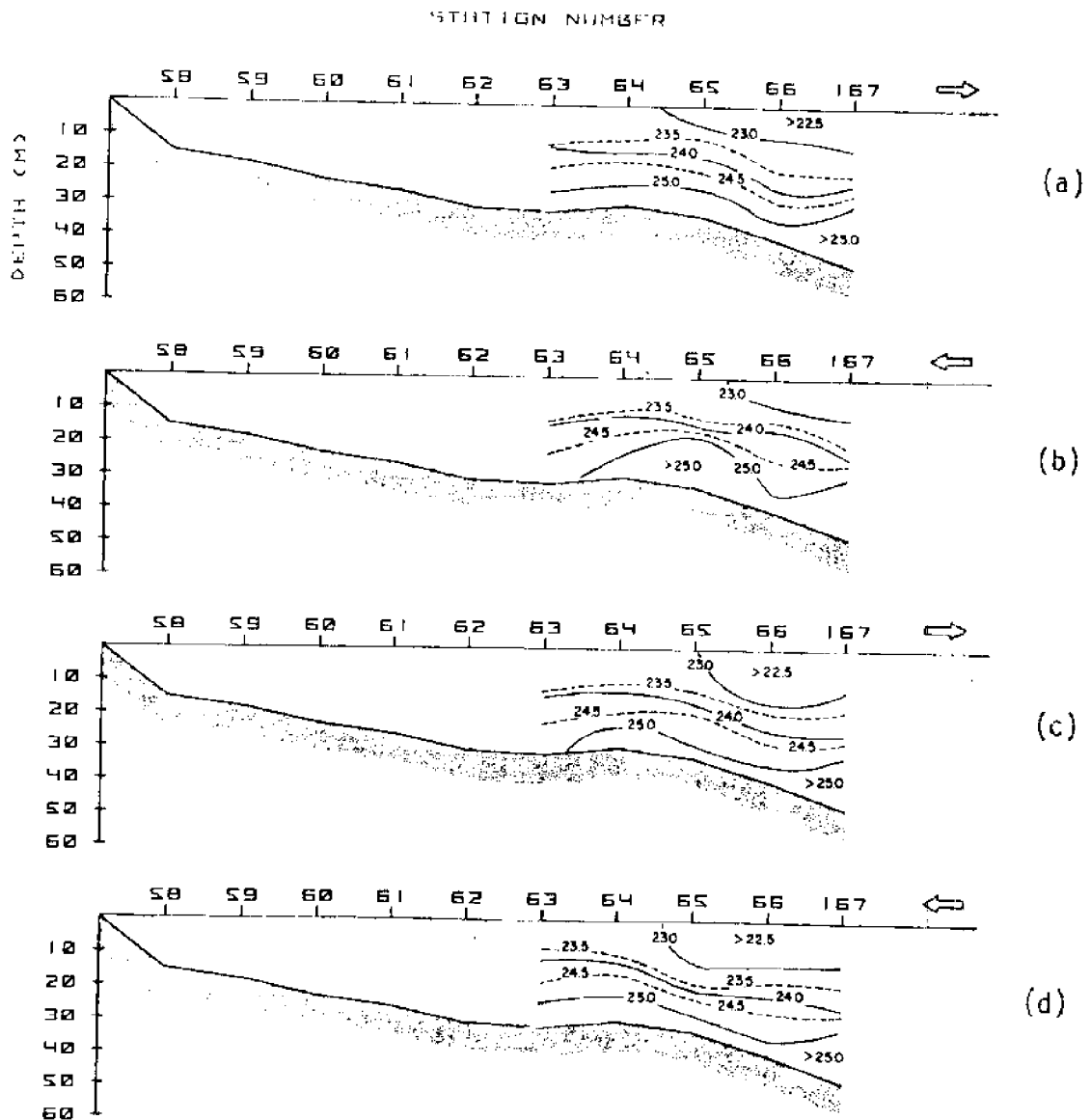


Figure 45. Vertical distribution of sigma-t (Bio Grid I).

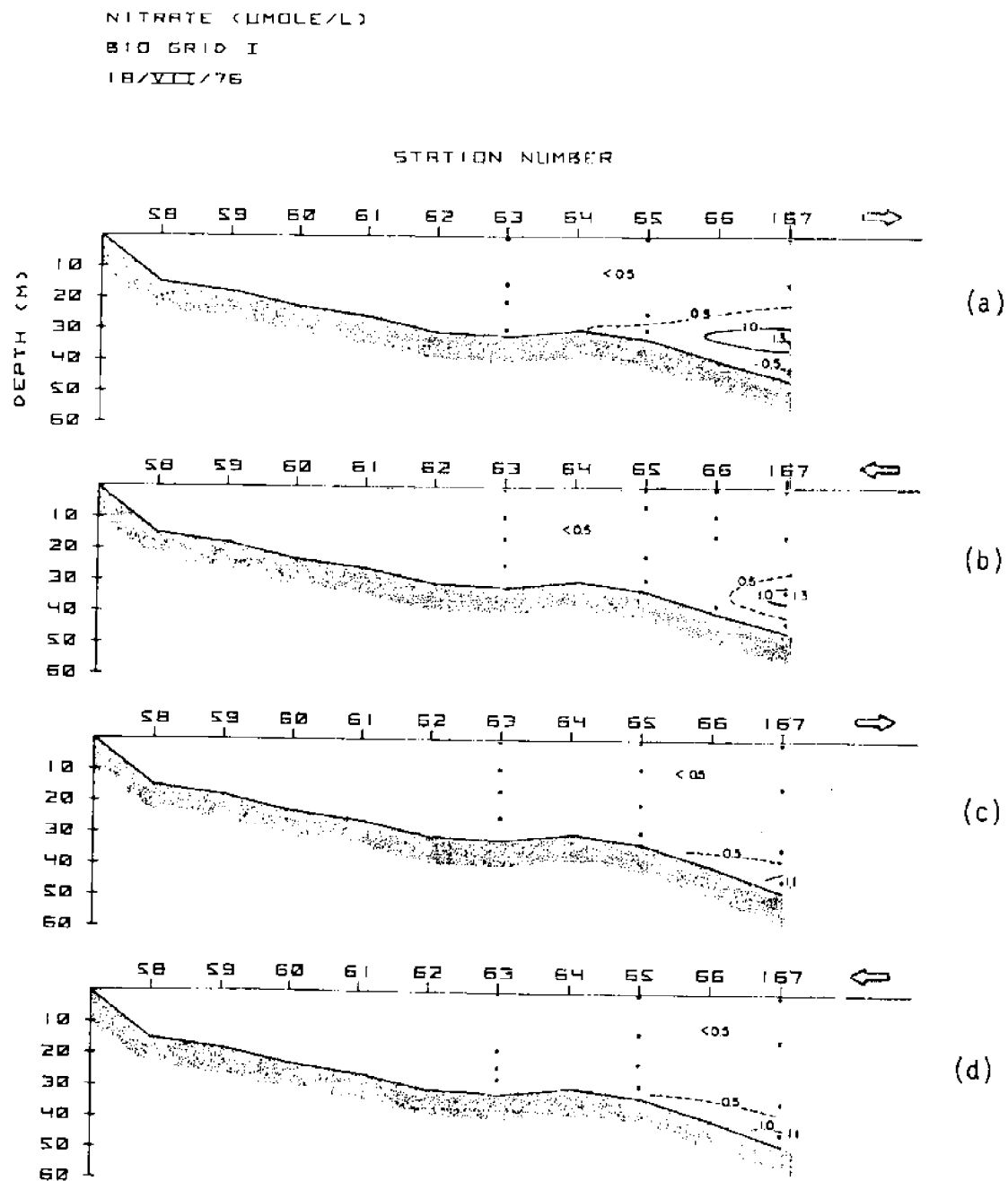


Figure 46. Vertical distribution of nitrate (Bio Grid I).

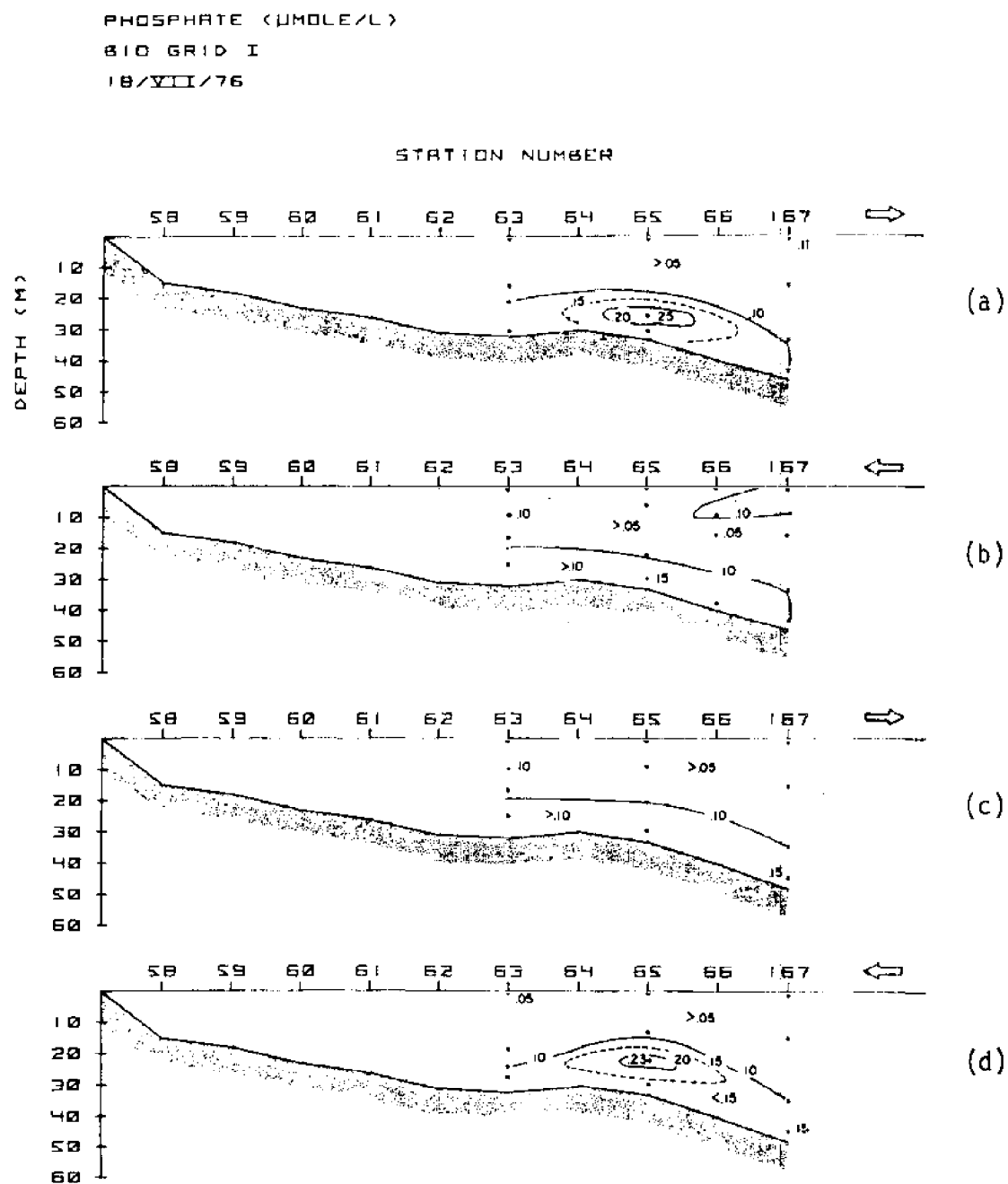


Figure 47. Vertical distribution of phosphate (Bio Grid I).

BIO GRID II

23/VII/76

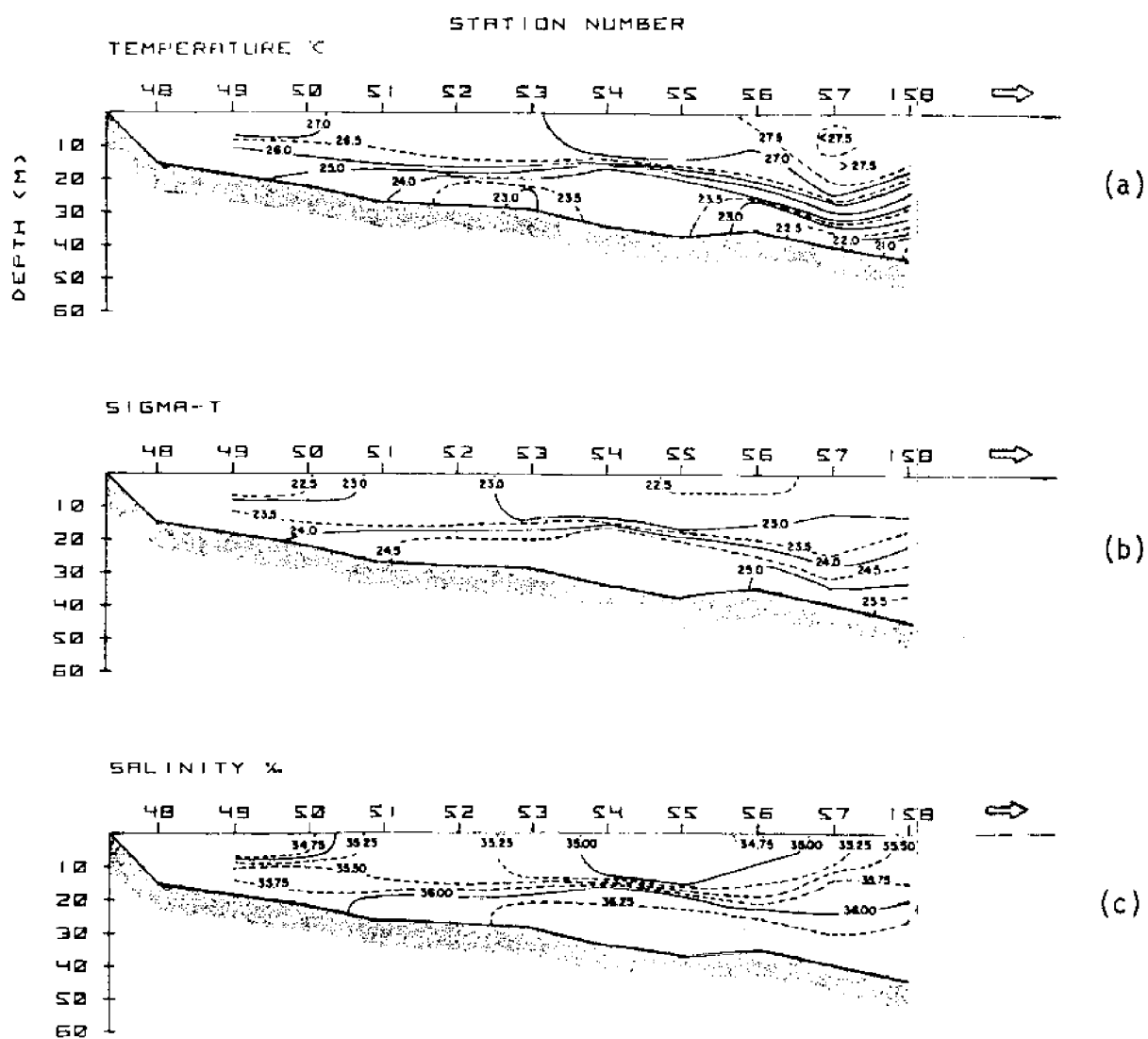


Figure 48. Vertical distribution of temperature, sigma-t and salinity (Bio Grid II).

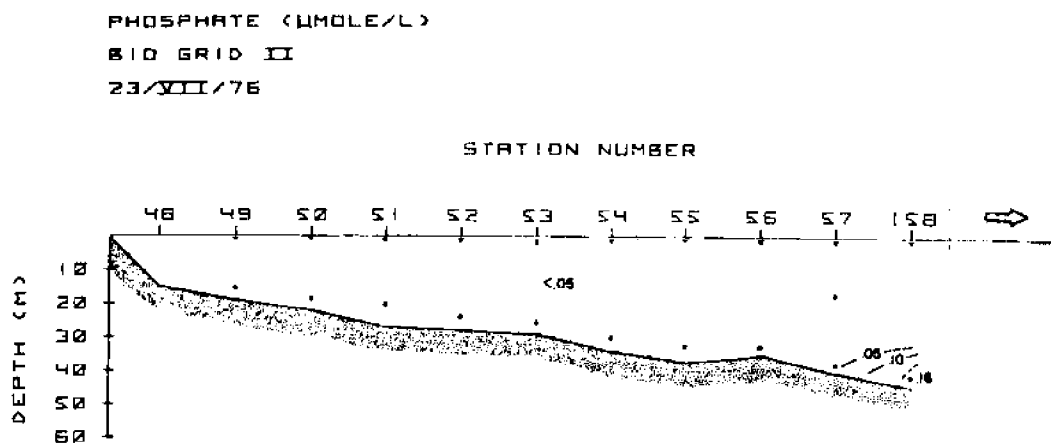
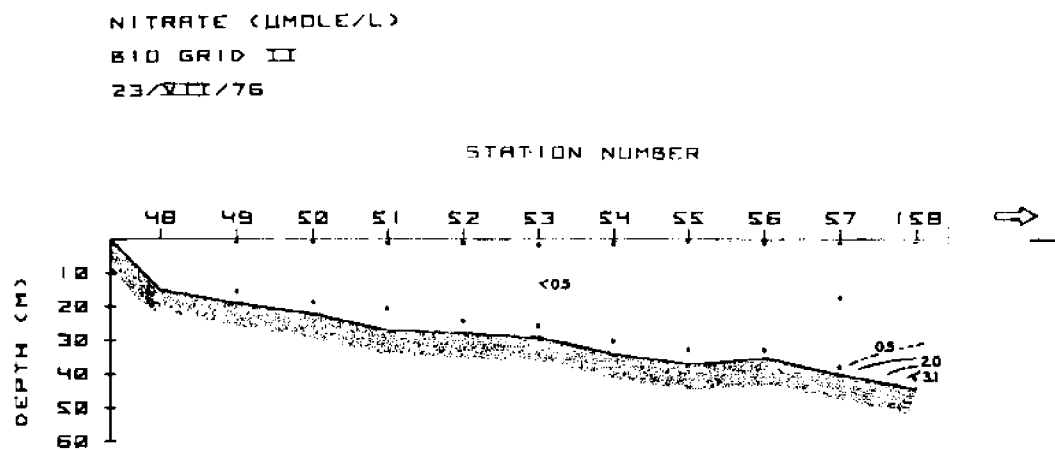


Figure 49. Vertical distribution of nitrate and phosphate (Bio Grid II).

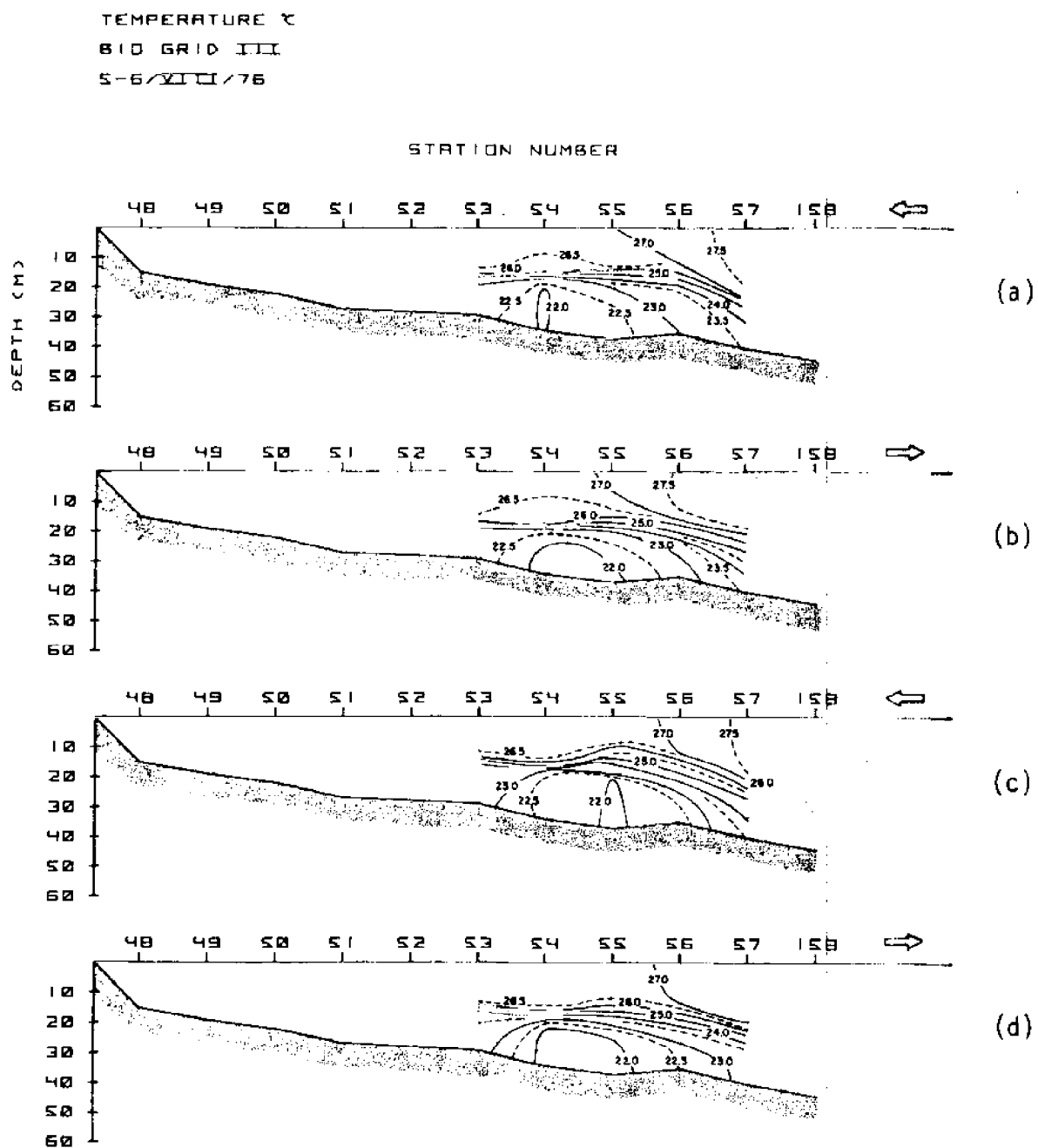


Figure 50. Vertical distribution of temperature (Bio Grid III).

SALINITY ‰
 BIO GRID III
 S-6/VIII/76

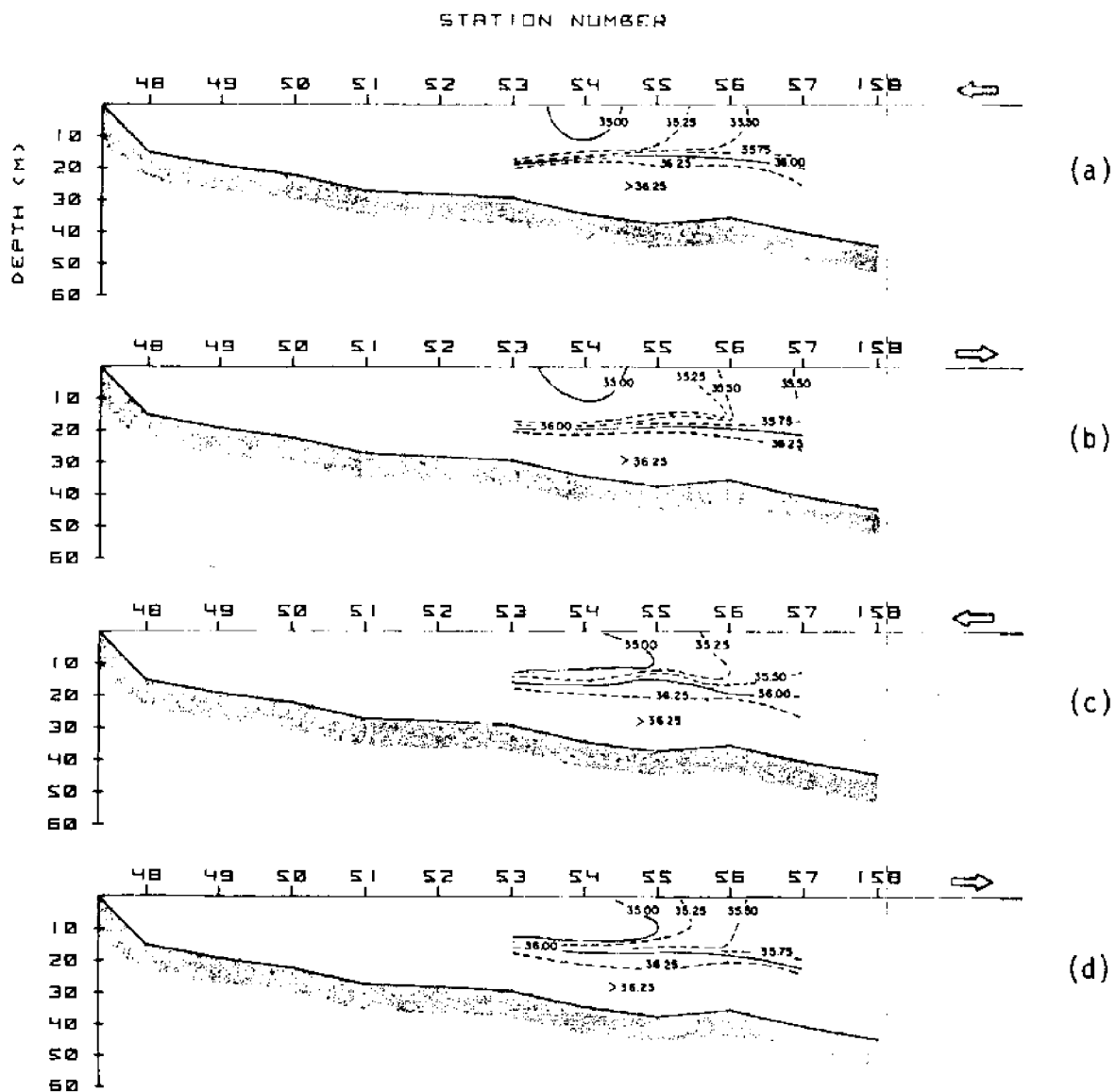


Figure 51. Vertical distribution of salinity (Bio Grid III).

SIGMA-T
 BIO GRID III
 5-6/VIII/76

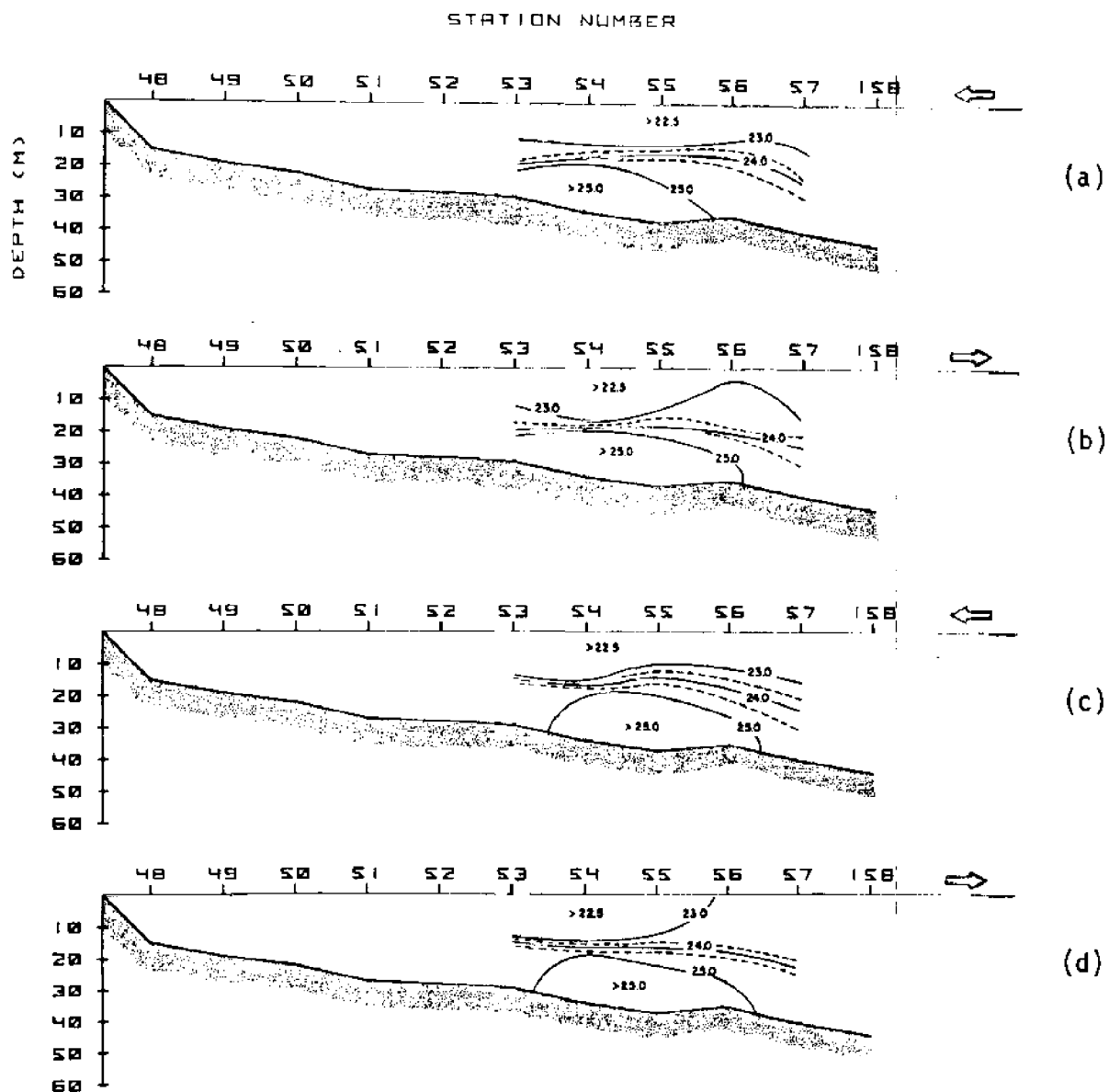


Figure 52. Vertical distribution of sigma-t (BIO Grid III).

NITRATE ($\mu\text{MOLE/L}$)
 BIO GRID III
 5-6/VIII/76

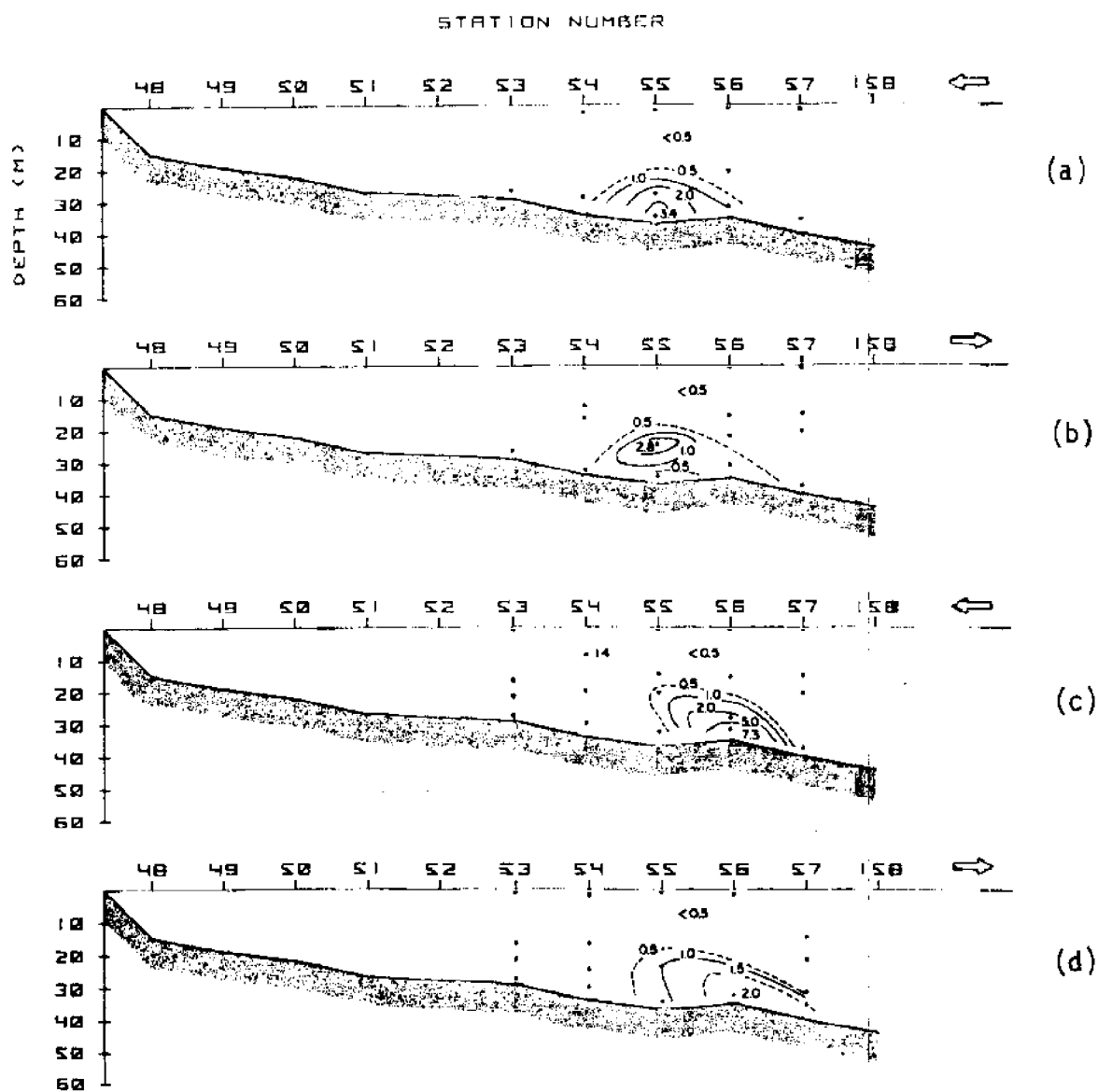


Figure 53. Vertical distribution of nitrate (Bio Grid III).

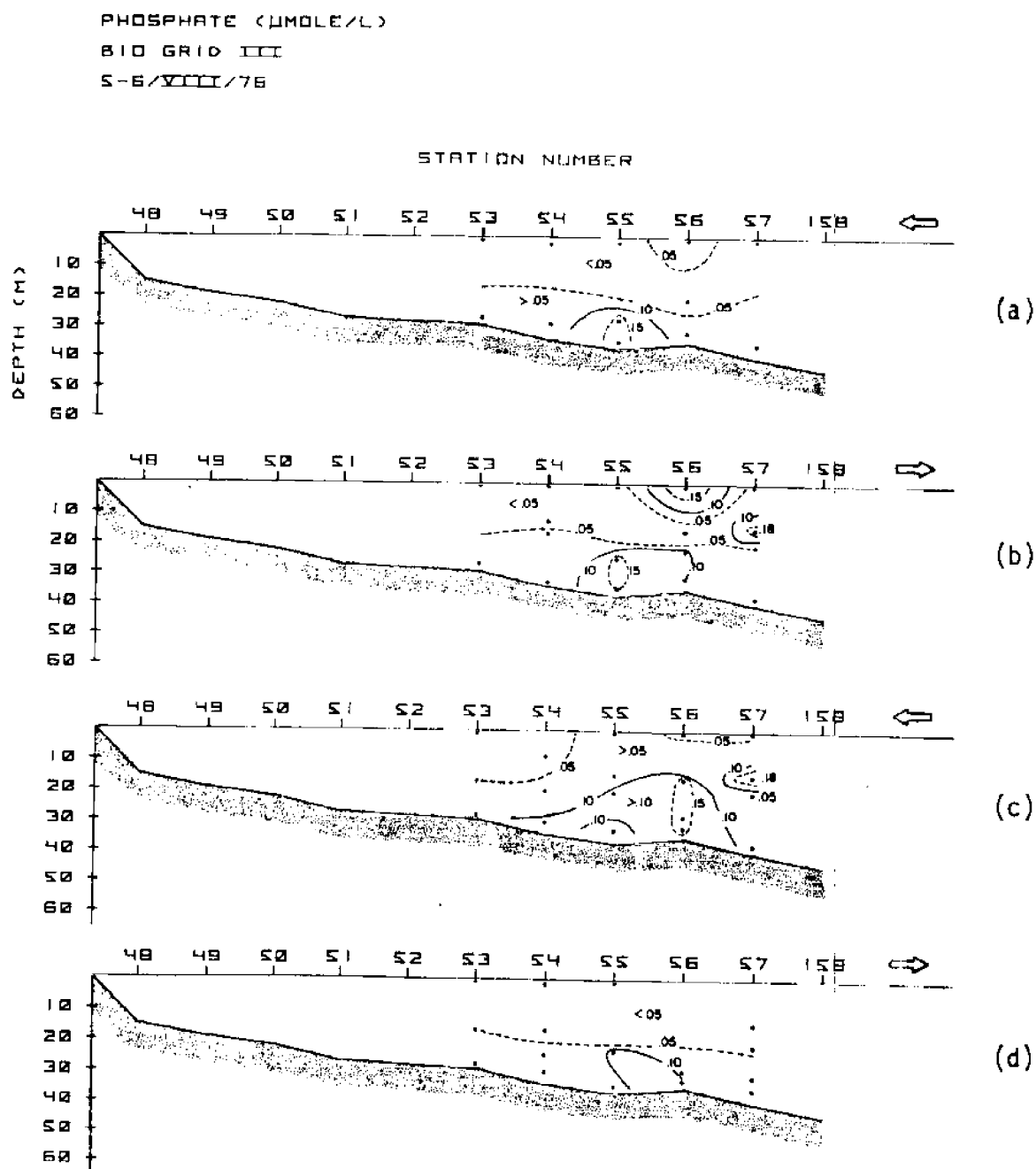


Figure 54. Vertical distribution of phosphate (Bio Grid III).

SILICATE ($\mu\text{MOLE/L}$)

BIO GRID III

5-6/VIII/76

STATION NUMBER

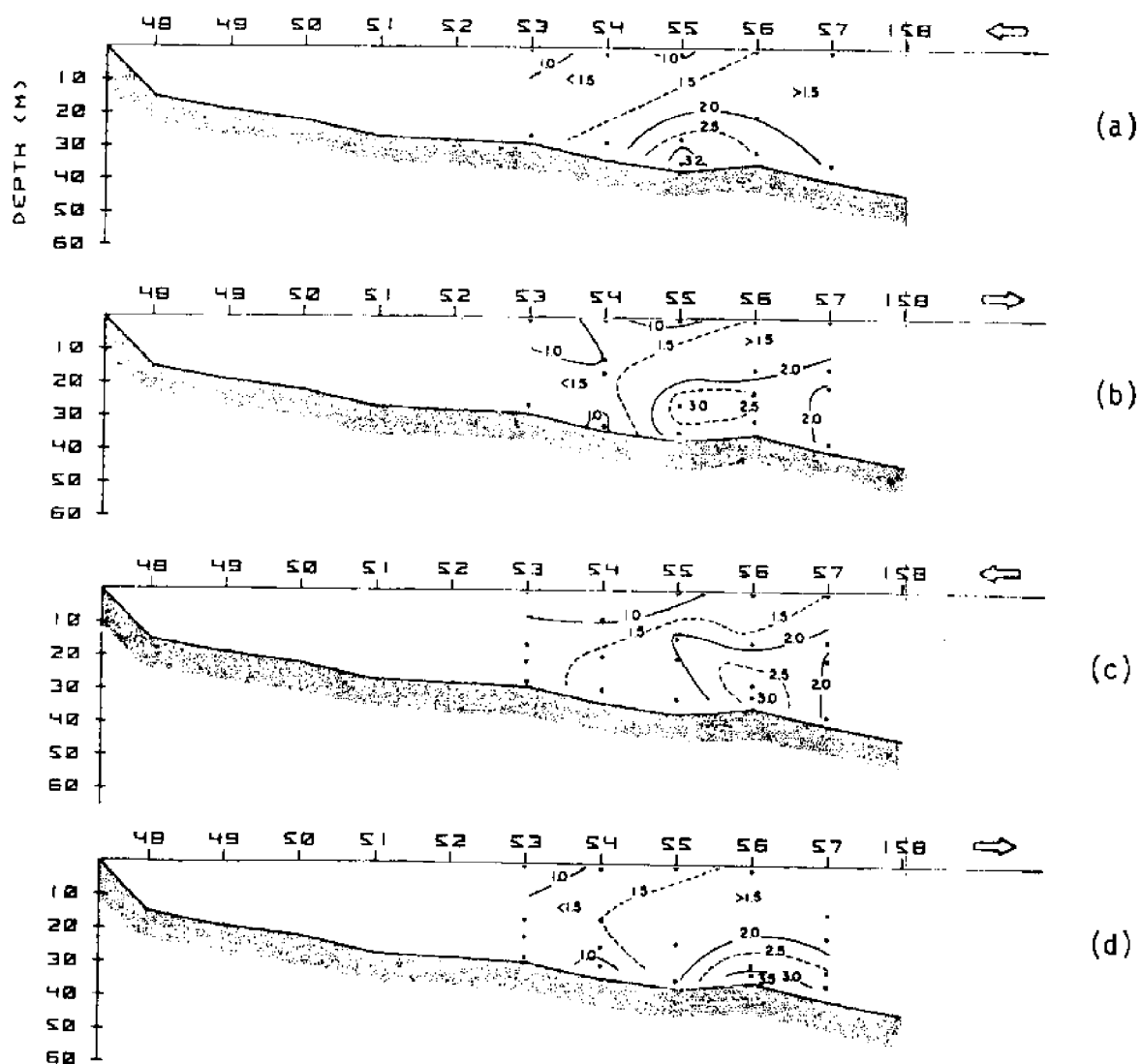
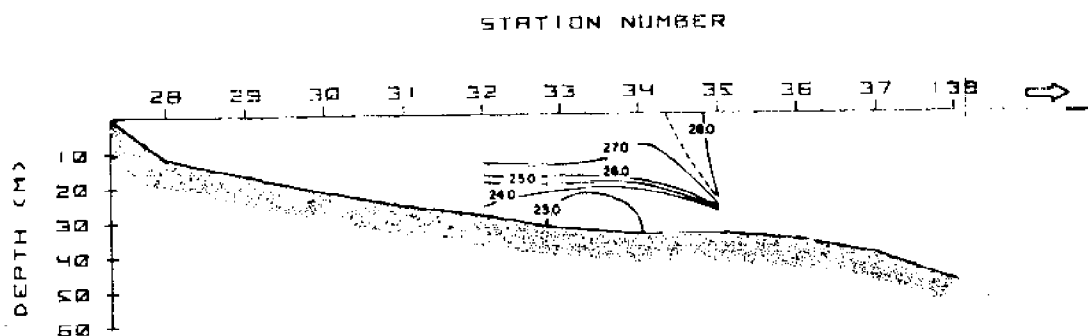
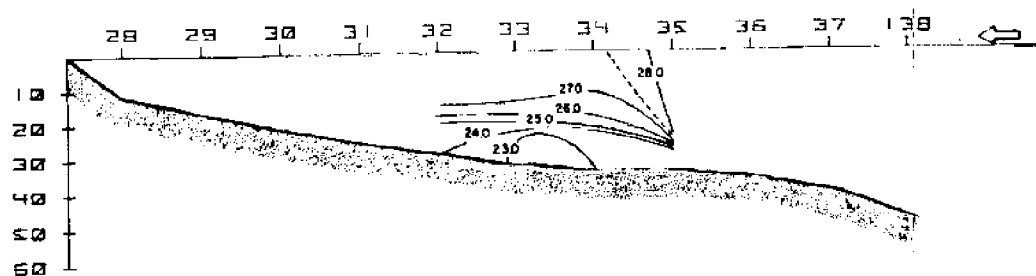


Figure 55. Vertical distribution of silicate (Bio Grid III).

TEMPERATURE °C
 BIO GRID IV
 16/VIII/76



(a)



(b)

Figure 56. Vertical distribution of temperature (Bio Grid IV).

SALINITY ‰
 BIO GRID IV
 16/VIII/76

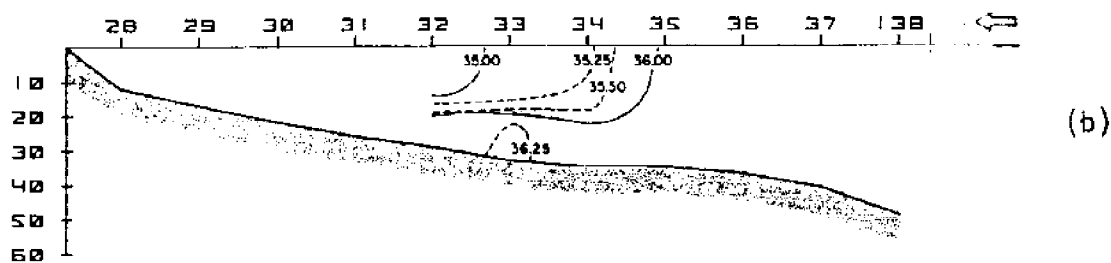
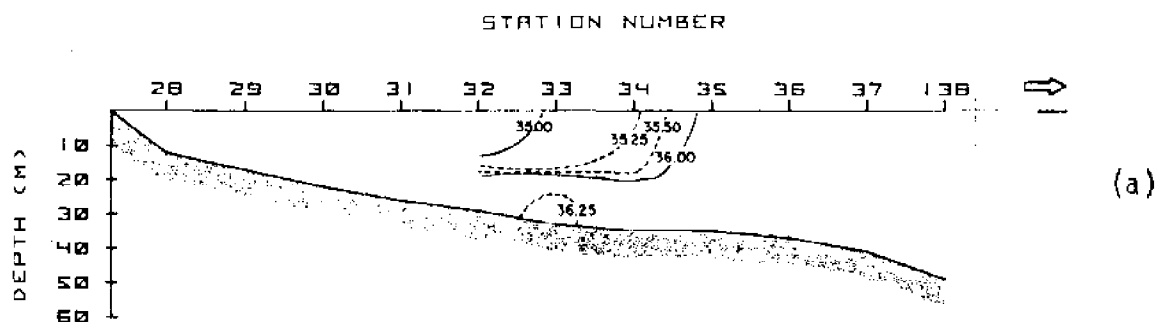


Figure 57. Vertical distribution of salinity (Bio Grid IV).

81

NITRATE ($\mu\text{MOL/L}$)

BIO GRID IV

16/VIII/76

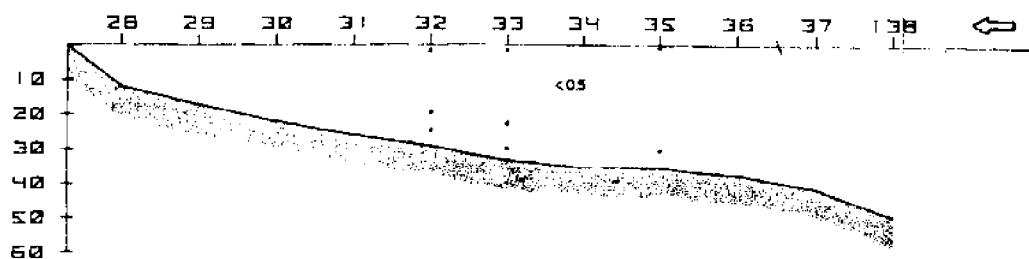
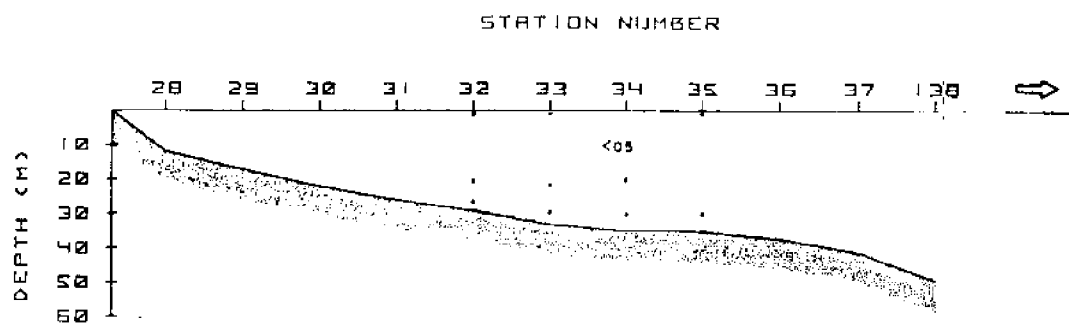


Figure 59. Vertical distribution of nitrate (Bio Grid IV).

NITRATE (μ MOLE/L)

BIO GRID IV

16/VIII/76

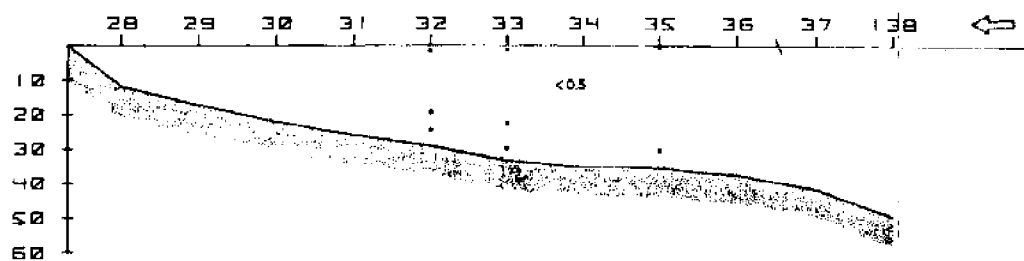
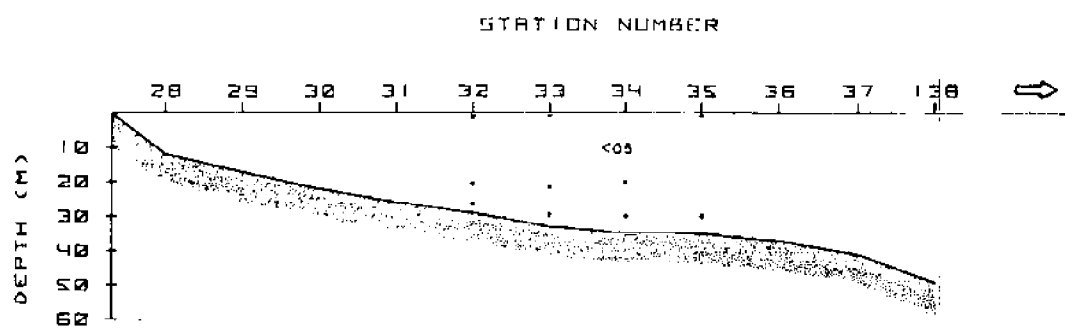
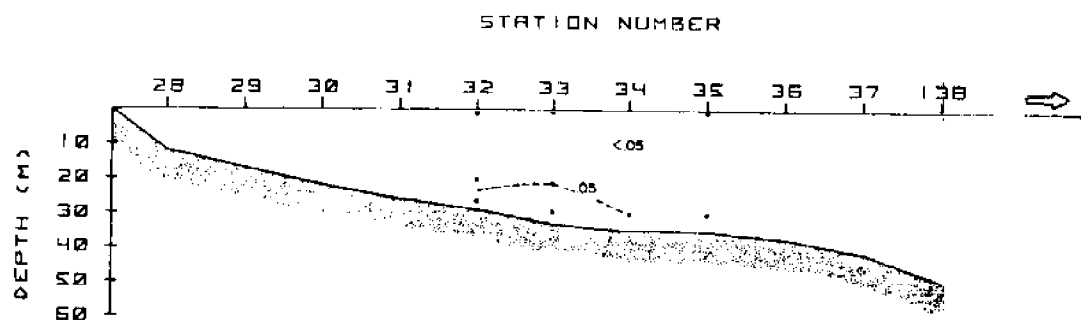
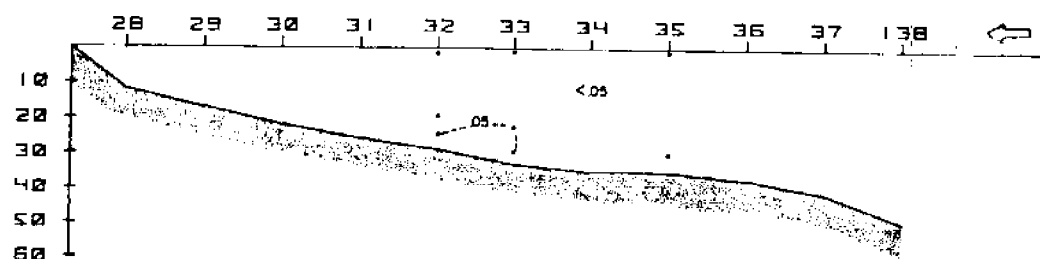


Figure 59. Vertical distribution of nitrate (Bio Grid IV).

PHOSPHATE ($\mu\text{MOLE/L}$)
 BIO GRID IV
 16/VIII/76



(a)



(b)

Figure 60. Vertical distribution of phosphate (Bio Grid IV).

SILICATE ($\mu\text{MOL/L}$)

BIO GRID IV

16/VIII/76

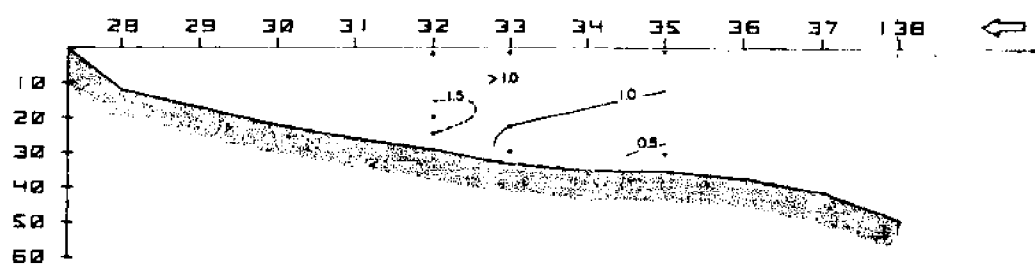
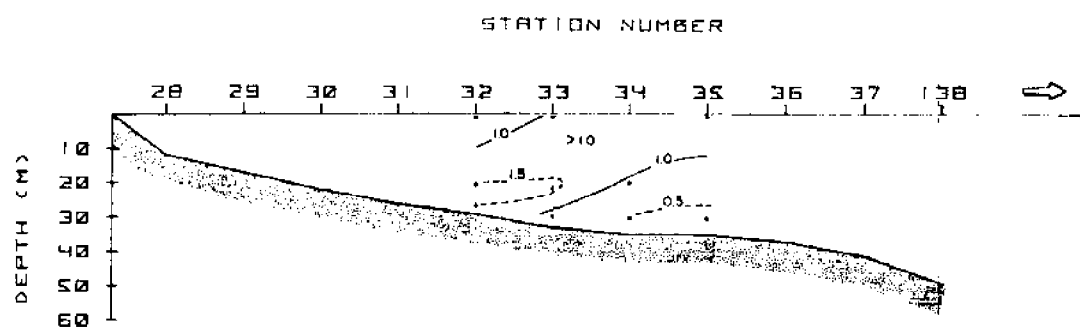


Figure 61. Vertical distribution of silicate (Bio Grid IV).

T-S Plot

A T-S plot of all temperature and salinity data is presented (Figure 62). The shelf waters are characterized by the low salinity-high temperature region of the plot. Gulf Stream waters are apparent in the highest temperature region and generally along the right hand edge of the plot. Slope waters are less easily defined but they occur between the shelf and Gulf Stream values (Stefánsson, Atkinson and Bumpus, 1971).

Nitrate vs. Phosphate

A plot of nitrate vs. phosphate is made of the entire data set (Figure 63). It reveals that most of the data are characterized by low values of these parameters. The lower values correspond to what are thought to be older intrusions with regenerated or unused phosphate and the higher value with the newer and cold intrusion events. A line drawn through zero and the higher nitrate concentrations would closely approximate the 16:1 ratio so characteristic of deeper off shelf waters.

Salinity vs. Silicate

This plot (Figure 64) is a composite of all silicate data collected during the study. It shows the high salinity region of the surface Gulf Stream waters with silicate in the 1.0 to 3.0 $\mu\text{mole/liter}$ range. Also, deeper Gulf Stream waters are represented by the higher silicate values in this region. The shelf waters are represented by silicate values less than 3.0 $\mu\text{mole/liter}$ in waters less than 36.00‰. No significant near-shore processes (runoff) appear to be evident from this plot. However, it should be noted that silicate data are not available for the first half of the study period (Hydro Grids I and II) and this may account for such an absence.

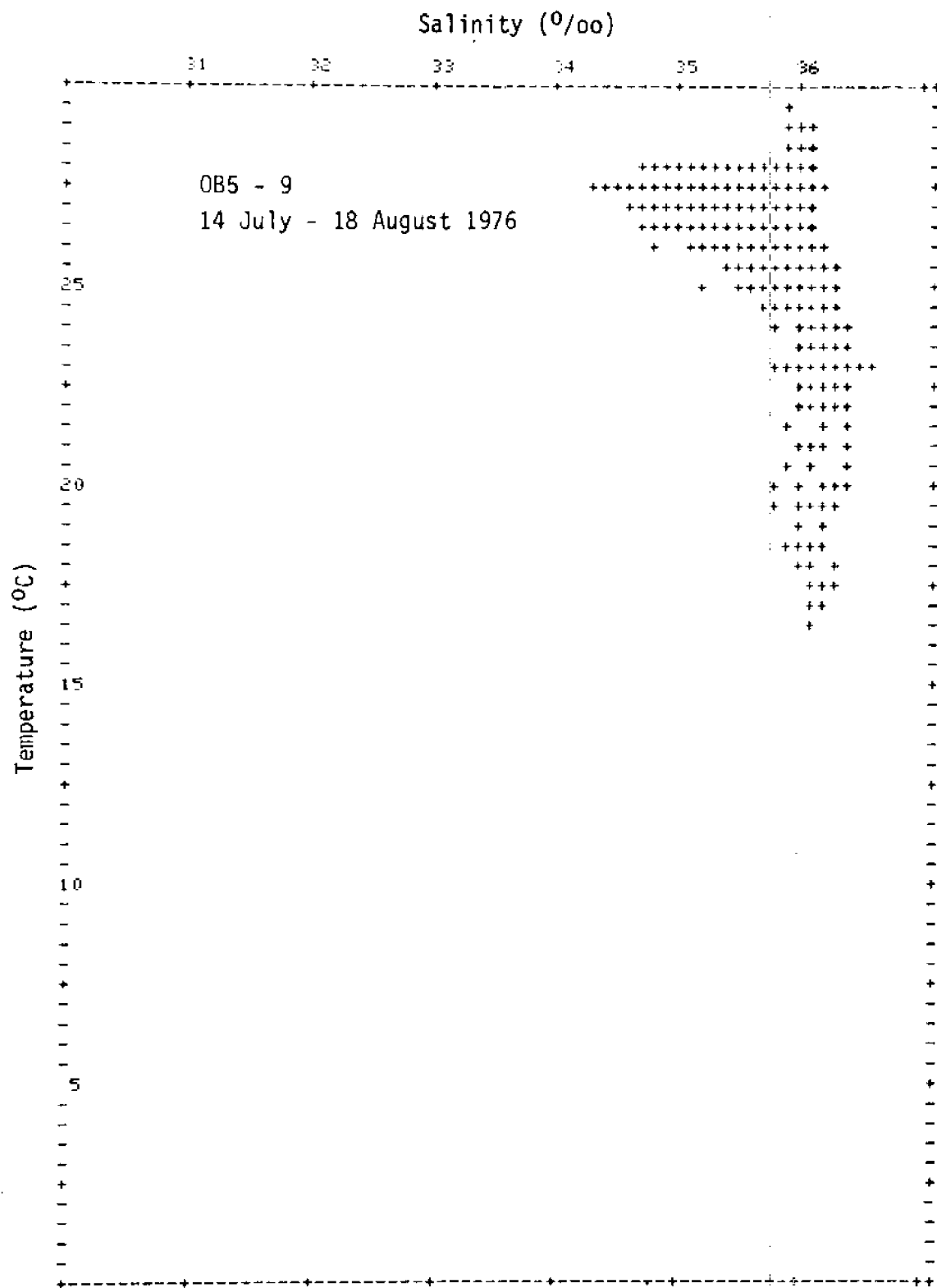


Figure 62. T-S plot (OBIS V).

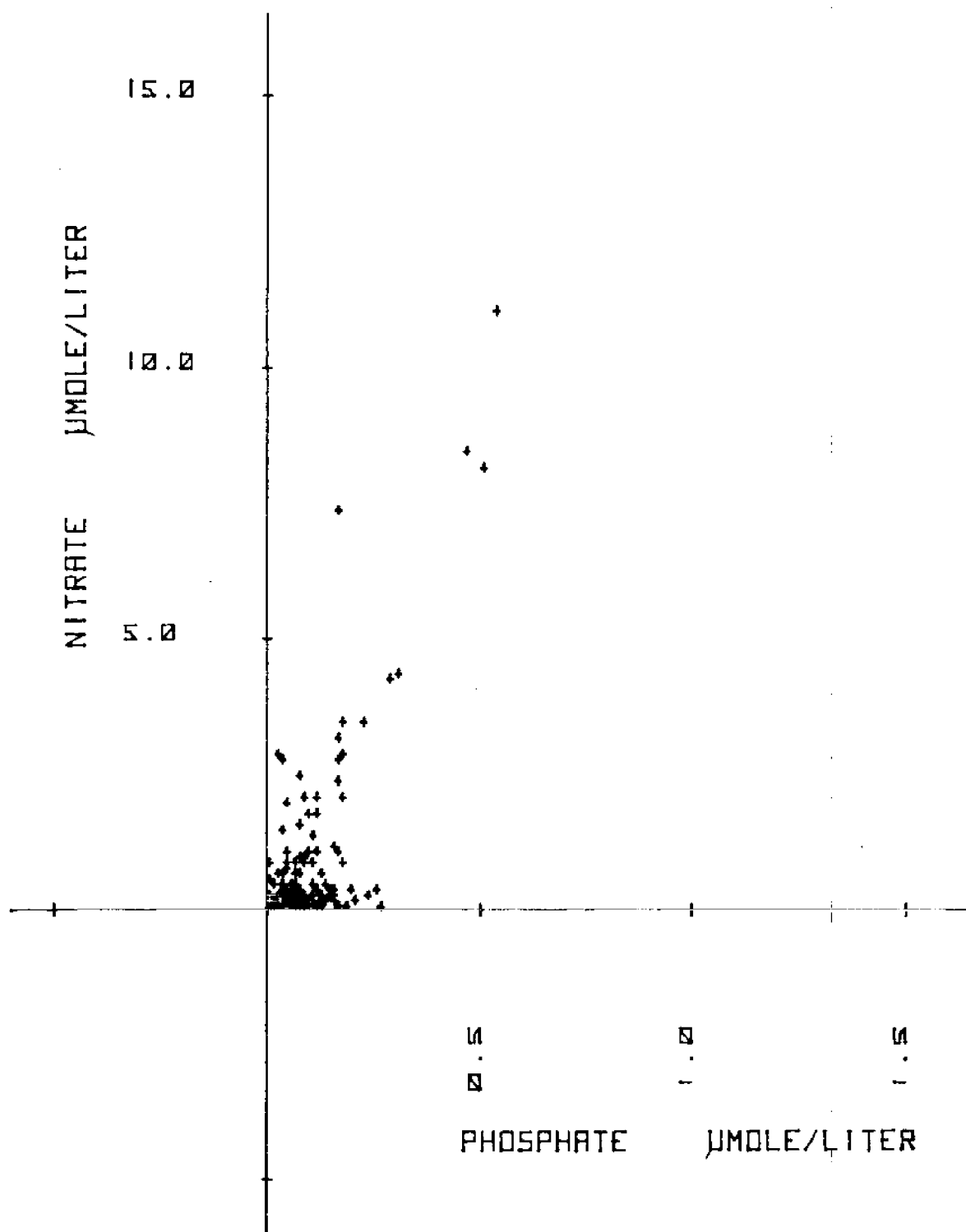


Figure 63. Plot of nitrate Vs. phosphate.

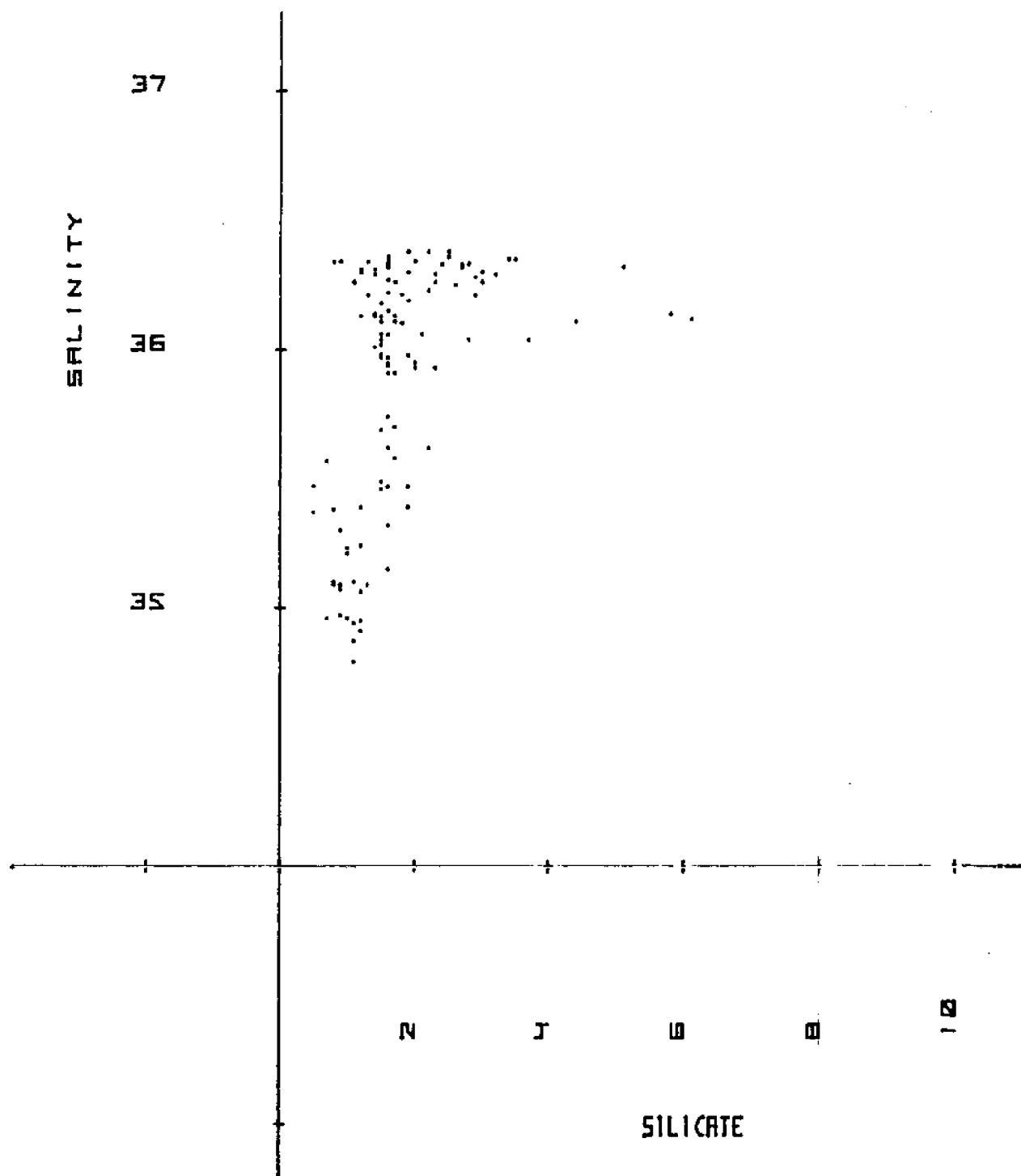


Figure 64. Plot of salinity Vs. silicate.

SUMMARY AND CONCLUSIONS

The data collected during OBIS V indicate the occurrence of at least four different intrusion events over the course of the study period. It seems probable that there were more than four such events and if so this should show up in the current meter data. Three intrusion cores were observed isolated on the shelf and three cold tongues were observed moving onto the shelf during the three hydro grids and the one XBT grid. In addition, there may be some correlation between some of these intrusion tongues and the isolated cores.

The passing of Hurricane Belle on 9 August may be responsible for the appearance of the cold water on the shelf on 14-16 August during Hydro Grid IV. This may also explain an intrusion event commencing in the northeastern offshore sector of Onslow Bay in advance of the southern sector where all previous intrusions had been observed to begin. The hurricane's closest passage of the Bay came in this same northeastern sector.

Low temperature, high salinity and high sigma-t values correlate to the intrusion phenomenon. In addition, relatively high nitrate and phosphate concentrations correspond to what appear to be the youngest intrusion events. In the older intrusion cores often times significant phosphate concentrations persist in spite of negligible nitrate concentrations. This is probably due to unused or regenerated phosphate. Silicate appears to be a more conservative tracer. However, it has the added complication that higher values are characteristic of both high salinity intrusion waters and lower salinity nearshore waters. Analysis of all of these data relative to the current meter data should provide a rather complete description of the Onslow Bay system during the observational period.

LIST OF REFERENCES

- Atkinson, L. P., J. J. Singer and L. J. Pietrafesa. 1976a. Onslow Bay intrusion study: Hydrographic observations during current meter servicing cruises in August, October and December 1975 (OBIS I, III and IV). Georgia Marine Science Center, Technical Report 76-4.
- Atkinson, L. P., J. J. Singer, W. M. Dunstan and L. J. Pietrafesa. 1976b. Hydrography of Onslow Bay, North Carolina: September 1975 (OBIS II). Georgia Marine Science Center, Technical Report 76-2.
- Bradshaw, A. and K. E. Schleicher. 1965. The effect of pressure on the electrical conductance of sea water. *Deep-Sea Res.*, 12:151-162.
- Gardner, W. S., D. S. Wynne and W. M. Dunstan. 1976. Simplified procedure for the manual analysis of nitrate in sea water. *Mar. Chem.*, 4:393-396.
- Jaeger, J. E. 1973. The determination of salinity from conductivity, temperature, and pressure measurements. *Proceedings Second S/T/D Conference and Workshop*, January 24-26, 1973, 29-43.
- Knowles, C. E. 1973. CTD sensors, specific conductance and the determination of salinity. University of North Carolina Sea Grant Program, Sea Grant Publication UNC-SG-73-16.
- Mullin, J. B. and J. P. Riley. 1955. The colorimetric determination of silicate with special reference to sea and natural waters. *Anal. Chim. Acta* 12:162-176.
- Murphy, J. and J. P. Riley. 1962. Modified single solution method for the determination of phosphate in natural waters. *Anal. Chim. Acta* 27:31-36.
- National Institute of Oceanography at Great Britain and UNESCO. 1966. *International Oceanographic Tables*, Wormley, Godalming, Surrey, England.

- National Institute of Oceanography of Great Britain and UNESCO. 1973. International Oceanographic Tables, Vol. 2, Wormley, Godalming, Surrey, England.
- Stefánsson, U., L. P. Atkinson and D. F. Bumpus. 1971. Hydrographic properties and circulation of the North Carolina shelf and slope waters. Deep-Sea Res., 18, 383-420.
- Strickland, J. D. H. and T. R. Parsons. 1965. A manual of sea water analysis. Fisheries Res. Board of Canada, Bull. No. 125 (2nd ed.), Ottawa.
- U. S. Department of Commerce, NOAA, EDS. 1976. Local climatological data, monthly summary, Cape Hatteras, North Carolina, July and August 1976. National Climatic Center, Asheville, N. C.

APPENDIX
SUMMARY OF EVENTS:
OBIS V

SUMMARY OF EVENTS: (OBIS V)

Cruise OB5 - OB9 (in EDT)

0923 - 8 July Departed Skidaway Institute, Savannah, GA (Atkinson
to Baker). Arrived at Duke University Marine Lab (DUML),
1445 - 9 July the land base for OBIS V.

0845 - 9 July Tested CTD while enroute to DUML (System inoperative -
repairs made).

1335 - 10 July Departed DUML (Atkinson, Singer, Chandler, Hofmann,
to Kelly, Porter, White, Baker, Paffenhofer, Diebel, Sands,
1737 - 10 July McIntyre, and Hosford). The purpose of this day cruise
was to test the repaired CTD and to allow all personnel
to become familiar with planned procedures. Carroll
Baker still had to work on the electronics. The Rosette
bottles were not tripping. We also later discovered that
the magnetic tape had not received the data signals (only
headers and blank data sets were recorded). It took a
week to discover this because the tapes were sent to the
computer center at UGA, and then from our terminal a
programming sequence was used to extract the data from
the tapes. Fortunately we had backup XYY trace for all
data sets.

11 July At the DUML dock Carroll Baker worked on the CTD. The
SCR in the Rosette was replaced, but still the bottles
were not tripping. The problem was found to be cold
solders in the Rosette deck unit.

1500 - 12 July Departed DUML (Atkinson, Singer, Kelly, Porter,
to White, Baker, Paffenhofer, Sands, McIntyre, and
1820 - 12 July Hosford) for HYDRO GRID I. We were delayed from an early
departure by an out of town trip for spare CTD electronics,
a trip to the hardware store by the crew, and having to
take the cook to the bus station after firing him. When
we did get off, six foot seas at the sea buoy and severe
storm warnings turned us back. However, we did make one
CTD cast and it was handled well from the A-frame off the
stern.

1915 - 13 July HYDRO GRID I. Departed DUML with the same scientific
to crew as for 12 July. At 0200 on 14 July we started
1940 - 15 July firing XBTs and hanging bottles because of a short in the
CTD cable. Both the Sandpiper depth finder and the
Raytheon fathometer were inoperable, so the last available
unit (Simrad) gave depths in fathoms with minimal
accuracy. At 1007, 14 July we resumed CTD casts after
replacing the CTD 9-pin conductor and fixing the short.
At 0300 15 July, the CTD shorted out again. It appeared
that the cable had been caught in the sheave of the
winch. We cut off 10 feet of sea cable, re-scotchcasted
it, and had the CTD operational at 0840, 15 July. In the
meantime, we fired XBTs and hung bottles. When CTD
operations resumed, the 'YYY' plotter could not be
calibrated with the 10V source so we had to use the
built-in settings of .25V/cm for depth and .5V/cm for

conductivity and temperature. Finally, as noted earlier, data was not recorded on magnetic tape during this cruise because of a problem with the Digital Data Logger (DDL) so data analysis relied on the XYY' traces. During the cruise we were unaware of this problem.

- 0947 - 17 July BIO GRID I. Departed DUML (Atkinson, Baker, Chandler, to Porter, Paffenhofer, Diebel, Sands, McIntyre, and 0335 - 18 July Hosford). An intrusion seen in the south end of Onslow Bay during HYDRO GRID I brought us back there for a biological and hydrographic transect. At 1846, 17 July an XBT was fired at Station 62. The results were unexciting, so we started the transect at Station 63, going offshore and including stations 64 through 167. We made four passes; the CTD operated perfectly! In heavy seas we used a lead weight to dampen the swinging Rosette. It was also necessary to dampen the slack in the sea cable as the boat rolled during a cast. The same lack of data transfer to the magnetic tape occurred as in HYDRO GRID I.
- 0825 - 21 July HYDRO/BIO II. Departed DUML (Singer, Chandler, White, to Kelly, Paffenhofer, Diebel, Sands, McIntyre, and Hosford). 0145 - 24 July We did a hydrogrid that covered the entire bay. It directed us to stations 49 - 157 for the subsequent biogrid along which a single transect was made. The CTD worked well. Personnel were instructed to zero and calibrate (full scale) the XYY' plotter more frequently

because data had not been going on the magnetic tapes. The 'YYY' plotter's autogrip did not hold very well for most of the cruise.

0810 - 28 July
to
1723 - 28 July

Departed DUML (Singer, Chandler, Hofmann, Porter, Paffenhofer, Diebel, Sands, Dunstan, and Hosford) for HYDRO/BIO III. After the first two hydrogrid stations, we proceeded to a current meter mooring to attach a buoy for NCSU. After completing the task, we returned to port because of poor radio communications. Carroll Baker had repaired the DDL so that data was being recorded; however, the headers did not have file gaps in front of them, and the depth signal was now folding at one quarter of what should have been full scale.

0800 - 30 July
to
0730 - 31 July

Departed DUML (Chandler, Hofmann, Porter, White, Paffenhofer, Diebel, Sands, Dunstan, and Hosford). This time we completed one track of HYDRO GRID III, but the seas became too rough (5 to 6 feet) to safely use the CTD. Consequently, XBTs were used for the next three stations before we retreated to port. Spiking occurred on the 'YYY' traces, possibly due to a loose connector to the CTD. We also had ship problems. One of the two generators broke down. When this happened, the power was cut off and then returned to the DDL. Subsequently, a new tape had to be loaded. Also radio communications were poor. Data went on magnetic tapes in the same way as the last cruise.

1114 - 2 August Departed DURL (Chandler, Hofmann, Porter, White,
to Paffenhofer, Diebel, Sands, Hosford, Kelly and
2345 - 2 August Waslenchuk). An XBT grid was planned instead of the
usual hydrogrid in order to make up for lost time. An
intrusion could be located by such a grid. After one
transect was completed, the sewage holding tanks backed
up and flooded the "stateroom", so we returned to port.

0811 - 4 August XBT/BIO III. Departed DURL (Atkinson, Singer, Hofmann,
to Kelly, Paffenhofer, Diebel, Sands, McIntyre, and Hosford).
1750 - 6 August An XBT grid was run in place of a hydrogrid; then a
biogrid was run at stations 53 - 57. It was observed
that radio communication interferes with the 'XXX' plotter.
Prior to the last station the BLUE FIN's v-drive broke.
The Coast Guard Cutter POINT MARTIN and later a smaller
CG vessel, towed the BLUE FIN to Southport, North
Carolina. Data went on the magnetic tapes in the same
way as the last cruise.

August 9 A hurricane warning and shaft repairs kept us in port.

0800 - 14 August HYDRO/BIO IV. Departed Southport (Atkinson, Singer,
to Porter, White, Paffenhofer, Diebel, Sands and Hosford).
1815 - 16 August After completing five hydrogrid stations the analog fold
on the depth scale was off. It cycled at 37.5 m instead
of 150 m. The 10V calibrating source became inoperable,
so built-in calibrated spans (.25V/cm for depth and .5V
for conductivity and temperature) had to be used. The
biogrid following the hydrogrid consisted of two transects
over an old intrusion (stations 32 - 35). It was noted

that entering a manual file gap before a new header permitted the recording of data and headers in separated files as desired. Consequently the tape quality was improved for the data set but still exhibited folding in the depth record.

- 0816 - 18 August HYDRO/BIO V. Departed DUMML (Singer, Chandler, White, Kelly, Paffenhofer, Diebel, Sands, Hosford and Gonsoulin).
- 0043 - 19 August We planned to use XBTs to locate a possible biogrid area, but the XBT was inoperable from the start (bad tube). Consequently CTD casts were made until rough seas terminated all work at 1646, 18 August, ending the '76 OBIS work. The magnetic tapes recorded data well, except for the folds in depth which were later corrected with software modifications.

